Dear Editor, Dear Reviewer,

We appreciated the very detailed and constructive comments on different aspects of the study. We have addressed the suggestions given by the reviewer; in the following we report the point-to-point reply to the comments.

Best regards,
Alice Vho and co-authors

At the date of review, the database, which is used for the modelling and which is fundamental for the models, is currently under review for another journal and can hence not be accessed. This is somewhat problematic regarding the final publication of this manuscript, at which point the database should be accessible to readers (see comment below).
The manuscript has been accepted and it will be available soon. For the moment, the fractionation factors used for the calculations are also provided with the program (folder "WorkingDirectoy" of PTloop). This has been added in the section "Code availability". The file DO18db2.0.3.dat contains the fractionation factors between quartz and any end-member used in the calculation.

10: For clarity, it should be added the Gibbs energy minimization is carried out for given whole-rock compositions.
The text has been modified accordingly (line 11).

15-20: The abstract would become clearer if a structure similar to the order/sections in the manuscript is adopted. For instance, the infiltration of an external fluid into mafic rocks is mentioned as point (1) in the abstract, but it is the last section in the results (3.3.4) and also near the end in the discussion. Better to first describe the simple case of dehydration only ("no interaction" case); it should also be mentioned that dehydration in the metasediments is also considered in the models. Second, the influx of MORB-derived fluid should be addressed; currently, MORB-derived fluids are not explicitly mentioned in the abstract, so this should be added as this process features prominently in the results and discussion. Finally, the influx of fluid derived from ultramafic rocks can be mentioned.
Abstract modified accordingly. The term "MORB" has been replaced by the term "metabasalt" when indicating the subducting mafic oceanic crust. Metabasalt$_{(h)}$ refers to the hydrated MORB composition, while metabasalt$_{(a)}$ to the altered mafic oceanic crust (lines 163 – 165).

82-90: Since sediment dehydration is also considered, this should be explicitly mentioned here. It is nicely described in the figure caption to Fig. 1 that the fluid produced in the "No Interaction" case is a mixture of MORB-derived and sediment-derived fluid.
Two sentences have been added to clarify this point (lines 95 – 99).

148: Reference to the database in Vho et al. (in review). As a reviewer of this manuscript for Solid Earth, I do not have access to this database and do not know the current status regarding publication of this database. This is somewhat problematic as the database is fundamental for the modelling performed in this manuscript. I am convinced that the authors are pursuing the publication of this accompanying manuscript as quickly and efficiently as possible, but I would like to see this the accompanying manuscript as accepted manuscript with doi number before the final version of this manuscript for Solid Earth goes online. The reason is that readers should be able to adequately follow and reconstruct all the information and proceedings of this article. This is difficult if the database is not accessible and may become problematic if the accompanying manuscript is never published (I do not expect this to happen, but it seems a sensible approach notwithstanding the impeccable reputation of the present author team).

See above.

194: As these fractionation factors are explicitly mentioned, it would be useful to specify for which temperature the fractionation of 2 ‰ is representative of.
It has been specified that this values if for T > 550 °C (line 209).

203: white mica: The phase diagrams in Fig. 3 show "ph" (phengite), but in the text mostly "white mica" is used (but see line 212). Does "white mica" always stands for a potassic white mica? For consistency, only one term should be used throughout, and an explanation regarding the composition of the white mica would also be useful (e.g. the modelled composition might be a typical muscovite at lower grades but becomes more phengitic at higher temperatures and pressures).
The composition of the modelled white mica has been added in the text. According to the composition, the term phengite was used, with the exception of the abstract where the term "white mica" (line 21) refers to all variety of potassic white mica compositions.

212-224: There are a few minor issues in this section that should be addressed:
a) Modal phase changes are referred to partly in a neutral way (increase/reduction) but in other cases specific reactions are invoked (e.g. gln consumed in favour of jd+ank, lws breakdown producing grt). From a perspective of a metamorphic petrologist, one would be interested to see the full reaction equations. Two examples: If ankerite is produced, carbonate or CO2 is required as reactant; which other phases are involved in the lawsonite breakdown reaction? However, in the context of this study, this detail may not be necessary, and it may be suffice to formulate in a way without referring to specific reactions.
This section was reformulated without referring to specific reactions since, as perceived also by the reviewer, this detail is not necessary.

b) Clinopyroxene composition: As the change from omphacite to jadeite is mentioned, please clarify at which compositional boundary (mol% jadeite component) the change in name is made. Or is it a pure end-member jadeite? The coexistence of jadeite and omphacite should also briefly be addressed as in natural rocks, one would presumably expect only one clinopyroxene with changes in the jadeite-component in omphacite.
Details on the pyroxene composition have been added in the text (lines 218 – 237). For consistency, also the composition of the garnet has been reported. A note about the interpretation of the coexistence of two pyroxenes has been added (lines 241 – 242) in line to what was already written for amphiboles.

The authors point out that the co-existence of two amphiboles is of little relevance for the oxygen isotope modelling – is this similar for the pyroxenes? This should be clarified.
Yes, it is similar for the pyroxenes and this point has been added in the text (lines 241 – 242).

227: Initial water-saturated conditions: Please explain and justify the choice of water-saturated conditions, in particular for the fresh MORB. If one assumes that fresh MORB is initially composed of nominally anhydrous minerals only, where does the water come from? In the discussion later, the water released from the slab is dominated by the MORB-derived fluid, and presumably this is due to amounts of water stored under water-saturated conditions initially. Hence, does this initial assumption affect (at least some) of the model calculations, and how large is the effect? I appreciate that not all possible scenarios can be addressed in a single manuscript, but a brief justification of the choices made would be useful.
In this case the main difference is that the amount of released fluid due to breakdown of hydrous phases would be smaller. This point has been added (lines 255-256).

234: Glaucophane and actinolite and the intermediate fluid pulse: It seems in the figure that the growth of talc takes up the water released by consumption of actinolite and glaucophane, as the modal proportion of talc increases from 580 to 600°C, whereas the amount of water appears to increase at >600 °C when the modal proportions of talc and then lawsonite decrease. Please check carefully and modify the text accordingly.

Talc takes only part (ca. 50%) of the water released by amphibole breakdown, because of the small abundance of talc (ca. 14 wt% in the metabasalt$_{(h)}$, ca. 6 wt% in the metabasalt$_{(a)}$, incorporating ca. 4 wt% of H_2O) with respect to the consumed amphiboles (ca. 50 wt% in the fresh MORB and ca. 40 wt% in the altered MORB, water content of 2.0 – 2.2 wt%). This results in a peak of fluid release at 600 °C as can be observed also in figure 5. This point has been specified in the text (line 254).

236: The liberation of water from the carbonate sediment is specified, but release of CO_2 is not mentioned. Does any release of CO_2 occur? Carbonate phases appear to remain stable, but the aspect should still be briefly explained for clarity.

This is an important point and we acknowledge both the reviewers for the comments. The main reasons why we did not to include CO_2 in the calculation are the following. (1) The amount of CO_2 involved in this model is limited. The maximum CO_2 content in the altered MORB-derived fluid is ca. 10 mol% at 700 °C and 2.6 GPa, and it is lower (2 – 7 mol%) at the conditions of the major fluid pulses. In the carbonate sediment the CO_2 content is > 7 mol% at T > 560 °C and P > 2.18 GPa, where a negligible amount of fluid (i.e. << 0.01 vol%) is released. (2) The oxygen isotope fractionation between CO_2 and H_2O is still poorly constrained and presents limitations (see below); therefore it was not included in the internally consistent database version used for this study. Published experimental calibrations involving CO_2 are limited (e.g., Böttcher, 1994 for norsetite-CO_2; O'Neil and Adami, 1969 for H_2O-CO_2) and were performed at T < 100 °C, making the validity of the available fractionation factors at high temperature questionable. Zheng (1994) provides fractionation data for calcite-CO_2, quartz-CO_2 and H_2O-CO_2; however, incremental calculations have strong limitations and must be used with caution (e.g., Chacko et al., 2001). For the H_2O-CO_2 pair, the available calibrations (Friedman and O'Neil, 1977; O'Neil and Adami, 1969; Zheng, 1994) are in strong disagreement and predict fractionations of 1.50 ‰, -1.87 ‰ and -4.41 ‰ at 700 °C and of -8.85 ‰, -11.45 ‰ and -10.99 ‰ at 350°C respectively. Overall, the H_2O-CO_2 fractionation is large (-5 – -12 ‰) at T < 440 °C, where CO_2 is absent or present in negligible amount in the fluid phase in our model; it decreases to -2 – -6 ‰ at T = 550 °C, where the amount of CO_2 present in the fluid phase in our model is minor (ca. 3 mol% in the fluid released by the MORB, ca. 6 mol% in the fluid released by the sediment); it is moderate (ca. -5 ‰) to absent (depending on the chosen calibration) at T ≥ 600 °C, where the amount of CO_2 in the fluid increases. The consideration of the CO_2 component would produce a negligible to minor shift on the fluid $\delta^{18}O$ at the condition of significant release (0.1 – 0.2 ‰ at 520 °C and 0.0 – 0.6 ‰ at 620 °C for the MORB-derived fluid and 0.1 – 0.3 ‰ at 480 °C and 0.2 – 1.1 ‰ at 620 °C for the sediment-derived fluid, depending on the calibration).

We added a paragraph in the section 3.2 describing the potential effect of the CO_2 component present in the fluid released by the altered MORB and the carbonate. The title of the section has been also changed from "Production of water" to "Production of aqueous fluid". However, we did not introduce CO_2 in the computation for the reasons discussed above.

282: Mafic fluid (see also 288, 297, 300 and elsewhere): Using the terms mafic fluid and ultramafic fluid is not appropriate and should be avoided. The term "mafic" is derived from magnesium and ferrum (iron) rich, which is appropriate for rock compositions but not for the fluids considered here. The same applies to "ultramafic fluids" (e.g. in lines 309, 311 and elsewhere), serpentinite-derived fluid should be used instead.

The term "mafic" has been replaced by "metabasalt-derived" and term "ultramafic" by "serpentinite-derived" when referring to fluids.

311: This statement is a bit vague. What exactly is the effect in the PI and NI cases on MORB? If the variations in the sedimentary rocks decrease to zero, does that mean there is no effect at all, or no change compared to the previous cases? Please formulate more precisely here.
The sentence has been rephrased and moved to the end of the section in order to make the point clearer.

331-337: The example of the granite appears to be out of place here, as granite has not been considered anywhere else in the manuscript. A dry basalt would be a more appropriate example, which can be linked to the scenarios considered much better. But the results presented show the limited effect on the O isotope variation anyway, so consider deleting this section altogether.
This example has been moved to the supplementary material S4.

363-364: This statement is important, and could be highlighted in abstract and/or conclusions.
The statement has been added in the abstract (line 17) and in the conclusions (lines 576 – 578).

387-393: This section would benefit from a few more details regarding the studies on oxygen isotope zoning in metamorphic minerals, and how the modelling results can be linked to these results (and possibly used to support interpretations or argue for alternative interpretations). Questions that are of interest to the reader include: What kind of zonation was observed in the minerals studied? With which of the modelled scenarios do these patterns coincide? Providing more details here and some specific examples would also be useful to emphasize the wider implications for studies based on natural samples.
Three examples of observed intragrain $\delta^{18}O$ variations in garnet from HP rocks have been reported (Martin et al., 2014; Rubatto and Angiboust, 2015; Vielzeuf et al., 2005b; lines 431 – 434).

403: Integrated Fluid/rock ratios: It is not entirely clear where the numbers come from as they have not been mentioned before. Please clarify.
The concept of integrated fluid/rock ratio has been now defined in the section 2.1 as "as the total mass of aqueous fluid that has passed through and interacted with the rock normalized to the mass of the rock".

410: Serpentinite-derived fluid input into the sedimentary layer: Is this fluid in the models not a mixture of serpentinite-derived fluid and MORB-derived fluid since MORB also dehydrates? If so, clarify this point.
Yes, it is a mixture and the point has been clarified (lines 453 – 454).

413-415: Detection of serpentinite-derived fluids: It would be useful if the authors could refer to the (possible) detection of such fluids in real sediments to underline the relevance of their study.
Two natural examples have been reported (lines 457 – 462). Martin et al. (2014) describe a shift in $\delta^{18}O$ of -2.5 ‰ among different generations of HP garnet in a sample from the Corsica continental basement (garnet mantle $\delta^{18}O = 7.2 \pm 0.4$ ‰, garnet rim $\delta^{18}O = 4.7 \pm 0.5$ ‰). The authors associate this shift to an infiltration of serpentinite-derived fluids and, to a lesser extent, altered gabbro-derived fluid. Williams (2019) describe an extreme $\delta^{18}O$ shift of -15 ‰ between garnet core and rim in a metasediment from the Lago di Cignana Unit. Such an oxygen isotope composition variation has been related to a strongly channelized fluid influx originated from the dehydration of serpentinites.

416-418: Effects: The relatively "dry" system still starts with a water-saturated MORB; so the reader may wonder how things change if the system is really dry – would the oxygen isotopic effects even larger? (see also earlier comments).

The terms “wet” and “dry” have been removed for clarity: relatively water-rich and relatively water-poor systems are used instead. The main difference with considering undersaturated basalt as starting composition would be the release of less fluid (as has been specified at lines 155-256) and therefore less capacity to infiltrate upper lithologies and modify their $\delta^{18}O$ value.

419-437: This section seems rather unnecessary because it does not add much to the discussion on oxygen isotopes, the main statement emphasizing that the trends are similar to the ones shown earlier. The discussion on water release is fine but key points could be incorporated into the section “Model geometry” where some of the differences between the P-T paths are already highlighted.
We believe that this section is important to provide an overview of the possible variations associated to the use of different P-T paths for the model. It also serves the purpose to clarify the doubt on whether the chosen geotherm is representative for any natural system (see the comment on figure 2 below). Therefore, it has been kept in the text.

450-468: Can the relevant equations that consider the subduction rate and the volumes of fluid released be shown here so that readers get a better understanding of the modelling approach?
A clarification about how the chosen subduction rate controls the amount of water infiltrating at a given point of the slab mantle interface has been added (lines 509 – 512). Given the column length of 1 m, a subduction rate of 1 cm/y implies that any fixed point (i.e. fixed P-T conditions) at the slab/mantle interface receives in 100 years the total amount of fluid that a single column can liberate at those conditions. Hence, in this example 4892.6 kg of water/100 years (i.e. the amount released by the considered column at the chosen conditions, as explained in the text) infiltrate the mantle wedge.

475: What exactly are “high” $\delta^{18}O$ arc lavas. Please provide some values or a range of values.
Values given in the cited studies have been reported (phenocrysts in lavas from Central Kamchatka: olivine $\delta^{18}O$ = 5.8 – 7.1 ‰ and clinopyroxenes $\delta^{18}O$ = 6.2 – 7.5 ‰, Dorendorf et al., 2000; New Guinea: silicate glass inclusions in olivine $\delta^{18}O$ = 8.8 – 12.2 ‰, clinopyroxenes in metasomatized lehrzolite $\delta^{18}O$ = 6.2 – 10.3 ‰, Eiler et al., 1998).

486: Another important statement relevant for the interpretation of natural samples, which may also be emphasized in the conclusions.
This statement has been added in the conclusions (lines 597 – 599).

515: Interesting aspect which may be of interest to studies on natural serpentinites. For instance, have such elevated O isotope signatures been observed in natural wedge serpentinites? Or can O isotopes be used to distinguish wedge from abyssal peridotites in the geological record? Briefly expanding on these aspects would widen the relevance of this study.
Theoretically, mantle wedge metasomatized/serpentinized rocks after interaction with slab-derived fluids are expected to increase the $\delta^{18}O$ with respect to the mantle signature of 5.5 ‰. It appears however impossibile to use this point as main discriminant to distinguish sea-floor (or in general low-T) serpentinites from HP ones because the first type is highly variable in oxygen isotope composition (ranging between 1 and more than 10 ‰).

Figure 1: As in the text, please avoid the terms “mafic fluid” and “ultramafic fluid”. Add $\delta^{18}O$ to the numbers given in the figure. Clarify that 4.5 ‰ is a fluid value, not the value of the serpentinite. Give the sources for the $\delta^{18}O$ values used in the figure, or refer to the text.
Figure and figure caption modified accordingly. To avoid confusion, only the $\delta^{18}O$ of the rocks (fluid sources) has been reported in the figure.

Figure 2: The meaning of the abbreviation D80 should be explained. Moreover, one may wonder whether an average geotherm is useful as it may not represent any real subduction zone. Typo in the figure "Syracuse". Regarding the lines in this figure and in other figures, they are dashed rather than dotted and should be labelled accordingly.
The meaning of D80 has been explained as "the geotherm dominated by a steep T gradient at 80 km depth, which occurs at the transition from partial to full coupling". The implications of the choice of a specific geotherm for the model, and the possible variations occurring when the P-T path is modified, are discussed in the section 4.4 "Effect of the subduction geotherm".
The typo has been corrected and "dashed" has been used for the lines.

Figure 3: Mineral abbreviations should be explained. It would also help to indicate initial water contents in the figure or the caption.
Mineral abbreviation reference to Whitney and Evans (2010) has been added. Titanite field colour has been changed to be consistent with Fig. 4. The initial water content in vol% (< 1 vol% for the MORBs and the carbonate sediment, ca. 3 vol% for the terrigenous sediment) have been added in the caption together with a reference to Table 1 for details.

Figure 4: The line for titanite is almost invisible in a print out, a somewhat darker colour would improve visibility. For diagrams (g) and (h), I recommend presenting separate diagrams for the partial and high interaction cases because the distinction of the lines marked with stars is not very clear (the bulk trend could be copied into the respective other diagram for comparison). As above, lines are dashed (short bars) rather than dotted (points).
The colour of the line for titanite has been modified. The term "dashed" has been used for the lines. The figure has been split into two figures in order to make the diagrams (g) and (h) clearer. Figure 4 includes the diagrams (a), (b), (c), (d), (e) and (f) of the original figure, while figure 5 include 4 diagrams showing separately the partial interaction and the high interaction cases for both the sediments. In all the diagrams we plotted the no interaction case lines for comparison. Figure captions and references in the text have been modified accordingly.

Figure 6: Avoid terms "mafic" and "ultramafic" fluid.

Figure and figure caption modified.

Technical corrections:

All addressed.

Dear Editor, Dear Reviewer,

We appreciated the constructive and helpful comments that shed light on important details that were missing in the previous version of the manuscript. We have addressed the suggestions given by the reviewer and the point-by-point response is reported in the following.

Best regards,
Alice Vho and co-authors

Chemical system: carbon is not present in the list at line 164.
It has been specified which lithologies contain carbon (line 177).

It is not clear if CO2 (as well as other species such as CH4 and H2) in the fluid was considered or forced not to form. It is clear, however, that CO2 and other species (if any) were not considered in the 18O budgets (line 118). Same for S. A sentence should be added.
We acknowledge the comments of both the reviewers about the importance of C since it is present both in the altered MORB and in the carbonate sediment. A sentence has been added at the end of the section 2.2 (line 118 in the original manuscript) that refers to the newly added discussion about the amount and possible effects of CO_2 in our model (section 3.2, see also the answer to the comments from reviewer 1). The implementation in the model of other species (i.e. CO_2 as well as CH_4, H_2) could be assessed, provided that (1) reliable constraints on the oxygen isotope fractionation between these species and water or minerals are determined and (2) their consistency with other available data is established. However, CH_4 and H2 do not contain any oxygen, being less relevant for the model than CO_2. This point has been added in the section 4.6 "Model applications and future directions".
S is not present in any of the considered bulk compositions and therefore no S species are involved in this model. Moreover, oxygen isotope fractionation between water and S-species is poorly constrained, especially at T > 350 °C, where no data are available.

The text should clarify if CO2 was considered as a negligible parameter in this model (non just not considered). To be honest, I do not see how percolation of potentially high fluid fluxes through the carbonate layer should not mobilize (not just equilibrate) a large portion of the bulk carbonate O. Take the example of Ague and Nicolescu (2013 Nat Geo): an almost complete carbonate devolatilization along a fluid channel. Or the reverse carbonation (Piccoli et al 2016; Scambelluri et al 2016). Can O-bearing fluid species other than H2O modify the model assumptions? If yes (e.g. Baumgartner and Rumble), something should be said. If not, why? The sentence at line 118 is not enough in my opinion and a more detailed presentation of the related biases should be provided.
A discussion on the possible effects of CO_2 in our model have been added in section 3.2 (see above and answer to reviewer 1). The anticipation of future directions that might consider decarbonation/carbonation reaction, or more in general mineral dissolution, transfer and re-precipitation has been added in the section 4.6 "Model applications and future directions".

There is no mention to the potential effect of evolving redox (e.g. when H2O+CH4 go to CO2 + H2) on the H2O δ18O. Of course, the cap delta between H2O and minerals would not change, but the relative signatures would. This should be at least mentioned and/or justified. This is relevant because, for example, in the terrigenous layer, a fluid in equilibrium with graphite (not considered in the model) may be strongly enriched in one or the other C-bearing species relative to H2O.

This effect of oxidation state on C, S and Cl stable isotope partitioning has been described (e.g., Chacko et al., 2001; Sharp, 2017). As explained by Sharp (2017), oxygen has one oxidation state and so it is not affected by the redox changes that occur in most of the other elements used for stable isotope studies. The heavy isotope of oxygen will be preferentially fractionated into short, strong chemical bonds (such as $Si^{4+)}$ generally with a high oxidation state, however this is not always the case (for example, uraninite $U^{4+}O_2$ strongly incorporates ^{16}O relative to quartz), so that oxidation state alone does not always correlate with oxygen isotope enrichment. Therefore no evolving redox effect has been considered.

Still on line 118: although the choice of considering molecular fluid species only does not fully reflect the technical means we have today (e.g. DEW model), I agree that this is probably the right choice for this early contribution. However, especially because this study centers on fluid-rock interactions and metasomatism, the effect of omitting ionic species and their effect of potentially large mineralogical/mass changes has to be introduced. The manuscript cites a series of natural examples of strong fluid-mediated O resets. These rocks are in most cases associated with dramatic major element variations that cannot be explained without species more complex than molecular H2O. The possibility that these species have a negligible effect on the δ18O of the system has to be demonstrated. For example, the capdelta between HCO3- and H2O at room T is about 40‰. At higher T it should be lower, but maybe still significant if present in large amounts. At least for the carbonate layer, species like HCO3- may be important at the considered conditions (see Facq et al 2014 GCA). Here again I suggest providing more details on these assumptions and potential biases.
Oxygen isotope partitioning between HCO_3^- and H_2O (as well as for other dissolved C-species) are poorly constrained and the data are obtained at low T (i.e. Halas and Wolacewicz, 1982, 25 – 45 °C; Usdowski and Hoefs, 1993, 19 – 25 °C). Therefore, any extrapolation to the temperature range relevant for this model and discussion on possible effects on the $\delta^{18}O$ partitioning among phases is disputable.
The study of Facq et al. (2014) points out the importance of HCO_3^- and CO_3^{2-} based on experiments on a very special system (a single aragonite crystal in water). They conclude that ion-pairing in deep crustal and mantle aqueous fluids may occur during the dissolution of carbonate minerals at high pressure, even if in natural system the complex interplay of pressure, temperature, and activity ratios imposed by the silicate and/or carbonate environment must be considered. Even if we would consider the presence of these C-species instead of CO_2 at high pressure, and we would assume to be able to extrapolate up to 700 °C the low T experimental data for oxygen isotope fractionation among them and H_2O (Usdowski and Hoefs, 1993), the fractionation between HCO_3^- / CO_3^{2-} and H_2O is smaller than the one between CO_2 and H_2O, resulting in an even smaller effect than the one discussed for CO_2 in section 3.2. We acknowledge the importance of this study, but we believe that this is a very specific point still under investigation and there are too many uncertainties in the available data to consider it at this stage of the model. However, we mention the possibility of introducing additional C-species in future developments in the section 4.6 “Model applications and future directions”.

See also the potential effect of pH on stable isotope variations (Ohmoto 1972).
Ohmoto (1972) described the effect of pH on S and C stable isotopes. The effect of pH state on C and S stable isotope partitioning has been described also in the more recent studies (Chacko et al., 2001; Sharp, 2017). No major pH effect on O stable isotope partitioning has been recognized with the exception of Fe(III)-oxides, for which large variations in experimental results at $T < 40$ °C might be attributed also – but not exclusively – to the difference in pH (Chacko et al., 2001).

F/R ratios. The only values of F/R ratios that I could find in the text (apologies if I am wrong) appear very low to me, especially in the case of channelized fluid flow. As time is present in the proposed model, it could help having some idea on how the proposed fluid/rock ratios translate

into time-integrated fluid fluxes. The proposed values should at least in part correspond to the time-integrated fluid fluxes estimated in pervasive vs. channelized fluid systems in crustal settings (see review by Ague 2014 for example). F/R ratios alone do not provide insights on the hydrology of the systems and are sometimes meaningless (Baumgartner and Ferry 1991). I understand that many times this choice is imposed by the numerical code itself, but here you have the means to do this conversion at least once in the text, for reference. This could be also introduced at line 52.

Values for integrated fluid/rock ratios (as defined in section 2.1, lines 88 – 89) in the sediments have been added in the results (section 3.3.1). In case of high interaction, the integrated F/R ratios are 0.75 kg/kg in the carbonate sediment (corresponding to 2.1 F/R volume ratio) and 0.35 kg/kg in the terrigenous sediment (corresponding to 0.98 F/R volume ratio). They drop to 1/2 in case of partial interaction. These values are consistent with the F/R ratios calculated by Konrad-Schmolke et al. (2011) of 0.15 – 0.3 for weakly deformed samples and 0.5 – 4 for mylonites in the Sesia Zone. Ague (2014) calculates fluid fluxes in the order of 1000 m^3/m^2 (and up to 10^4 – 10^5 m^3/m^2 in case of channelized fluid flow) for crustal column of 15 km. Our crust is 1 km thick and the fluid fluxes are 160 – 170 m^3/m^2, therefore comparable in the order of magnitude with the one calculated by Ague (2014).

Line 19: bulk δ18O value: in the source?
Yes. It has been specified (line 17).

Line 85: and also on the fluid speciation that is not considered here but that can strongly modify the δ18O evolution of the fluid/rock system. For example, at 500 °C the Cc-H2O and CC-CO2 cap delta for O differ by about 6‰.
A discussion about the effect of a mixed H_2O-CO_2 fluid on the $\delta^{18}O$ has been added in the section 3.2 “Production of aqueous fluid” (see above).

Line110:“excluding” is misleading in my opinion. You mean removing from the reactive bulk, right?
The term “removing” has been used instead of “excluding”.

161: can you clarify the meaning of natural profiles?
The sentence has been modified for clarity (line 173).

Line 181-182: do the chosen values take into account processes like decarbonation?
Those are the starting $\delta^{18}O$ values (25 – 35 ‰, retrieved from marine sediment measurements, where no decarbonation occurred). Possible decarbonation during subduction might decrease the starting $\delta^{18}O$ (i.e. because calcium carbonate has usually higher $\delta^{18}O$ than the bulk $\delta^{18}O$), and indeed the $\delta^{18}O$ of carbonate in HP metamorphic terrains could be lower. However, as already mentioned, decarbonation has not been considered at this stage of the investigation, but represents an important, although challenging, development as has been stated in the section 4.6.

193: this sounds like a model-driven assumption. Could you clarify?
The sentence has been modified (lines 206 – 208) to clarify that the choice of the serpentine $\delta^{18}O$ = 2.5 ‰ has been done in order to maximize the difference in $\delta^{18}O$ between the fluid-source and the fluid-sink lithologies, while using a feasible value for natural serpentinites. Any interaction with higher- $\delta^{18}O$ serpentinite-derived fluids will just reduce the effects described in this study.

323: δ18O of the water: this is still a model assumption. I would say fluid instead.
The text has been modified accordingly (line 357).

344: increase in bulk δ18O: increase in the reactive bulk δ18O?

Yes, the text has been modified accordingly (line 373).
.

345: reactive bulk δ18O?
Yes, the text has been modified accordingly(line 373).

361-366: Here is where I miss the effect of decarbonation/dissolution and species other than H2O in the model. I suggest adding a sentence to recall the assumptions.
The assumption has been recalled (line 393).

492: Airaghi et al: I suggest adding a couple more references on this topic.
Few more references have been added (Cartwright and Barnicoat, 2003; Engi et al., 2018; Konrad-Schmolke et al., 2011; Rubatto and Angiboust, 2015) (line 549).

Tracing fluid transfers in subduction zones: an integrated thermodynamic and $\delta^{18}O$ fractionation modelling approach

Alice Vho[1], Pierre Lanari[1], Daniela Rubatto[1,2], Jörg Hermann[1]

[1] Institute of Geological Sciences, University of Bern, CH-3012 Bern, Switzerland
[2] Institut de Sciences de la Terre, University of Lausanne, CH-1015 Lausanne, Switzerland

Correspondence to: Alice Vho (alice.vho@geo.unibe.ch)

Abstract. Oxygen isotope geochemistry is a powerful tool for investigating rocks that interacted with fluids, to assess fluid sources and quantify the conditions of fluid-rock interaction. We present an integrated modelling approach and the computer program PTLOOP that combine thermodynamic and oxygen isotope fractionation modelling for multi-rock open systems. The strategy involves a robust petrological model performing on-the-fly Gibbs energy minimizations coupled to an oxygen fractionation model for a given chemical and isotopic bulk rock composition; both models are based on internally consistent databases. This approach is applied to subduction zone metamorphism to predict the possible range of $\delta^{18}O$ values for stable phases and aqueous fluids at various pressure- (*P*) and temperature (~~P-~~*T*) conditions in the subducting slab. The modelled system is composed ~~by~~ of a mafic oceanic crust with a sedimentary cover ~~a sequence of oceanic crust (mafic) with sedimentary cover~~ of known initial chemical composition and bulk $\delta^{18}O$. The evolution of mineral assemblages and $\delta^{18}O$ values of each phase is calculated along a defined *P-T* path for two typical compositions of basalts and sediments. In a closed system, the dehydration reactions, fluid loss and mineral fractionation produce minor to negligible variations (i.e. within 1 ‰) in the bulk δ18O values of the rocks, which are likely to remain representative of the protolith composition. In an open system, fluid-rock interaction may occur (1) in the metasediment, as consequence of infiltration of the fluid liberated by dehydration reactions occurring in the metamorphosed mafic oceanic crust, and (2) in the metabasalt, as consequence of infiltration of an external fluid originated by dehydration of underlying serpentinites. In each rock type, the interaction with external fluids may lead to shifts in δ18O up to one order of magnitude larger than those calculated for closed systems. ~~. Fluid-rock interactions may occur as consequence of (1) infiltration of an external fluid into the mafic rocks or (2) transfer of the fluid liberated by dehydration reactions occurring in the mafic rocks into the sedimentary rocks. The effects of interaction with externally derived fluids on the mineral and bulk $\delta^{18}O$ of each rock are quantified for two typical compositions of metabasalts and metasediments with external fluid influx from serpentinite. The dehydration reactions, fluid loss and mineral fractionation produce minor to negligible variations in bulk $\delta^{18}O$ values, i.e. within 1 ‰. By contrast, the interaction with external fluids may lead to shifts in $\delta^{18}O$ up to one order of magnitude larger.~~ Such variations can be detected by analysing in-situ oxygen isotope in key metamorphic minerals such as garnet, white mica and quartz. The simulations show that~~,~~ when the water released by the slab infiltrates the forearc mantle wedge, it can cause extensive serpentinization within fractions of a Myr and significant oxygen isotope variation at the interface. The approach presented here ~~This technique~~ opens new perspectives for tracking ~~to track~~ fluid pathways in subduction zones, to distinguish porous from channelized fluid flows, and to determine the *P-T* conditions and the extent of fluid/rock interaction.

1 Introduction

The subducting oceanic slab is composed of a sequence of rock types corresponding to chemical systems that undergo continuous and discontinuous ~~phase~~ reactions in response to pressure (*P*) and temperature (*T*) changes. Through its metamorphic history, ~~altered~~ hydrated oceanic lithosphere undergoes extensive dehydration by the breakdown of low-temperature, volatile rich minerals (e.g., Baumgartner and Valley, 2001; Baxter and Caddick, 2013; Hacker, 2008; Manning, 2004; Page et al., 2013; Poli and Schmidt, 2002). The expelled aqueous fluid~~water~~ migrates through the slab towards the slab-mantle interface and it may continue

rising to the mantle wedge playing a major role in triggering mass transfer and melting (Barnicoat and Cartwright, 1995; Bebout and Penniston-Dorland, 2016). Evidence ~~of~~ for fluid circulation in subducted rocks has been extensively observed in exhumed high-pressure/ultra-high-pressure (HP/UHP) terrains (e.g., Zack and John, 2007; Baxter and Caddick, 2013; Martin *et al.*, 2014; Rubatto and Angiboust, 2015; Engi *et al.*, 2018), but a direct link to the primary source production is often missing and the main source remains matter of debate. The characterization of fluid pathways in subduction zones has been addressed by using a variety of methods (i.e., seismicity, thermodynamic modelling, fluid inclusions, HP veins, trace element and stable isotope studies on metamorphic minerals) (e.g., Baxter and Caddick, 2013; Hacker, 2008; Hernández-Uribe and Palin, 2019; Scambelluri and Philippot, 2001; Spandler and Hermann, 2005). In particular, oxygen isotope compositions of metamorphic minerals from exhumed HP rocks shed light on the nature of the fluid reacting with those systems during metamorphism. Thus, oxygen isotope studies of HP rocks have the potential to make important contributions to the investigation of fluid sources and pathways in subduction zones (e.g., O'Neil and Taylor, 1967; Muehlenbachs and Clayton, 1972; Hoefs, 1997; Baumgartner and Valley, 2001; Page *et al.*, 2013; Martin *et al.*, 2014; White and Klein, 2014; Rubatto and Angiboust, 2015).

Modelling of oxygen isotopic fractionation has been traditionally addressed as equilibrium calculation between individual mineral couples. An alternative approach follows what has been extensively adopted in the last decades for thermodynamic modelling (see reviews by Lanari and Duesterhoeft, ~~2018~~2019; Powell and Holland, 2008; Spear et al., 2017) and considers an evolving mineral assemblage. A pioneer model ~~was~~ proposed by Kohn (1993) can be applied to single and closed chemical systems~~, limited to single and closed chemical systems~~, i.e. for which no infiltration of external fluids in isotopic disequilibrium ~~was~~ is allowed. Such an approach can ~~evaluate~~ simulate how the oxygen isotopic composition changes with *P* and *T*, but it remains too simple for subduction zone settings, where significant fluid exchange occurs between different lithologies within the subducting slab. Baumgartner and Valley (2001) proposed a model for stable isotope fluid-rock exchange based on continuum mechanics~~a continuum mechanics model for stable isotope fluid-rock exchange~~, where infiltration profiles can be calculated, but no information is provided about the different components (minerals) of the rock, as it is considered as a continuum. The fluid/rock (F/R) ratios obtained with this strategy do not correspond to the physical ~~fluid~~ amount of fluid, but ~~just~~ rather represent~~s~~ a measurement of exchange progress.

We present a new approach that combines equilibrium thermodynamics and oxygen isotope fractionation modelling applied to multi-rock systems. This modelling technique takes advantage of the increased capability of forward modelling of complex systems achieved in the last two decades (Lanari and Duesterhoeft, 2019). A MATLAB©-based modelling program PTLOOP has been developed to calculate oxygen isotope fractionation between stable phases from the results of Gibbs energy minimization performed by Theriak-Domino (de Capitani and Brown, 1987; de Capitani and Petrakakis, 2010) along any fixed P-T trajectory. The oxygen isotope variation of each mineral within the evolving assemblage is tracked using an extensive and internally consistent database for oxygen isotope fractionation (Vho et al., 2020 ~~in review~~). A graphical user interface (GUI) provides the representation of the results. The capabilities of this software solution will be discussed in detail~~s~~ with an example that focuses on the characterization of (1) the effect of the dehydration reactions on the bulk $\delta^{18}O$ of a rock, (2) the effect of the influx into a subducting rock of an external fluid of distinct isotopic composition~~signature~~ and (3) the final amount and isotopic composition~~signature~~ of the fluid leaving the multi-rock system, e.g. infiltrating an upper unit or the mantle wedge. Petrological implications of relevant computational results are also discussed.

2 Modelling

2.1 Model geometry

~~On average, t~~The subducting oceanic lithosphere is typically composed of a section of igneous oceanic crust with its sedimentary cover (mostly < 1 km) above~~,~~ and an ultramafic lithospheric mantle section beneath. The geometry of the model is illustrated in

Fig. 1. The target column represents a simplified section of the upper part of such oceanic lithosphere. It is composed of a layer of basaltic composition (*Rock1*) overlaid by a layer of sediments (*Rock2*, see below for details). Two different rock columns are considered: (1) a relatively ~~"wet"~~water-rich system with altered basalts and terrigenous sediments, and (2) a relatively ~~"dry"~~water-poor system with unaltered basalts (MORB composition) and carbonate sediments~~fresh MORB and carbonates~~. The column has a fixed section of 1 m^2, while the thickness of each rock unit can be set by the user. The model is conservative with respect to the mass, while the volume of each rock type is changing according to fluid loss and density variation along the P-T path. The P-T structure of subduction zones depends on numerous variables, including the age of the incoming lithosphere and the amount of previously subducted lithosphere (e.g., Peacock, 1990). In this study, the calculation was performed following the subduction geotherm from Gerya *et al.*, (2002) (Fig. 2) over a pressure range of 1.3 – 2.6 GPa, corresponding to a depth of ~ 45 to ~ 85 km to encompass the conditions of interest for the investigated processes. The modelled temperatures range from a minimum of 350 °C to a maximum of 700 °C. The lower limit was chosen to take into account ~~is due to~~ the large uncertainties in the thermodynamic databases for many common low-T metamorphic minerals that lead to unsatisfactory~~not satisfactorily~~ models for phase equilibria and mineral parageneses for low-grade ~~metabasites~~ rocks (Frey et al., 1991; Vidal et al. 2016). The upper limit is fixed by the wet solidus of metasediments ~~is fixed before the melting region of metasediment~~ – the present model strictly applies to subsolidus conditions.

During burial and heating the different slab lithologies undergo dehydration reactions. The produced fluid escapes from the source rock and migrates upward, likely interacting with the surrounding units of different chemical and isotopic composition. The effect of an external fluid input on the $\delta^{18}O$ value of growing minerals is strongly dependent on the isotopic composition of the infiltrating fluid ($\delta^{18}O_{fluid}$) and on the degree of fluid/rock interaction. The integrated F/R ratio is defined here as the total mass of aqueous fluid that has passed through and interacted with the rock normalized to the mass of the rock. ~~(fluid-rock ratio, expressed as mass ratio).~~ To explore different scenarios, three models are discussed involving different associations of fresh or altered oceanic basalts with terrigenous or carbonate~~calcareous~~ sediments (Fig. 1b): (1) the interaction between the fluid released from the metamorphosed mafic crust and the overlying metasediment~~the oceanic crust derived fluid and the overlying sediment~~ is negligible and the two rocks evolve independently (*No Interaction* case, *NI*), (2) part of the fluid derived from the metabasalt ~~of the oceanic crust derived fluid~~ (50% when not specified differently) equilibrates with the metasediment, while the other part leaves the system (*Partial Interaction* case, *PI*) and (3) all the fluid released by the metamorphosed mafic crust ~~the MORB~~ equilibrates with the metasediment before escaping the system (*High Interaction* case, *HI*). The fluid released by the entire system is a mixture of fluids derived from the progressive dehydration of the metabasalt and metasedimentary layers. In the *NI* case, both rock types behave as closed systems and the fluid is liberated from the metabasalt and from the metasediment separately. In case of infiltration of fluid derived from the metabasalt in the metasediment, the amount of fluid released by this latter includes the fluid produced by dehydration reactions plus the excess fluid that enters the metasediment and cannot be incorporated in stable hydrous minerals.

The thickness and the degree of serpentinization of the lithospheric mantle subducting beneath the oceanic crust can be highly variable. The most important dehydration reactions in partly or fully serpentinised mantle ~~in these rocks~~ are related to antigorite breakdown, which can release up to 12 wt% of water, playing an important role for water flows in subduction zones. Deserpentinization is assumed to result in two main subsequent fluid peaks (Padrón-Navarta et al., 2013; Scambelluri et al., 2004) related to the reactions

antigorite + brucite → olivine + chlorite + water (~ 480 °C, 1.7 GPa; 1 to 2 wt% water released, up to ~ 50 kg/m^3) (1)

antigorite → olivine + orthopyroxene + chlorite + water (~ 660 °C, 2.5 GPa; ≥ 6.5 wt% water released, ≥ 170 kg/m^3) (2)

The effect on the $\delta^{18}O$ of the metabsalts and metasediments ~~of oceanic crust and sediments~~ of an external fluid influx, i.e. caused by dehydration of the underlying serpentinites, was investigated by defining an amount of fluid with a specific $\delta^{18}O$ value that infiltrates the basaltic layer (*Rock 1*) at two steps of the model (480 °C and 660 °C along the chosen *P-T* path) ~~*Rock 1* at two steps of the model (480 °C and 660 °C)~~ (Fig. 1c,2).

2.2 Model strategy

The strategy behind PTLOOP consists of forward modelling the evolution of the mineral assemblage and the oxygen isotope composition of a rock column composed by two lithologies (Fig. 1a) of assigned thickness and starting bulk chemical and oxygen isotope compositions along a defined ~~Pressure (P)–Temperature (T)~~*P-T* path using a stepwise procedure (Fig. 2). At each *P-T* step, (1) the equilibrium mineral assemblage, oxygen isotope composition of stable phases (δ18O ‰ vs. Vienna Standard Mean Ocean Water, VSMOW), mass (in kg) and isotopic composition of the excess fluid for the metabasalt are calculated~~and isotopic signature (δ^{18}O ‰ vs. Standard Mean Ocean Water, SMOW) of the excess fluid for the metabasalts are calculated~~; (2) any fraction of excess fluid deriving from dehydration reactions in the metabasalt~~s~~ can be transferred to the metasediment~~s~~ or directly escapes the system; (3) the equilibrium mineral assemblage, δ^{18}O value of stable phases, amount and δ^{18}O~~signature~~ of the excess fluid for the ~~metasedimens~~ metasediment are evaluated by accounting the changes caused by the fluid input from the metabasalt~~s~~; (4) the mass ~~(in kg)~~ and δ^{18}O ~~signature~~ of the total fluid leaving the system is calculated. Furthermore, at each step a chosen amount of external fluid with a given δ^{18}O can be input in the metabasalt~~s~~ and its contribution is accounted for in the subsequent steps. This model is based on the assumption of thermodynamic equilibrium applied to a partially reactive system, whereby phases are assumed to reach chemical and isotopic equilibrium at all steps within the reactive part of the system, i.e. removing from the reactive bulk the phases that are fractionated~~i.e. excluding the phases that are fractionated~~ (Lanari and Engi, 2017). Such petrological models can account for element sequestration during prograde metamorphism. Mineral fractionation in relicts and fluid input/loss are two processes that are allowed to modify the reactive bulk composition. No mineral resorption is permitted. Any fluid liberated during dehydration (excess fluid) does not further interact and leaves the rock. This process is termed *Rayleigh volatilization* (Rumble, 1982; Valley, 1986). In natural rocks, it occurs often combined with the opposite end-member, the *batch volatilization*, where the produced fluid stays within the system as the mineral reaction proceeds, and remains in isotopic equilibrium with the rock until the reaction is completed. In most natural cases involving oxygen isotopes, the difference between the results calculated using the two processes is negligible (Baumgartner and Valley, 2001). The released fluid is considered as pure H_2O~~;~~. Any other effect related to solute-transport by the fluid is ignored in the calculation; the potential effect of a CO_2 component in the fluid is discussed in section 3.2.~~therefore any other solute-transport effect is ignored.~~

2.3 Governing equations

Equilibrium assemblage calculation for a given bulk rock composition at any *P* and *T* is performed with the ~~software~~ program Theriak (de Capitani and Brown, 1987; de Capitani and Petrakakis, 2010) and is based on Gibbs energy minimization. A complete description of the ~~Theriak~~ minimization algorithm is given by de Capitani and Brown (1987). The reacting bulk composition may evolve in the course of the metamorphic history of a rock because of mineral fractionation, fluid loss or input of external fluids. The effective bulk composition is recalculated by PTLOOP at each subsequent stage following the strategy of Lanari et al. (2017).

As for phase assemblage determination, equilibrium is a common assumption of stable isotope transport (Baumgartner and Rumble, 1988; Baumgartner and Valley, 2001; Bowman et al., 1994; Gerdes et al., 1995a, 1995b). Thus, a molar equilibrium constant (*K*) can be defined to describe the thermodynamic stable isotope equilibrium between two substances *i* and *j* (Sharp, 2017)

$$K = \frac{^{18}O_i/^{16}O_i}{^{18}O_j/^{16}O_j} \quad (3)$$

The fractionation factor (α) can be related to the equilibrium constant K as

$$\alpha = K^{1/n} \quad (4)$$

where *n* is the number of exchanged atoms, normally 1 for simplicity. In isotope geochemistry, the isotopic composition is commonly expressed in terms of δ values

$$\delta_i = \left(\frac{R_i}{R_{St}} - 1\right) \cdot 10^3 \ (‰) \quad (5)$$

where R_i and R_{St} are the isotope ratio measurements for the compound i and the defined isotope ratio of a standard sample respectively. For differences in δ values or for δ values of less than ~ 10 ‰, ~~it is valid the approximation~~

$$1000 ln\alpha_{i-j} = \delta_i - \delta_j \quad (6)$$

is a valid approximation that is used in most cases ~~that is used in most cases~~ (Hoefs, 1997; Sharp, 2017). For oxygen isotope fractionation, the equation that can reproduce most of the available calibrations describing the stable isotope fractionation function between two phases is a second order polynomial of $10^3/T$. Hence the stable isotope fractionation between two phases i (with k end-members) and j (pure) as a function of T is described by Eq. (7):

$$\delta^{18}O_i - \delta^{18}O_j = \sum_1^k \left(\frac{A_{k,j} \cdot 10^6}{T^2} + \frac{B_{k,j} \cdot 10^3}{T} + C_{k,j}\right) \cdot X_{k,i} \cdot \frac{N_{k,i}}{N_i} \quad (7)$$

and the conservation of the bulk $\delta^{18}O$ in the system by Eq. (8):

$$\delta^{18}O_{sys} \cdot N_{sys} = \sum_{k=1}^{p} M_k \cdot N_k \cdot \delta^{18}O_k \quad (8)$$

where $\delta^{18}O_i$, $\delta^{18}O_j$ and $\delta^{18}O_{sys}$ are the isotopic compositions of phase i, phase j and the system (bulk $\delta^{18}O$) respectively, $A_{k,j}$, $B_{k,j}$ and $C_{k,j}$ the fractionation parameters for end-member k of mineral i *vs.* phase j, $X_{k,i}$ the fraction of end-member k in the phase i, $N_{k,i}$, N_i and N_{sys} the total number of moles of oxygen in end-member k, in mineral i and in the system respectively, p is the number of phases, M_k the number of moles of phase k, N_k the its number of oxygen and $\delta^{18}O_k$ its oxygen isotope composition. Given a stable mineral assemblage at any P-T condition, the oxygen isotope partitioning among the stable phases is calculated by solving the linear system described by the sets of p-1 Eq. of type (7) and the Eq. (8) (Kohn, 1993; Vho et al., ~~in review~~2020). In closed systems, the first term in Eq. (8) is constant. Open system behaviour can either modify the $\delta^{18}O_{sys}$ or the number of moles of the phases (N_{sys}). The parameters A, B and C between phases were taken from the internally consistent database for oxygen isotope fractionation DBOXYGEN version 2.0.3 ~~by~~ (Vho et al., ~~in review~~2020).

2.4 Starting assumptions

In order to represent the variability in the basaltic portion of the oceanic crust two different bulk compositions were used (Table 1): (1) a representative average MORB basalt (Gale et al., 2013) that has been hydrated but without any other addition or removal of element (metabasalt$_{(h)}$) and (2) a basalt that underwent extensive sea-floor alteration during hydration (Baxter and Caddick, 2013 after Staudigel et al., 1996) that will be referred to as metabasalt$_{(a)}$ in the following. ~~(1) a representative unaltered oceanic basalt (Gale et al., 2013) and (2) a hydrated basalt (Baxter and Caddick, 2013 after Staudigel *et al.*, 1996).~~ Those compositions are in good agreement with other compilations reported in literature (e.g., Sun and McDonough, 1989; Albarède, 2005; Staudigel, 2014; White and Klein, 2014). Oceanic sediments were modelled with two distinct bulk compositions (Table 1): (1) terrigenous sediment, metasediment$_{(t)}$ (clay from Mariana trench, Hacker, 2008 after Plank and Langmuir, 1998) and (2) nanno ooze carbonate, metasediment$_{(c)}$ (Plank, 2014). ~~): (1) terrigenous sediment (clay from Mariana trench, Hacker, 2008 after Plank and Langmuir, 1998) and (2) nanno ooze carbonate sediment (Plank, 2014).~~ Nanno oozes are widespread carbonate sea-floor sediments (Plank, 2014) and they are close in composition to carbonate-rich sediments observed in HP terrains (e.g., Bebout et al., 2013; Kuhn et al., 2005). Thicknesses of 1000 m for the basaltic layer, of 175 m for the clay sediment and 75 m for the ~~carbonatic~~ carbonate sediment were chosen in order to maintain proportions between oceanic crust and sediments comparable with the values reported in various compilations (e.g., Hacker, 2008; Plank, 2014). This results in a total thickness of the rock column 2 to 3 times

smaller than the real thickness ~~natural profiles~~ to encompass the assumption of homogeneous temperature over the whole column within ~ 20 °C. To overcome the effects of possible temperature variations within the column, a discretization step size of ~ 20 °C along the *P-T* path was applied.

The bulk compositions were simplified to the Na_2O–CaO–K_2O–MgO–FeO–Al_2O_3–TiO_2–SiO_2–H_2O system; C is present in the initial bulk composition of the metabasalt$_{(a)}$ and the metasediment$_{(c)}$ (Table 1). MnO was excluded because it overemphasizes the stability of garnet at low metamorphic conditions ($T \leq 350$ °C). The conditions of the garnet-in reaction in Mn-absent systems ~~(MORB, altered MORB)~~ match the results obtained for garnet nucleation in natural rocks (e.g., Laurent et al., 2018). Thermodynamic modelling was performed using the internally consistent dataset of Holland and Powell (1998) and subsequent updates (tc55, distributed with Theriak-Domino 04.02.2017, see Supplementary ~~material~~ Material S1). The following activity models where used for the solid solutions: Holland and Powell (2003) for calcite-dolomite-magnesite; Holland and Powell (1998) for garnet, white mica and talc; Holland and Powell (1996) for omphacite; Holland et al. (1998) for chlorite; Diener et al. (2007) for amphibole. In the presented model garnet undergoes fractional crystallization both in *Rock 1* and *Rock 2* fractionating the reactive bulk for the subsequent~~following~~ steps. The amount of initial H_2O in each rock was set at saturation and is reported in Table 1. No pore fluid expulsion, diagenetic and low-grade ($T < 350$ °C) devolatilization reactions are considered in this study (see above).

A starting bulk $\delta^{18}O$ for the metabasalt$_{(h)}$ ~~MORB~~ of 5.7 ‰ was chosen and represents the reference value for an unaltered MORB (e.g., Cartwright and Barnicoat, 1999; Eiler, 2001; Staudigel, 2014; White and Klein, 2014), while a starting bulk $\delta^{18}O$ of 9.0 ‰ is used for metabasalt$_{(a)}$~~,is~~ representative of basaltic material that underwent sea-floor alteration at $T \leq 400$ °C (e.g., Alt et al., 1986; Cartwright and Barnicoat, 1999; Eiler, 2001; Gregory and Taylor Jr, 1981; Miller and Cartwright, 2000; Staudigel, 2014; White and Klein, 2014). The starting bulk of the terrigenous sediment of 15 ‰ represents the average for the $\delta^{18}O$ of clastic sediments reported by Eiler (2001). The chosen $\delta^{18}O$ starting bulk of the carbonate sediment is 25 ‰, which represents a conservative estimate of marine carbonate $\delta^{18}O$ (typically 25 – 35 ‰, Eiler, 2001). It is ~ 5 ‰ higher than the values for metasedimentary carbonates in the Italian Alps (e.g., Cook-Kollars et al., 2014) that are likely to have interacted with lower- $\delta^{18}O$ fluids during subduction.

In order to define the contribution of an external fluid originating in the lithospheric mantle by serpentine breakdown, a layer of 150 m of pure serpentine containing 12 wt% bulk H_2O was considered and the mass of water released at each reaction was calculated by mass balance, resulting in an~~d~~ input of 7800 kg of water at 480 °C and of 25350 kg at 660 °C to satisfy reactions (#~~7~~1) and (#8~~2~~) respectively. In order to fit the thicknesses chosen for the oceanic crust and the sedimentary layer (2 to 3 times thinner than an average lithospheric section), the 150 m of pure serpentine correspond to a conservative estimate of 3000 m of serpentinized peridotite with an average serpentine content of 5 % in volume. This is in agreement with the values used by Barnes and Straub (2010) and John et al. (2011) based on the estimate by Sharp and Barnes (2004). Serpentine oxygen isotope compositions reported in literature are highly variable (Cartwright and Barnicoat, 1999, 2003; Früh-Green et al., 2001; Mével, 2003; Miller et al., 2001), typically ranging from 1 to 10 ‰. In mid-oceanic ridge environments, the distribution has a peak between 2 and 5 ‰ (Mével, 2003). A value of 2.5 ‰ was chosen from the lower-$\delta^{18}O$ side of this peak. This results in the liberation of a fluid with a characteristic low $\delta^{18}O$ value, but still feasible for natural serpentinites; this value is clearly distinct with respect to the overlying lithologies. The effect of infiltration in the metabasalts and metasediments of serpentinite-derived fluids will become smaller as the fluid $\delta^{18}O$ becomes higher, approaching the equilibrium with the overlying lithologies. The $\delta^{18}O$ value of the released fluid is ~ 4.5 ‰ at $T > 550$ °C (serpentine/water oxygen isotope fractionation, see Vho et al., 2020). ~~, as the effect of interaction with the overlying, higher $\delta^{18}O$, rocks is expected to become smaller when the two isotopic compositions get closer to each other. This leads to a $\delta^{18}O$ value of the released fluid of ~ 4.5 ‰ (serpentine/water fractionation factors compiled in Vho et al., in review).~~ Further details on the modelling input data are given in Supplementary ~~material~~ Material S2.

3 Results

3.1 Stable mineral assemblage

The evolving stable mineral assemblages and bulk water contents of each lithology, without external fluid input, were calculated for each rock composition along the prograde *P-T* path. Results are provided as mode-box diagrams in Fig. 3. The H_2O field represents the volume fraction of excess water in each rock type. The fluid is progressively extracted becoming isolated from the reactive part of the system. Garnet is the only phase prevented from re-equilibrating in the model, thus fractionating from the reactive bulk composition. Below 450 °C and 1.80 GPa, ~~for~~ in the metabasalts~~MORB compositions,~~ glaucophane, actinolite and lawsonite comprise ~ 80 vol. % of the paragenesis, with minor phengite (Si_{apfu} = 3.67 – 3.63, X_{Mg} = 0.62 – 0.56 in metabasalt$_{(h)}$; Si_{apfu} = 3.68 – 3.65, X_{Mg} = 0.67 – 0.58 in metabasalt$_{(a)}$), omphacite (X_{Na} = 0.45 – 0.42, X_{Mg} = 0.81 – 0.72),~~white mica, omphacite,~~ chlorite and titanite. Metabasalt$_{(h)}$ ~~The fresh MORB~~ is richer in SiO_2, FeO and MgO with respect to the metabasalt$_{(a)}$ ~~altered MORB~~ and chlorite is stable up to 480 °C. Metabasalt$_{(a)}$ ~~Altered MORB~~ contains ~ 5 vol% of Ca-carbonate that remains stable over the entire *P-T* path. For either composition, the volume of glaucophane, actinolite and lawsonite gradually decreases from 480 °C and ~ 1.90 GPa until complete consumption ~~In either compositions, from 480 °C and ~ 1.90 GPa, the volume of glaucophane, actinolite and lawsonite gradually decreases until complete consumption~~ at 600 – 620 °C and 2.30 – 2.36 GPa~~~ 2.30 GPa~~. Those represent the major hydrous phases contributing to the dehydration, while a secondary role is played by talc and zoisite at higher *P-T* conditions ($T \geq 580$ °C, $P \geq 2.24$ GPa). Most of the water still retained in the rocks is stored in ~~white mica~~phengite, the abundance of which is primarily controlled by bulk K_2O content, higher in the metabasalt$_{(a)}$~~altered MORB~~, and that remains stable beyond the model conditions. Garnet production starts at ~ 500 °C and ~ 2.00 GPa (X_{alm} = 0.60, X_{grs} = 0.35)~~in the MORBs~~ and ~~it~~ garnet grows continuously until constituting ~ 20 vol% of the metabasalt$_{(a)}$~~altered MORB,~~ and ~ 35 % of the metabasalt$_{(h)}$~~fresh MORB~~.

In the metasediment$_{(c)}$ calcium carbonate, quartz, phengite (Si_{apfu} = 3.42, X_{Mg} = 0.53) and jadeite (jadeite content X_{jd} = 0.95, X_{Na} = 0.96, X_{Mg} = 0.39) compose ~ 80 vol% of the solids at 350 °C and 1.30 GPa. ~~In the carbonate sediment at 350 °C and 1.30 GPa calcium carbonate, quartz, phengite and omphacite compose ~ 80 vol% of the solids.~~ Glaucophane and lawsonite are stable up to 460 °C and 560 °C respectively. Jadeite abundance increases from ~ 10 vol% at 440 °C to ~ 16 vol% at 460 °C, ankerite is stable in minor amounts (≤ 3 vol%) at 440 – 560 °C. Garnet (X_{alm} = 0.57, X_{grs} = 0.41) is stable only at 540 – 580 °C and 2.12 – 2.24 GPa reaching ~ 5 vol% and is then preserved because of the assumption of fractionation from the bulk in the model. ~~Glaucophane and lawsonite are stable up to 460 °C and 560 °C respectively. Glaucophane is consumed in favour of jadeite and ankerite, and lawsonite breakdown produces garnet.~~ The metasediment$_{(t)}$ at T < 500 °C~~terrigenous sediment~~ shows a paragenesis of phengite (Si_{apfu} = 3.68 – 3.55, X_{Mg} = 0.53 – 0.44)~~white mica~~, glaucophane, lawsonite, quartz and omphacite (X_{Na} = 0.50 – 0.48, X_{Mg} = 0.87 – 0.70), with minor titanite~~, at T < 500 °C~~. At ~~500~~ 520 °C and 2.~~00~~ 06 GPa, lawsonite is consumed and the amphibole proportion reduces from ~ 30 vol% to < 20 vol%, while garnet (X_{alm} = 0.63, X_{grs} = 0.34) is produced and reaches ~ 10 vol%. ~~producing garnet.~~ At these conditions, the omphacite content decreases and a clinopyroxene of more jadeitic composition (X_{jd} = 0.72, X_{Na} = 0.76, X_{Mg} = 0.45) becomes stable. ~~The clinopyroxene composition changes from omphacite to jadeite. Also in the terrigenous sediment, garnet appears at ~ 500 °C and ~ 2.00 GPa and it reaches ~ 15 vol% of the terrigenous sediment. In the carbonate sediment, garnet is stable only at 540 – 580 °C and 2.12 – 2.24 GPa reaching ~5 vol% and is then preserved because of the assumption of fractionation from the bulk in the model.~~ These models are in line with the first-order mineralogical changes observed in subducted (and exhumed) crustal material. Thermodynamic calculations predict the coexistence of a calcic amphibole and a sodic amphibole in the metabasalts~~MORBs~~ and of jadeite and omphacite in the metasediment$_{(t)}$~~terrigenous sediment~~. From an oxygen isotope partitioning perspective, the interpretation~~s~~ of the modelled coexistence of a sodic and a calcic amphibole~~s~~ either as two end-members of a solid solution or as coexisting minerals ~~are~~ is equivalent. The same applies to pyroxenes, for which the modelled coexistence of two pyroxenes can be interpreted as a continuous solid solution. Therefore, this does not affect the oxygen isotope partition model final results for the other phases and the bulk.

3.2 Production of aqueous fluid~~water~~

At the initial conditions, all the lithologies are saturated in H_2O (Table 1). Up to 500 °C, lawsonite, actinolite and glaucophane are the main repositories of H_2O in the metabasalts~~MORBs~~, followed by chlorite ~~in the fresh MORB~~ and minor phengite. A significant pulse of water is modelled at 500 – 520 °C and 2.00 – 2.~~60~~ 06 GPa for both the metabasalts ~~in the fresh and altered MORB~~ (Fig. 3a,b). This pulse is caused by decreasing abundance of lawsonite and amphiboles and breakdown of chlorite to produce garnet and omphacite. This first dehydration stage releases ~ 25 % of the total water loss from the metabasalt$_{(a)}$ ~~altered MORB~~ (~ 4.0 vol% H_2O liberated) and ~ 45 % from the metabasalt$_{(h)}$~~fresh MORB~~ (~ 6.5 vol% H_2O liberated). The second significant pulse in the metabasalts~~MORBs~~ occurs at 620 – 640 °C and 2.36 – 2.42 GPa, releasing ~ 40 % of the total water loss from the metabasalt$_{(a)}$~~altered MORB~~ and ~ 15 % from the metabasalt$_{(h)}$~~fresh MORB~~. This pulse is caused by the final breakdown of lawsonite and of amphibole in the metabasalt$_{(a)}$ ~~and in the altered MORB of amphibole~~ (Fig. 3b). In the metabasalt$_{(h)}$~~the fresh MORB~~, glaucophane and actinolite breakdown takes place at 600 °C and 2.~~03~~ 30 GPa~~,~~. Growth of talc only incorporates half of the water released by amphibole breakdown, causing an intermediate fluid pulse of minor magnitude at these *P-T* conditions (Fig. 3a). If an initial undersaturated basaltic composition was considered, the amount of released fluid due to breakdown of hydrous phases would be smaller.~~causing an intermediate fluid pulse of minor magnitude (Fig. 3a).~~

The metasediment$_{(c)}$ ~~carbonate sediment~~ is the rock-type~~composition~~ that dehydrates the least: the two main pulses of fluid production are at 480 °C and 1.92 GPa (~ 0.4 vol% H_2O liberated) and from 540 °C and 2.12 GPa to 560 °C and 2.18 GPa (~ 1.7 vol% H_2O liberated), caused by breakdown of glaucophane and lawsonite respectively (Fig. 3c). The water produced from these two dehydration stages represents < 0.02 wt% of the total water released by the system composed of metabasalt$_{(h)}$ and metasediment$_{(c)}$. ~~by fresh MORB and carbonate sediment.~~ In the metasediment$_{(t)}$, ~~terrigenous sediment~~ the main fluid pulse occurs at 520 °C and 2.06 GPa (~ 3.0 vol% of H_2O liberated), caused by the breakdown of lawsonite and a decrease of glaucophane abundance~~of glaucophane at the expense of garnet and clinopyroxene growth~~ (Fig. 3d). The water produced from this dehydration stage represents ~ 0.07 wt% of the total water released by the system composed of metabasalt$_{(a)}$ and metasediment$_{(t)}$~~by altered MORB and terrigenous sediment~~.

As specified in section 2.2, the aqueous fluid used for the calculation considers only the water component (a_{H2O} = 1). Release of CO_2 occurs during progressive metamorphism of metabasalt$_{(a)}$ and metasediment$_{(c)}$. CO_2 is absent or present in negligible amount (< 1 mol% of the total fluid) up to 440 °C and 1.76 GPa. At higher temperatures, the X(CO_2) content increases significantly up to ~ 10 mol% in the fluid released by metabasalt$_{(a)}$ and ~ 30 mol% in the fluid released by metasediment$_{(c)}$ at 700 °C and 2.60 GPa. However, the total amount of fluid produced at these conditions is negligible (< 0.01 vol%). The oxygen isotope fractionation database used for this study (Vho et al., 2020) does not include fractionation data for CO_2. Limited calibrations are available for oxygen isotope fractionation between H_2O and CO_2 (Friedman and O'Neil, 1977; O'Neil and Adami, 1969; Zheng, 1994). The fractionation values diverge significantly, for example between -4.9 ‰ and -8.3 ‰ at 450 °C, and between 1.5 ‰ and -4.4 ‰ at 700 °C. At 520 °C, the fluid released by metabasalt$_{(a)}$ contains 2 mol% of CO_2 and 6 – 7 mol% at 620 – 640 °C. The consideration of CO_2 would produce a negligible shift on the fluid $\delta^{18}O$ (0.1 – 0.2 ‰ at 520 °C and 0.0 – 0.6 ‰ at 620 °C, depending on the calibration used). The amount of CO_2 in metasediment$_{(c)}$ derived-fluid is 2 mol% at 480 °C and 5 mol% at 540 °C. The consideration of CO_2 would also produce negligible to minor shifts in the fluid $\delta^{18}O$ (0.1 – 0.3 ‰ at 480 °C and 0.2 – 1.1 ‰ at 620 °C, depending on the calibration).

3.3 Oxygen isotope compositions

The largest initial bulk $\delta^{18}O$ difference occurs between metabasalt$_{(h)}$ and metasediment$_{(c)}$ ~~fresh MORB and carbonate sediment~~ (14.3 ‰, the relatively ~~dry~~ water-poor system), while the smallest initial bulk $\delta^{18}O$ difference is observed between metabasalt$_{(a)}$ and metasediment$_{(t)}$ ~~altered MORB and terrigenous sediment~~ (6.0 ‰, the relatively ~~wet~~ water-rich system). In the following, the results are presented in details for a selection of two end-member scenarios (Fig. 4, 5): (1) metasediment$_{(c)}$ associated to metabasalt$_{(h)}$ and (2) metasediment$_{(t)}$ associated to metabasalt$_{(a)}$ ~~(1) carbonate sediment associated to fresh MORB and (2) terrigenous sediment associated to altered MORB~~ when not specified differently. Other scenarios (i.e., metabasalt$_{(h)}$ associated to metasediment$_{(t)}$ and metabasalt$_{(a)}$ associated to metasediment$_{(c)}$~~fresh MORB associated with the terrigenous sediment and altered MORB associated with the carbonate sediment~~) give intermediate results in terms of oxygen isotope composition variations as consequence of fluid/rock interaction. Further details and the results for the intermediate scenarios are given in Supplementary Material S3.

3.3.1 Bulk oxygen isotope compositions

For rocks that undergo only dehydration reactions the staritng bulk $\delta^{18}O$ evolves as consequence of garnet and fluid fractionation (~~black solid lines in~~ Fig. 4). The bulk $\delta^{18}O$ shift related to water fractionation is within 0.2 ‰, while the shift due to garnet fractionation is within 0.5 ‰ (Fig. 4c,d). Since water has typically heavier $\delta^{18}O$ ~~signature~~ with respect to the bulk and the garnet a lighter one, the two effects produce opposite trends. The combination of both effects results in a shift of the bulk $\delta^{18}O$ in the considered lithologies restricted to < 0.3 ‰. This in turn leads to negligible (< 0.2 ‰) variations in the $\delta^{18}O$ values of the stable phases.

In the metasediments, the progressive interaction with the fluid from the metabasalts ~~mafic rocks~~ causes a decrease in the bulk $\delta^{18}O$ (Fig. ~~4g,h~~5) that is controlled by the amount and $\delta^{18}O$~~signature~~ of the incoming fluid. A significant decrease starts at 480 °C, where the amount of water released by the metabasalts ~~mafic rocks~~ increases of about one order of magnitude from < 0.05 vol% to ~ 0.3 vol% due to partial consumption of amphiboles and lawsonite. The maximum shift in bulk $\delta^{18}O$ was calculated for the metasediment$_{(c)}$~~carbonate~~ interacting with the metabasalt$_{(h)}$~~fresh MORB~~ at ~~~~ 12.9 ‰ for the *HI* case (integrated F/R ratio = 0.75 kg/kg), while it is ~~~~ 8.7 ‰ for the *PI* case (integrated F/R ratio = 0.38). The shift of the bulk $\delta^{18}O$ of the metasediment$_{(t)}$~~terrigenous sediment~~ interacting with the metabasalt$_{(a)}$~~altered MORB~~ is ~~~~ 1.5 ‰ for the *HI* case (integrated F/R ratio = 0.35) and ~~~~ 2.7 ‰ for the *PI* case (integrated F/R ratio = 0.18).

3.3.2 Oxygen isotope composition of mineral phases

Since at infinite temperature the fractionation between any two phases approaches 0 ‰, a general trend of reduction of oxygen isotope fractionation between the stable phases with increasing metamorphic grade is observed in all lithologies and is a result of the temperature increase (~~coloured lines in~~ Fig. 4a,b,e,f). As a consequence, mineral phases typically heavier than the bulk (i.e. quartz and carbonates) become isotopically lighter with increasing metamorphic conditions, and the mineral phases typically lighter than the bulk (i.e. rutile, garnet and titanite) become isotopically heavier. Such variations are limited (i.e. within 1.0 ‰) for most of the phases, with the exception of quartz, calcite and rutile that may vary up to 3.0 ‰ in response to temperature variation only in the considered range.

In the case of ingress of the low $\delta^{18}O$ fluid from the metabasalts in the metasedimentary ~~MORB in the sedimentary~~ rocks (*PI* and *HI* cases), the mineral $\delta^{18}O$ values decrease progressively with respect to the *NI* case following the trend of the bulk $\delta^{18}O$ (Fig. ~~4g,h~~5). For instance, in case of *NI* the $\delta^{18}O$ of quartz in the metasediment$_{(t)}$~~terrigenous sediment~~ decreases from 19.4 ‰ to 17.3 ‰ (~~–~~2.1 ‰) and of quartz in the metasediment$_{(c)}$~~carbonate sediment~~ from 28.0 ‰ to 26.5 ‰ (-1.5 ‰) over the total temperature range modelled~~because of increasing temperature~~. In the *PI* and *HI* cases, the $\delta^{18}O$ shift of quartz is respectively -3.8 ‰ and -5.0 ‰ in the metasediment$_{(t)}$~~terrigenous sediment~~, and -10.0 ‰ and -13.9 ‰ in the metasediment$_{(c)}$~~carbonate sediment~~. Hence, the

final quartz $\delta^{18}O$ values (at 700 °C, 2.60 GPa) for the *HI* case in the metasediment$_{(t)}$ and in the metasediment$_{(c)}$~~terrigenous and in the carbonated sediment~~ are respectively 3.0 ‰ and 13.0 ‰ isotopically lower than the expected values in case of *NI* (Fig. ~~4c h~~5). The maximum shift of $\delta^{18}O$ (i.e. between *NI* and *HI* cases) for the other stable phases is within those values. In the metasediment$_{(t)}$~~terrigenous sediment~~, the $\delta^{18}O$ values of phengite, galucophane, jadeite, rutile and garnet decrease by 3.0 ‰ and of omphacite by 2.4 ‰ from the *NI* to the *HI* case. Lawsonite and titanite are not stable after the first significant input of metabasalt-derived fluid ~~mafic fluid input~~ (500 °C, 2.00 GPa), and their $\delta^{18}O$ values decrease ~~of~~ by 1.1 ‰ and 0.3 ‰ respectively from the *NI* to the *HI* case. In the metasediment$_{(c)}$~~carbonate sediment~~, the $\delta^{18}O$ values of dolomite, jadeite, phengite, rutile and aragonite decrease ~~of~~ by a maximum of 13.1 ‰, of lawsonite and ankerite ~~of~~ by a maximum of 10.3 ‰ and 9.5 ‰ respectively. Garnet crystallizes only between 540 °C and 580 °C and its $\delta^{18}O$ value in the *HI* case is 5.9 ‰ lower than the one in the *NI* case.

3.3.3 Oxygen isotope composition of the fractionated fluids

The $\delta^{18}O$ of the fractionated water from each rock type at each step is in isotopic equilibrium with the stable mineral assemblage at the given conditions. In the temperature range where ~~the~~ most of the fluid is released (i.e. T -> 480 °C), the $\delta^{18}O$ of the ~~mafic~~ fluid is 7.0 ± 0.5 ‰ for the metabasalt$_{(h)}$~~fresh MORB~~ and 10.0 ± 0.5 ‰ for the metabasalt$_{(a)}$~~altered MORB~~. At T > 480 °C, the water released in the *NI* case by the metasediment$_{(c)}$~~carbonate sediment~~ has a $\delta^{18}O$ = 24.2 – 25.6 ‰ and from the metasediment$_{(t)}$~~terrigenous sediment~~ of 15.4 – 16.4 ‰ (Fig. ~~5~~6). The $\delta^{18}O$ of the fluid leaving the system, e.g.~~,~~ infiltrating an upper layer or the mantle wedge, results from the mixing of the water released from the metabasalts~~MORB~~ and the overlying metasediments, and it derives from the balance between the amount of fluid released by each rock type and its $\delta^{18}O$ value (~~blue lines in~~ Fig. ~~5a~~6a,b).

In the *NI* case, the $\delta^{18}O$ of water leaving the system is up to 1 ‰ higher than the composition of the fluid released by the metabasalt~~MORB~~ because of the minor input from the metasediment at around 500 – 550 °C. The only exceptions are for the interaction between the metabasalt$_{(a)}$ and the metasediment$_{(t)}$~~altered MORB and the terrigenous sediment~~ at T of ~ 450 °C and ~ 700 °C. At these conditions, the $\delta^{18}O$ values of the final fluid are up to 5 ‰ higher than the metabasalt$_{(h)}$-derived ~~mafic~~ fluid (~~thick dark blue line in~~ Fig. ~~5b~~6b). This increase is caused by a proportion in favour of the metasediment-derived ~~sedimentary~~ fluid~~s~~ at those conditions; however, the amount of high-$\delta^{18}O$ fluid represents < 0.1 wt% of the rock column and ~ 1 wt% of the total released fluid (~~grey field in~~ Fig. ~~5b~~6b).

In the case of interaction between the metasediments and the metabasalt-derived~~mafic~~ fluid, part of or all ~~the mafic~~this fluid reacts with the overlying metasediments~~sediment~~ before leaving the system. The~~and the~~ final $\delta^{18}O$ ~~signature~~ of the fluid is controlled by the integrated F/R ratio~~mafic fluid/rock ratio~~ in the metasediments and their buffering capacity. In the *HI* case, the $\delta^{18}O$ of the released fluid has a dominant sedimentary signature at T < 500 – 520 °C, before the first fluid pulse from the ~~MORBs~~ metabasalts ~~(T < 500 – 520 °C)~~ (14.5 – 15.5 ‰ for the metasediment$_{(t)}$~~terrigenous sediment~~ and 23.0 – 24.0 ‰ for the metasediment$_{(c)}$~~carbonate sediment~~, ~~light blue lines in~~ Fig. ~~5~~6). The first metabasalt-derived~~mafic~~ fluid pulse (500 – 520 °C, see above) causes a drop in the bulk $\delta^{18}O$ values of the total released fluids of 0.7 ‰ for the metabasalt$_{(a)}$/metasediment$_{(t)}$~~altered MORB/terrigenous sediment~~ association and of 6.3 ‰ for the metabasalt$_{(h)}$/metasediment$_{(c)}$~~fresh MORB/carbonate sediment~~ association. The second metabasalt-derived~~mafic~~ fluid pulse (620 – 640 °C, see above) causes a second decrease of the $\delta^{18}O$ values of the total released fluid equal to 1.0 ‰ for both the lithological associations.

3.3.4 Input of serpentinite-derived fluid~~ultramafic fluid~~

Ultramafic rocks tend to undergo episodic dehydration (see above). In the following, the effects caused by the input of a serpentinite-derived~~an ultramafic~~ fluid at the base of the rock column in case of *HI* are described (Fig. ~~6~~7). ~~In the *PI* and *NI* cases, the effect of the ultramafic fluid on the MORB remains the same, while the variations in the sedimentary rocks will decrease to zero (Supplementary Material S3).~~ The input of the amount of water corresponding to the dehydration of 150 m of pure serpentine

at 480 °C (2.0 wt% H_2O) and 660 °C (6.5 wt% H_2O) having a $\delta^{18}O$ = 4.5 ‰~~,~~ (see above) produces a decrease of < 0.2 ‰ in the final bulk $\delta^{18}O$ of the ~~MORBs~~metabasalts, up to ~ 1.0 ‰ in the metasediment$_{(c)}$~~carbonate sediment~~ (Fig. ~~6a~~7a) and of < 0.5 ‰ in the metasediment$_{(t)}$~~terrigenous sediment~~ (Fig. ~~6b~~7b) with respect to the *HI* case with~~out~~ no serpentinite-derived~~ultramafic~~ fluid. The largest decrease occurs at 660 °C, where the second pulse of serpentinite-derived~~ultramafic~~ fluid enters the system, resulting in ca. -0.1 ‰, -0.3 ‰ and -1.0 ‰ for the metabasalts, metasediment$_{(t)}$ and metasediment$_{(c)}$ $\delta^{18}O$ bulk values, respectively (Fig. 7)~~for the MORBs, the terrigenous sediment and the carbonate sediment respectively (Fig. 6)~~. Even by increasing the thickness of the serpentinite by a factor of two, the variations in bulk $\delta^{18}O$ values with respect to the *HI* case with no serpentinite-derived fluid are < 1.0 ‰ for any rock type with the exception of the metasediment$_{(c)}$~~carbonate sediment~~, for which the bulk $\delta^{18}O$ decreases ~~of~~ by 2.0 ‰ with respect to the serpentinite-derived~~ultramafic~~ fluid-absent *HI* case (Supplementary Material S3). The effect of the serpentinite-derived fluid on the metabasalts remains the same for any interaction case (*NI*, *PI* and *HI*), while the variations in the $\delta^{18}O$ of metasedimentary rocks decreases to zero with decreasing infiltration of external fluid (Supplementary Material S3).

4 Discussion

4.1 Effect of stable assemblage evolution and phase fractionation on the bulk $\delta^{18}O$

The changes in mineral assemblage, modes and compositions along a prograde *P-T* path control (1) the oxygen isotope partitioning between the stable phases and (2) the amount and $\delta^{18}O$ of the ~~water~~ fluid released by the system. At the same time, oxygen isotope fractionation between the stable phases is controlled by temperature. Thus, the effects of evolving paragenesis and increasing temperature are systematically overlapping in nature. In the case of a closed system, the bulk concentrations of ^{18}O and ^{16}O remain constant and a change in one phase is compensated exactly by adjustments in other phases (Baumgartner and Valley, 2001; Kohn, 1993). In this situation, major changes in mineral assemblage do not play a significant role in shifting the $\delta^{18}O$ of stable phases: this is demonstrated by the limited (< 0.5 ‰) shift in $\delta^{18}O$ values of quartz, garnet, phengite, omphacite and rutile in the metabasalt$_{(h)}$~~MORB~~ after (1) the breakdown of amphibole and lawsonite and (2) the crystallization of talc and kyanite over a narrow ~~T~~ temperature range between 500 and 580 °C (Fig. 4a,b).~~-~~ Similar effects can be anticipated also for rocks with different chemical composition that undergo major changes in the mineral assemblage (see Supplementary Material S4).~~The limited effect of changing assemblages on the variation in oxygen isotope composition can be evaluated with an extreme example. A granite composed of quartz + K feldspar + plagioclase + biotite + accessory ilmenite and zircon at 700 °C and 0.3 GPa is subducted to 700 °C and 2.5 GPa. If lack of hydration prevents the rock from re-equilibration, the granite can preserve a metastable mineral assemblage during subduction. Assuming a pervasive hydration at 700 °C and 2.5 GPa, a re-equilibration into a full eclogite facies assemblage of quartz + white mica + garnet + clinopyroxene + accessory rutile and zircon occurs. The temperature was kept constant in order to remove any T related effect and the fluid was assumed to be in equilibrium with the mineral assemblage. Quartz $\delta^{18}O$ variation between the two parageneses, as well the difference between ilmenite and rutile $\delta^{18}O$, are within 1 ‰.~~

In a closed system evolving at equilibrium, the initial chemical bulk composition and bulk $\delta^{18}O$ do not change along the *P-T* evolution. However, in metamorphic rocks, compositional zoning and metamorphic overgrowths are often preserved in refractory minerals (Lanari and Engi, 2017) indicating that parts of the minerals became isolated from the reactive volume of the rock. This scenario is commonly referred to as *partially re-equilibrated open systems*, because the chemical and the isotopic compositions vary as a consequence of fractionation of solid and fluid phases (i.e. garnet fractionation and excess fluid removal) even in absence of external fluid input. Phase fractionation is expected to affect the bulk $\delta^{18}O$ as function of both the amount of fractionated or expelled phases and their isotopic composition. Fractionation of a phase lighter than the bulk in $\delta^{18}O$ leads to an increase ~~in~~ of the reactive bulk $\delta^{18}O$ value, while fractionation of an isotopic heavier phase leads to a decrease ~~in~~ of the reactive bulk $\delta^{18}O$ value.~~-~~ The most common example of fractionating metamorphic mineral is garnet, which systematically records compositional zonation at low- to medium-grade (Evans, 2004; Giuntoli et al., 2018; Konrad-Schmolke et al., 2008; Spear, 1988;

Tracy, 1982). Therefore, garnet fractionation was incorporated in the model in order to better approximate the behaviour of natural systems. Note that this effect is reduced at higher grade where intra-crystalline diffusion becomes efficient to partially re-equilibrate garnet (Caddick et al., 2010; Lanari and Duesterhoeft, 2018). As already documented by Konrad-Schmolke et al. (2008), garnet fractionation controls the ~~extend~~ extent of the garnet stability field. Garnet crystallization is not systematically expected to occur near the peak conditions, if the matrix was strongly depleted due to garnet fractionation and the volume of garnet remains constant (i.e. for the metabasalt$_{(a)}$~~altered MORB composition~~, Fig. 3b). While garnet fractionation is recognized to significantly affect isopleth thermobarometry and volume fractions (Lanari and Engi, 2017), its effect on oxygen isotope bulk composition and partitioning is negligible (< 0.5 ‰) in all the studied lithologies. In the model, the garnet fraction varies from ~ 5 vol% in the metasediment$_{(c)}$~~the carbonate sediment~~ to ~ 35 vol% in the metabasalt$_{(h)}$~~fresh MORB~~ (Fig. 3) and its $\delta^{18}O$ is 0.8 to 1.7 ‰ lower than the bulk (Fig. 4a,b,e,f). Beside garnet fractionation, dehydration due to hydrous mineral breakdown and expulsion of excess water may contribute to changing the starting chemical and isotopic bulk compositions. Baumgartner and Valley (2001) postulated that the liberation of metamorphic fluids might have a profound effect on the stable isotope composition of the residual rock. In the present study, the maximum fluid loss is from the ~~MORBs~~ metabasalts that release ~ 15 vol% (~ 5 wt%) of H_2O with $\delta^{18}O$ values 0.9 to 1.5 ‰ higher than the bulk rock (Fig. 4a,b) at $T \geq 500$ °C. This significant fluid flux produces a decrease in the bulk $\delta^{18}O$ of less than 0.2 ‰ (Fig. 4c,d). Even if more extensive dehydration occurs, the effect on the ~~value of~~bulk $\delta^{18}O$ value will be typically lower than 1.0 ‰. No significant differences in the effect of stable assemblage evolution and phase fractionation are observed between the four lithologies. Therefore, the bulk $\delta^{18}O$ of a rock that experienced a succession of dehydration reactions, without rehydration by external fluids or major compositional changes through decarbonation or mineral dissolution, is likely to be representative of its protolith composition. In this regard, integrated thermodynamics and oxygen isotope modelling represents a key tool for quantifying the potential effects of different processes and for assessing closed or open system behaviours.

4.2 Mineral $\delta^{18}O$ zoning as indicator of open system behaviour

In the last decades, the significant advances of oxygen stable isotope analyses by SIMS (secondary ion mass spectrometer) allowed zoned metamorphic minerals to be analysed in situ with a precision down to 0.2 – 0.3 ‰ (2σ) (e.g., Ferry et al., 2014; Martin et al., 2014; Page et al., 2010). The magnitude of the intra-crystalline $\delta^{18}O$ variation in key metamorphic minerals has been widely used to target whether a metasomatic stage is related to an internal fluid deriving from the breakdown of hydrous phases or if it reflects equilibration with an external fluid of different isotopic composition (e.g., Putlitz et al., 2000; Errico et al., 2013; Page et al., 2013; Russell et al., 2013; Martin et al., 2014; Rubatto and Angiboust, 2015; Engi et al., 2018). Understanding the scale of fluid migration at depth and the magnitude of the interaction between fluids and minerals is of special interest and can be enhanced by modelling of such fluid flow and isotopic exchange (Baumgartner and Valley, 2001). The definition of different *interaction cases* (*NI*, *PI*, *HI*) is useful to represent various degrees of isotopic exchange between the fluid and the rock. If the flow is channelized, all the *interaction cases* can possibly occur in close proximity and the modelled scenarios can be linked to the evolution of different domains around the vein (Fig. ~~7~~8). The flow of a pervasive fluid leads to homogenization of the chemical potential of all components, including stable isotopes (Baumgartner and Valley, 2001), and it is represented by the *HI* case, as long as integrated fluid/rock ratios are high. In contrast, the flow of a channelled fluid results in local chemical heterogeneities, allowing some portions of the rock and of the fluid to remain unaffected (*NI* case) and some other to be only partially affected (*PI* case).

The first step for a meaningful interpretation of an observed intra-grain variation in $\delta^{18}O$ value is the quantification of the possible effects of changes in *T* and mineral assemblage. Such effects are characteristic of each phase (Fig. 4a,b,e,f). Quartz, calcite and rutile are the most sensitive minerals to ~~such~~ temperature changes. Their composition is expected to vary up to 1 ‰ per 100 °C and they are stable over a wide range of temperature. For such phases, care is required in interpreting significant intra-grain $\delta^{18}O$ variations (i.e. up to 3.0 ‰) since it does not necessarily reflect interaction with an external fluid having a different isotopic ~~signature~~composition. However, quartz and calcite are not necessarily robust minerals that can preserve chemical and isotopic

zoning during metamorphism. On the other hand, the variation in $\delta^{18}O$ value over 150 °C in a mineral such as garnet that commonly retains growth zoning is typically within 0.5 ‰ when no phase fractionation is involved and still less than 1.0 ‰ when considering the effect of previous garnet and/or excess fluid fractionation (Fig. 4a,b,e,f). ~~However, the variation of garnet $\delta^{18}O$ over 150 °C is typically within 0.5 ‰ when no phase fractionation is involved and still less than 1.0 ‰ when considering the effect of previous garnet and/or excess fluid fractionation (Fig. 4a,b,e,f).~~ Thus, any larger variation has to be linked to a significant change in bulk $\delta^{18}O$. Similar behaviour is observed for other key metamorphic minerals such as ~~white mica~~phengite, amphibole and clinopyroxene. These minerals have been widely used in metamorphic petrology as thermometers and geobarometers (Dubacq et al., 2010; Ferry and Spear, 1978; Parra et al., 2002) and are expected to be robust targets to link the fluid evolution along the *P*–*T* path, especially when mineral relics are preserved. Due to its large capacity to preserve growth chemistry, garnet has been a primary target for microscale measurement of oxygen isotopes. Protocols and reference materials for SIMS measurements for a range of garnet compositions are well established (e.g., Martin et al., 2014; Page et al., 2010; Vielzeuf et al., 2005b) and its retentivity to high *T* resetting by diffusion has been investigated (Higashino et al., 2018; Vielzeuf et al., 2005a). In HP rocks, various degrees of intragrain variations in garnet $\delta^{18}O$ associated to external fluid infiltration have been reported in literature. Where field constraints on the fluid source (i.e. oxygen isotope measurements on the feasible source lithologies) are available, the intragrain variation can assist in the calculation of F/R ratios. Martin et al. (2014) describe a shift of -2.5 ‰ associated to infiltration of serpentinite- or altered gabbro-derived fluids in metasediments from the continental basement in Corsica. Rubatto and Angiboust (2015) observed a shift of 3.5 – 4.0 ‰ in garnet from an eclogite from Monviso that they attributed to sediment-derived fluid infiltration. Vielzeuf et al. (2005b) measured a decrease of 2.5 – 3.0 ‰ between garnet core and rim in the Dora Maira gneiss probably caused by the interaction with a fluid derived from the whiteschists (Gauthiez-Putallaz et al., 2016). Studies that used in-situ measurement of micas are limited (Bulle et al., 2019; Siron et al., 2017) and thus the potential of mica to trace fluid-rock interaction is still underexplored. The matrix complexity of pyroxenes and amphiboles remains a challenge for SIMS measurements.

4.3 Interaction with fluids from an ultramafic source

The effect of pervasive fluid flow deriving from the breakdown of serpentine ~~serpentine breakdown~~ ($\delta^{18}O$ = 4.5 ‰) in a serpentine layer of different thicknesses (150 m, 300 m, 600 m, see above) on the bulk $\delta^{18}O$ of the two metabasalts is negligible~~on the bulk $\delta^{18}O$ of the fresh and altered MORBs calculated for different thicknesses of pure serpentine (150 m, 300 m, 600 m, see above) is negligible~~ (< 0.5 ‰, Fig. ~~6~~7, Supplementary Material S3). This is mainly due to (1) the minor difference in $\delta^{18}O$ between the serpentinite-derived~~ultramafic~~ fluid and the metabasalts~~MORB~~ (1.2 ‰ for the $metabasalt_{(h)}$ ~~fresh MORB~~ and 4.5 ‰ for the $metabasalt_{(a)}$~~altered MORB~~) and (2) the very low integrated F/R ratio (0.01, 0.02 and 0.04 for the 3 cases). In this case, the integrated F/R ratio~~The latter~~ seems to play a bigger role, since the limited change in $\delta^{18}O$ is similar for both the metabasalts~~MORBs~~ even if the initial $\Delta^{18}O$ between fluid and rock is larger for the $metabasalt_{(a)}$~~difference in $\delta^{18}O$ between input fluids and receiving rock is larger for the altered MORB~~. With the same total volume of fluid and rock, a channelized fluid flow would imply larger volumes of fluid interacting with smaller volumes of rock (higher ~~fluid/rock~~F/R ratios) and would thus be expected to drive larger variations in isotopic composition. For instance, by increasing ~~of~~ by a factor of 10 the F/R ratio (from 0.01 to 0.1) the bulk $\delta^{18}O$ decreases of 0.6 ‰ ($metabasalt_{(h)}$) and 1.1 ‰ ($metabasalt_{(a)}$) upon infiltration of the serpentine-derived fluids.~~the fresh and altered MORB bulk $\delta^{18}O$ decreases of 0.6 ‰ and 1.1 ‰ respectively.~~

In contrast to the metabasaltic~~MORB~~ layers, the overlying metasediments have (1) larger compositional differences with the serpentinite-derived~~ultramafic~~ fluid and (2) a smaller mass. The effect of the serpentinite-derived fluid input at the base of the column on the metasediment bulk $\delta^{18}O$ compositions can be up to 10 times larger than the effect that the same amount of fluid has on basaltic compositions. This is the case even when the serpentinite-derived fluid completely equilibrates with the metabasalt before interacting with the overlying metasediment. In our model, the fluid infiltrating the metasediment is always a mixture of metabasalt-derived and serpentinite-derived fluid. Considering instead an input of serpentinite-derived fluid directly in the

metasediment and applying a F/R ratio of 0.1, the final bulk $\delta^{18}O$ of the metasediment$_{(c)}$ decreases of 4.6 ‰ and of the metasediment$_{(t)}$ of 2.6 ‰. These values are significant and are comparable with variations observed in natural samples. For instance, Martin et al. (2014) describe a shift in $\delta^{18}O$ of -2.5 ‰ among different generations of HP garnet in a sample from the Corsica continental basement (garnet mantle $\delta^{18}O$ = 7.2 ± 0.4 ‰, garnet rim $\delta^{18}O$ = 4.7 ± 0.5 ‰). The authors associate this shift to an infiltration of serpentinite-derived fluids and, to a lesser extent, altered gabbro-derived fluid. Williams (2019) describe an extreme $\delta^{18}O$ shift of -15 ‰ between garnet core and rim in a metasediment from the Lago di Cignana Unit. Such an oxygen isotope composition variation has been related to a strongly channelized fluid influx originated from the dehydration of serpentinites. ~~The consequence is that the effect of the ultramafic fluid input on the sediment bulk $\delta^{18}O$ compositions can be up to 10 times larger than in the MORBs, even when the ultramafic fluid completely equilibrates with the MORBs before interacting with the sediments. By applying a F/R ratio of 0.1, the final bulk $\delta^{18}O$ of the carbonate sediment decreases of 4.6 ‰ and of the terrigenous sediment of 2.6 ‰.~~ These results demonstrate that~~These values are significant and demonstrate how~~ metasediments can be a good target to detect fluids from an ultramafic source migrating upward through the subducting slab or along the subduction interface, even though the two lithologies may not be in direct contact in the field.

It is important to note that the relatively water-poor ~~"dry"~~ system composed by the metabasalt$_{(h)}$ and the metasediment$_{(c)}$ ~~fresh MORB and carbonate sediment~~ is more sensitive to external fluid infiltration and thus affected by the highest changes in $\delta^{18}O$, according with observation in natural systems (e.g., Page et al., 2019).

4.4 Effect of the subduction geotherm

As discussed in detail by previous studies (Baxter and Caddick, 2013; Hacker, 2008; Hernández-Uribe and Palin, 2019; Syracuse et al., 2010), the subduction geotherm has an important effect on hydrous phase stability and *P-T* conditions of fluid release into the mantle wedge. Along the average D80 geotherm by Syracuse et al. (2010) (Fig. 2), the top of the slab crust releases ~ 95% of the water at ~ 80 km, during the transition from partial to full coupling. Along the cold geotherm by Penniston-Dorland et al. (2015), the first significant fluid pulse (20 – 40 % of water released) occurs as a consequence of the breakdown of glaucophane and actinolite at greater depths than predicted by our model (~ 500 °C and 2.7 – 2.8 GPa, 90 – 100 km depth), and the remaining water is released at depth > 100 km. Both those models imply a relatively dry mantle forearc region, contradicting what has been described by Bostock et al. (2002). By contrast, along the warm geotherm by Penniston-Dorland et al. (2015), the breakdown of chlorite, epidote and actinolite releases 40 – 50 % of the water at 460 – 470 °C and ~ 0.6 GPa (~ 20 km depth); after this stage, ~ 95 % of the water is released at depth < 70 km. This implies that little to no water is available at subarc depths. The average geotherm by Penniston-Dorland et al. (2015) is hotter than the one by Gerya et al. (2002) used in our model for T < 650 °C and P < 2.5 GPa (Fig. 2). Along this *P-T* gradient, chlorite is the main water carrier at low ~~depths~~ grade conditions and the first two main dehydration pulses occur at depths of 30 – 40 km (significant decrease of chlorite, 20 – 25 % of water released) and of ~ 50 km (complete breakdown of chlorite, 20 – 25 % of water released). Along this geotherm, the most water is released at shallower depths than in our model. Differences can be investigated in detail by modelling each case with PTLOOP. Nevertheless, the effects of fluid-rock interaction on the bulk and mineral $\delta^{18}O$ compositions follow the general trends described above. Different parageneses are expected to form during hydration, but the shift in bulk $\delta^{18}O$ remains constrained by the F/R ratio and the isotopic composition of the incoming fluid.

4.5 Implication for mantle-wedge hydration

Infiltration of the slab-derived fluid into the mantle wedge is important for subduction zone settings because mantle minerals are strongly depleted in volatiles. At equilibrium, a free aqueous fluid is not stable in the mantle wedge at T < 650 °C until a fully hydrated mineral assemblage has formed (i.e. serpentine, chlorite, talc, and amphibole) (Manning, 2004). As shown above, the *P-T* conditions of H_2O release from the subducting slab, as well as the volume and the $\delta^{18}O$ of the liberated H_2O can vary according

to the geometry of the subduction zone and the composition of the subducting lithosphere (e.g., Hacker, 2008; Hernández-Uribe and Palin, 2019; Poli and Schmidt, 2002). The program PTLOOP allows the *P-T* conditions, amount and oxygen isotope composition of the released fluid to be calculated for the system of interest. The presented model uses an intermediate *P-T* gradient that stabilizes lawsonite and results in a first significant fluid pulse at 65 – 70 km depth and a second pulse at ~ 80 km depth. Below that depth, phengite is the main carrier of H_2O. This implies that the majority of fluid is released in the forearc region, in agreement with previous studies investigating the dehydration of basaltic~~MORB~~ and sedimentary components of the slab (e.g., Baxter and Caddick, 2013; Kerrick and Connolly, 2001; Schmidt and Poli, 1994).

The influence of the slab-derived fluid on (1) the degree of hydration and (2) the $\delta^{18}O$ modification of the overlying mantle rocks was estimated on the basis of the results presented above. A slab composed by the metabasalt$_{(a)}$ and the metasediment$_{(t)}$ ~~altered MORB and terrigenous sediments~~ (left column in Fig. 1a, assuming the real thickness of the slab to be 3 times the modelled one) subducting at 1 cm/y was considered (Fig. ~~8a~~9a)~~. This~~. This subduction rate represents a conservative estimate, considering that previous averages have proposed 4 – 5 cm/y ~~an average of 4 – 5 cm/y~~ (Stern, 2002).~~ Any faster subducting rate may shorten the timescale of the processes discussed below, allowing larger fluid fluxes in the mantle wedge over the same interval.~~ Mechanical decoupling between the slab and the wedge, and steady state cold mantle wedge are assumed (e.g., Abers et al., 2006; Hirauchi and Katayama, 2013; Wada et al., 2008). The fluid released by the slab at 500 – 520 °C with a characteristic $\delta^{18}O$ = 15.0 ‰ (Fig. ~~5a~~6a) was let infiltrate in an initially dry peridotite (composition KLB-1 from Walter, 1998, simplified to the FMAS system, Table S2.4 in Supplementary Material S2) with *T* = 570 °C and an initial $\delta^{18}O$ = 5.5 ‰ (Eiler et al., 1997; Mattey et al., 1994). This simplified model ignores the dynamics of fluid infiltration and assumes pervasive flow. Given the column length of 1 m, a subduction rate of 1 cm/y implies that any fixed point (i.e. fixed *P-T* conditions) at the slab/mantle interface receives in 100 years the total amount of fluid that a single column can liberate at those conditions. Hence, in this example 4892.6 kg of water/100 years (i.e. the amount released by the considered column at the chosen conditions, see above) infiltrate the mantle wedge. The released fluid first interacts with a small volume at the slab-mantle interface (V1 1000 x 1000 x 1 m, Fig. ~~8b~~9b) and once it has equilibrated and saturated V1, it infiltrates volume V2 (3000 x 2000 x 1 m, Fig. 9b). Both~~Fig. 8b). Both~~ the volumes were scaled to 1:3 for the calculation in order to maintain the volume proportion with the modelled slab. The slab-derived fluid, which is in continuous supply during subduction of new material, infiltrates V1 and causes a progressively change in mineralogy from olivine + orthopyroxene + garnet to serpentine + chlorite + minor olivine until the rock reaches saturation after 0.35 Myr of subduction. At this stage, V1 has a bulk $\delta^{18}O$ of ~ 8 ‰ that is significantly higher with respect to the initial mantle value (Fig. 9c). With~~(Fig. 8c). With~~ ongoing subduction, the continuing release of water from new slab material under a static mantle drives the $\delta^{18}O$ of the volume of mantle wedge toward higher values. The water that will infiltrate V2 has a $\delta^{18}O$ that depends on (1) the $\delta^{18}O$ of the slab-derived water and (2) the buffering capacity of V1. The same changes in mineral assemblage described for V1 occur also in V2, while the bulk $\delta^{18}O$ of V2 increases more moderately than the one of V1 and reaches a $\delta^{18}O$ of ~ 6 ‰ after 0.75 Myr of subduction (Supplementary Material S4).

In the proposed model, most of the fluid is released by the slab at forearc depths. However, in most subduction zones no melting appears to occur in the forearc region and the serpentinite acts as the effective H_2O-absorber (Iwamori, 1998), recording the possible variation in $\delta^{18}O$ induced by the slab-derived fluid. Progressive oceanward migration of the slab ("slab rollback") has been considered as an important mechanism acting in most active subduction zones (e.g., Heuret and Lallemand, 2005; Nakakuki and Mura, 2013). The rollback of the slab results in a lateral extension of the serpentinized wedge. As consequence, the melt ascending below the arc can interact with serpentinized, high $\delta^{18}O$ mantle portions that were originally part of the forearc mantle and modify its original isotopic composition. High $\delta^{18}O$ arc lavas and melt in arc-setting peridotites have been described (e.g., phenocrysts in lavas from Central Kamchatka: olivine $\delta^{18}O$ = 5.8 – 7.1 ‰ and clinopyroxenes $\delta^{18}O$ = 6.2 – 7.5 ‰, Dorendorf et al., 2000; New Guinea: silicate glass inclusions in olivine $\delta^{18}O$ = 8.8 – 12.2 ‰, clinopyroxenes in metasomatized lehrzolite $\delta^{18}O$ = 6.2 – 10.3 ‰, Eiler et al., 1998)~~have been described (e.g., Dorendorf et al., 2000; Eiler et al., 1998)~~, but the mechanism of crustal contamination is still debated. Our results support the model proposed by Auer et al. (2009) that relates such high $\delta^{18}O$ lavas to the

interaction between primitive basaltic melts with ~~the~~ an uppermost mantle that was ~~once~~ hydrated and enriched as part of the forearc mantle prior to trench migration.

4.6 Model applications and future directions

The presented approach has a broad range of applications for modelling fluid/rock interaction in different tectonic settings. We have presented here an example of subducted crust but the same principles apply also for regional metamorphism or hydrothermal systems. The model also provides new ways to quantify the degree of interaction of an external fluid within the same rock unit. We have shown that the observed effect on the $\delta^{18}O$ of a rock of channelized *vs* ~~extensive~~ pervasive hydration is strictly coupled with the composition of the fluid source. Nevertheless, important insights can be given by linking observations of ideal cases with modelling even if the composition of the infiltrating fluid is not known a priori. For instance, the oxygen isotope composition of a fluid source can be retrieved when a variation in $\delta^{18}O$ is observed within the same rock type from the more hydrated to the less hydrated portions, even in absence of a clear presence of a vein or vein system. Alternatively, the degree of equilibration of the host rock around a vein can be calculated when the isotopic composition of the fluid is known. Therefore, the combination of mineral-scale in-situ oxygen isotope analyses with major and trace element mapping will provide much more detailed information on quantitative element mobility during fluid-rock interaction.

Fluids play a central role as catalyst for chemical reactions in rocks. Generally re-equilibration reactions occur only in presence of fluids that either derive from breakdown of hydrous phases or from external sources (e.g., Airaghi et al., 2017; Cartwright and Barnicoat, 2003; Engi et al., 2018; Konrad-Schmolke et al., 2011; Rubatto and Angiboust, 2015). The program PTLOOP calculates at which *P-T* conditions breakdown of hydrous phases ~~dehydration reactions~~ occurs and, consequently, metamorphic reactions and free fluid are expected. If in a rock fluid-driven reactions occurred at *P-T* conditions where no release of internal fluid is expected~~mineral growth occurs at *P-T* conditions where no internal fluid is buffered~~, the role of an external fluid should be considered and its amount and isotopic composition can be retrieved using the approach outlined in this paper.

Fluid/rock reactions in subducted lithosphere are likely to involve more complex open-system processes than the dehydration and rehydration considered for this model, driving silicate and carbonate dissolution, transport and re-precipitation (e.g., Ague and Nicolescu, 2013; Piccoli et al., 2016). Carbon release via dissolution of calcium carbonate has been recognized to have important implications for CO_2 release from subduction zones and it is controlled by H_2O-rich fluid infiltration (e.g., Ague and Nicolescu, 2013; Frezzotti et al, 2011; Gorman et al., 2006; Kerrick and Connolly, 2001). Future models may account for such variations in reactive major element bulk composition of the rocks along the *P-T* evolution as consequence of mineral net transfer reactions occurring simultaneously with fluid/rock exchange (Baumgartner and Valley, 2001), in addition to water liberation and mineral fractionation (see above). This would require additional considerations on the changes in the fluid isotopic composition during transfer of solute species through the fluid. Implementation of other fluid species beside H_2O, such as CO_2, could be assessed, provided that (1) reliable constraints on the oxygen isotope fractionation between these species and water or minerals are determined and (2) their consistency with other available data is established. Other species such as CH_4 and H_2 do not contain any oxygen, and thus they are likely to be less relevant to this model.

5 Conclusions

We developed a user-friendly tool that combines equilibrium thermodynamic with oxygen isotope fractionation modelling for investigating the interaction between fluids and minerals in rocks during their metamorphic evolution. The program simulates along any given *P-T* path the stable mineral assemblages, bulk $\delta^{18}O$ and $\delta^{18}O$ of stable phases and the amount and oxygen isotope composition of the fluid released.

The capabilities of the program PTLOOP are illustrated by an application to subduction zones, but the presented modelling strategy can be applied to various metamorphic and tectonic settings. In this study, the chosen system represents a section of subducting oceanic crust composed by a lower layer of metabasalt~~either fresh or altered MORB~~ and an upper layer of metasediments of carbonaceous~~carbonatic~~ or pelitic composition. The calculation follows a step-wise procedure along the chosen *P-T* path. During the prograde evolution, any mineral and excess fluid can be fractionated from the reactive bulk composition.

Mineral fractionation and/or excess fluid loss produce only minor (i.e. < 1.0 ‰) shifts in the bulk $\delta^{18}O$ of any lithology. Hence, the bulk $\delta^{18}O$ of a rock that experienced a succession of such processes without interaction with external fluids is likely to be representative of its protolith composition. Variations in $\delta^{18}O$ of stable phases due to mineral fractionation and/or excess fluid loss ~~is typically~~are as well negligible (i.e. < 0.5 ‰), while the effect of temperature variation over a range of ~150 °C on the mineral $\delta^{18}O$ is phase dependent and may be significant (> 1.0 ‰). Interaction with an external fluid of different oxygen isotope composition leads to shifts in bulk and mineral $\delta^{18}O$ values ~~that are marked when the major fluid pulses from the source rock occur,~~ according to the degree of fluid/rock interaction and $\delta^{18}O$ difference between the rock and the fluid. Extreme large variations in bulk $\delta^{18}O$ of ~ 12 ‰ are calculated for the carbonate metasediment equilibrating with a fluid derived from a metabasalt with an initial hydrated MORB composition~~with a fresh MORB derived fluid~~, while small variations of ~ 3 ‰ are calculated for the terrigenous metasediment equilibrating with a fluid from a metabasalt that derives from an altered oceanic crust~~an altered MORB derived fluid~~. When 50 % or more of the fluid deriving from dehydration of the ~~basaltic crust~~metabasalts equilibrates with any of the overlying metasediments, the final $\delta^{18}O$ of the fluid released by the system has a dominant sedimentary signature, with values between 12 and 18 ‰. Such fluids have $\delta^{18}O$ values significantly higher than the mantle value (5.5 ‰) and~~Such fluid with $\delta^{18}O$ values of 6.5 to 12.5 ‰ higher than the mantle value (5.5 ‰)~~ have a great potential to modify the oxygen isotope composition of the mantle wedge at the slab-mantle interface. Extensive serpentinization and $\delta^{18}O$ increase of ~ 2.5 ‰ are modelled at the interface already after 0.35 Myr of ongoing subduction.

PTLOOP provides a powerful way to evaluate the effect of closed system *vs* open system behaviour with respect to oxygen isotopes during the evolution of the rocks. Different degrees of interaction between the external fluids and the sink lithology can be simulated and the effects of internally *vs* externally buffered fluids on the mineral paragenesis and on the mineral isotopic composition investigated.

Measured oxygen isotope compositions in minerals, intra-grain or bulk $\delta^{18}O$ variations at different scales, can be compared with the results of the model for specific scenarios. If the measured isotopic compositions are not consistent with the behaviour of a closed system, the presented ~~model~~ approach can be used to determine feasible external fluid sources, to estimate the degree of fluid-rock interaction and the metamorphic conditions at which this happened. This modelling strategy can assist also in retrieving the oxygen isotope composition of a fluid source when a variation in $\delta^{18}O$ is observed within the same rock type from the more hydrated to the less hydrated portions, even in absence of a clear presence of a vein or vein system. Our model thus opens new avenues for mapping fluid pathways related to external fluid infiltration during the metamorphic evolution of the crust, with important consequences for element recycling in subduction zones and investigation of fluid-induced earthquakes.

Code availability

A compiled version of the program PTLOOP, the oxygen isotope fractionation database and the thermodynamic database used for this study are available at http://oxygen.petrochronology.org.~~A compiled version of the program PTLOOP is available for download for the purpose of review at the temporary link https://www.dropbox.com/sh/h2objjchbd6plwv/AABzPSSPfKmG1KBxc-qiDPf2a?dl=0.~~

Author contributions

Alice Vho developed the model and performed the calculations. Pierre Lanari supervised the software development and contributed to the code implementation. Daniela Rubatto and Jörg Hermann contributed to formulate and design the model and to the interpretation of the results. Alice Vho prepared the manuscript with contributions from all co-authors. Daniela Rubatto conceived the project and secured funding.

Competing interest

The authors declare that they have no conflict of interest.

Acknowledgements

We thank the conveners and the participants of the EGU Galileo conference "Exploring new frontiers in fluid processes in subduction zones" for constructive discussions. We also thank Ulrich Linden for the technical support.

Financial support

This work was supported by the Swiss National Science Foundation (grant no. 200021_166280 to Daniela Rubatto and grant no. 200021_169062 to Jörg Hermann).~~This work was supported by the Swiss National Science Foundation [Project N. 200021_166280].~~

REFERENCES

Abers, G. A., van Keken, P. E., Kneller, E. A., Ferris, A. and Stachnik, J. C.: The thermal structure of subduction zones constrained by seismic imaging: Implications for slab dehydration and wedge flow, Earth and Planetary Science Letters, 241(3–4), 387–397, https://doi.org/10.1016/j.epsl.2005.11.055, 2006.

Ague J. J. and Nicolescu, S.: Carbon dioxide released from subduction zones by fluid-mediated reactions, Nature Geoscience, 7(5), 355–360, https://doi.org/10.1038/ngeo2143, 2014.

Airaghi, L., Lanari, P., de Sigoyer, J. and Guillot, S.: Microstructural vs compositional preservation and pseudomorphic replacement of muscovite in deformed metapelites from the Longmen Shan (Sichuan, China), Lithos, 282, 262–280, https://doi.org/10.1016/j.lithos.2017.03.013, 2017.

Albarède, F.: The survival of mantle geochemical heterogeneities, Washington DC American Geophysical Union Geophysical Monograph Series, 160, 27–46, 10.1029/160GM04, 2005.

Alt, J. C., Muehlenbachs, K. and Honnorez, J.: An oxygen isotopic profile through the upper kilometer of the oceanic crust, DSDP Hole 504B, Earth and Planetary Science Letters, 80(3), 217–229, https://doi.org/10.1016/0012-821X(86)90106-8, 1986.

Auer, S., Bindeman, I., Wallace, P., Ponomareva, V. and Portnyagin, M.: The origin of hydrous, high-$\delta^{18}O$ voluminous volcanism: diverse oxygen isotope values and high magmatic water contents within the volcanic record of Klyuchevskoy volcano, Kamchatka, Russia, Contributions to Mineralogy and Petrology, 157(2), 209, https://doi.org/10.1007/s00410-008-0330-0, 2009.

Barnes, J. D. and Straub, S. M.: Chorine stable isotope variations in Izu Bonin tephra: implications for serpentinite subduction, Chemical Geology, 272(1), 62–74, https://doi.org/10.1016/j.chemgeo.2010.02.005, 2010.

Barnicoat, A. C. and Cartwright, I.: Focused fluid flow during subduction: oxygen isotope data from high-pressure ophiolites of the western Alps, Earth and Planetary Science Letters, 132(1–4), 53–61, https://doi.org/10.1016/0012-821X(95)00040-J, 1995.

Baumgartner, L. P. and Rumble, D.: Transport of stable isotopes: I: Development of a kinetic continuum theory for stable isotope transport, Contributions to Mineralogy and Petrology, 98(4), 417–430, https://doi.org/10.1007/BF00372362, 1988.

Baumgartner, L. P. and Valley, J. W.: Stable isotope transport and contact metamorphic fluid flow, Reviews in Mineralogy and Geochemistry, 43(1), 415–467, https://doi.org/10.2138/gsrmg.43.1.415, 2001.

Baxter, E. F. and Caddick, M. J.: Garnet growth as a proxy for progressive subduction zone dehydration, Geology, 41(6), 643–646, https://doi.org/10.1130/G34004.1, 2013.

Bebout, G. E. and Penniston-Dorland, S. C.: Fluid and mass transfer at subduction interfaces—The field metamorphic record, Lithos, 240, 228–258, https://doi.org/10.1016/j.lithos.2015.10.007, 2016.

Bebout, G. E., Agard, P., Kobayashi, K., Moriguti, T. and Nakamura, E.: Devolatilization history and trace element mobility in deeply subducted sedimentary rocks: Evidence from Western Alps HP/UHP suites, Chemical Geology, 342, 1–20, https://doi.org/10.1016/j.chemgeo.2013.01.009, 2013.

Bostock, M. G., Hyndman, R. D., Rondenay, S. and Peacock, S. M.: An inverted continental Moho and serpentinization of the forearc mantle, Nature, 417(6888), 536, https://doi.org/10.1038/417536a, 2002.
Bowman, J. R., Willett, S. D. and Cook, S. J.: Oxygen isotopic transport and exchange during fluid flow: One-dimensional models and applications, American Journal of Science; (United States), 294(1), 10.2475/ajs.294.1.1, 1994.
Bulle, F., Rubatto, D., Ruggieri, G., Luisier, C., Villa, I. M. and Baumgartner, L.: Episodic hydrothermal alteration recorded by microscale oxygen isotope analysis of white mica in the Larderello-Travale Geothermal Field, Italy, Chemical Geology, 119288, https://doi.org/10.1016/j.chemgeo.2019.119288, 2019.
Caddick, M. J., Konopásek, J. and Thompson, A. B.: Preservation of garnet growth zoning and the duration of prograde metamorphism, Journal of Petrology, 51(11), 2327–2347, https://doi.org/10.1093/petrology/egq059, 2010.
de Capitani, C. and Brown, T. H.: The computation of chemical equilibrium in complex systems containing non-ideal solutions, Geochimica et Cosmochimica Acta, 51(10), 2639–2652, https://doi.org/10.1016/0016-7037(87)90145-1, 1987.
de Capitani, C. and Petrakakis, K.: The computation of equilibrium assemblage diagrams with Theriak/Domino software, American Mineralogist, 95(7), 1006–1016, https://doi.org/10.2138/am.2010.3354, 2010.
Cartwright, I. and Barnicoat, A. C.: Stable isotope geochemistry of Alpine ophiolites: a window to ocean-floor hydrothermal alteration and constraints on fluid–rock interaction during high-pressure metamorphism, International Journal of Earth Sciences, 88(2), 219–235, https://doi.org/10.1007/s005310050261, 1999.
Cartwright, I. and Barnicoat, A. C.: Geochemical and stable isotope resetting in shear zones from Täschalp: constraints on fluid flow during exhumation in the Western Alps, Journal of Metamorphic Geology, 21(2), 143–161, https://doi.org/10.1046/j.1525-1314.2003.00423.x, 2003.
Cook-Kollars, J., Bebout, G. E., Collins, N. C., Angiboust, S. and Agard, P.: Subduction zone metamorphic pathway for deep carbon cycling: I. Evidence from HP/UHP metasedimentary rocks, Italian Alps, Chemical Geology, 386, 31–48, https://doi.org/10.1016/j.chemgeo.2014.07.013, 2014.
Diener, J. F. A., Powell, R., White, R. W. and Holland, T. J. B.: A new thermodynamic model for clino-and orthoamphiboles in the system Na2O–CaO–FeO–MgO–Al2O3–SiO2–H2O–O, Journal of Metamorphic Geology, 25(6), 631–656, https://doi.org/10.1111/j.1525-1314.2007.00720.x, 2007.
Dorendorf, F., Wiechert, U. and Wörner, G.: Hydrated sub-arc mantle: a source for the Kluchevskoy volcano, Kamchatka/Russia, Earth and Planetary Science Letters, 175(1), 69–86, https://doi.org/10.1016/S0012-821X(99)00288-5, 2000.
Dubacq, B., Vidal, O. and De Andrade, V.: Dehydration of dioctahedral aluminous phyllosilicates: thermodynamic modelling and implications for thermobarometric estimates, Contributions to Mineralogy and Petrology, 159(2), 159, https://doi.org/10.1007/s00410-009-0421-6, 2010.
Eiler, J. M.: Oxygen isotope variations of basaltic lavas and upper mantle rocks, Reviews in mineralogy and geochemistry, 43(1), 319–364, https://doi.org/10.2138/gsrmg.43.1.319, 2001.
Eiler, J. M., Farley, K. A., Valley, J. W., Hauri, E., Craig, H., Hart, S. R. and Stolper, E. M.: Oxygen isotope variations in ocean island basalt phenocrysts, Geochimica et Cosmochimica Acta, 61(11), 2281–2293, https://doi.org/10.1016/S0016-7037(97)00075-6, 1997.
Eiler, J. M., McInnes, B., Valley, J. W., Graham, C. M. and Stolper, E. M.: Oxygen isotope evidence for slab-derived fluids in the sub-arc mantle, Nature, 393(6687), 777, https://doi.org/10.1038/31679, 1998.
Engi, M., Giuntoli, F., Lanari, P., Burn, M., Kunz, B. and Bouvier, A.-S.: Pervasive Eclogitization Due to Brittle Deformation and Rehydration of Subducted Basement: Effects on Continental Recycling?, Geochemistry, Geophysics, Geosystems, 19(3), 865–881, https://doi.org/10.1002/2017GC007215, 2018.
Errico, J. C., Barnes, J. D., Strickland, A. and Valley, J. W.: Oxygen isotope zoning in garnets from Franciscan eclogite blocks: evidence for rock–buffered fluid interaction in the mantle wedge, Contributions to Mineralogy and Petrology, 166(4), 1161–1176, https://doi.org/10.1007/s00410-013-0915-0, 2013.
Evans, T. P.: A method for calculating effective bulk composition modification due to crystal fractionation in garnet-bearing schist: implications for isopleth thermobarometry, Journal of Metamorphic Geology, 22(6), 547–557, https://doi.org/10.1111/j.1525-1314.2004.00532.x, 2004.
Ferry, J. M., Kitajima, K., Strickland, A. and Valley, J. W.: Ion microprobe survey of the grain-scale oxygen isotope geochemistry of minerals in metamorphic rocks, Geochimica and Cosmochimica Acta, 144, 403–433, https://doi.org/10.1016/j.gca.2014.08.021, 2014.
Ferry, J. M. and Spear, F. S.: Experimental calibration of the partitioning of Fe and Mg between biotite and garnet, Contributions to mineralogy and petrology, 66(2), 113–117, https://doi.org/10.1007/BF00372150, 1978.
Frey, M., Capitani, C. de and Liou, J. G.: A new petrogenetic grid for low-grade metabasites, Journal of Metamorphic Geology, 9(4), 497–509, https://doi.org/10.1111/j.1525-1314.1991.tb00542.x, 1991.
Frezzotti, M. L., Selverstone, J., Sharp, Z. D. and Compagnoni, R.: Carbonate dissolution during subduction revealed by diamond-bearing rocks from the Alps, Nature Geoscience, 4(10), 703–706, https://doi.org/10.1038/ngeo1246, 2011.
Friedman, I. and O'Neil, J. R.: Compilation of stable isotope fractionation factors of geochemical interest, US Government Printing Office, Washington, D. C., 1977.
Früh-Green, G. L., Scambelluri, M. and Vallis, F.: O–H isotope ratios of high pressure ultramafic rocks: implications for fluid sources and mobility in the subducted hydrous mantle, Contributions to Mineralogy and Petrology, 141(2), 145–159, https://doi.org/10.1007/s004100000228, 2001.
Gale, A., Dalton, C. A., Langmuir, C. H., Su, Y. and Schilling, J.-G.: The mean composition of ocean ridge basalts, Geochemistry, Geophysics, Geosystems, 14(3), 489–518, https://doi.org/10.1029/2012GC004334, 2013.
Gauthiez-Putallaz, L., Rubatto, D. and Hermann, J.: Dating prograde fluid pulses during subduction by in situ U–Pb and oxygen isotope analysis, Contributions to mineralogy and petrology, 171(2), 15, https://doi.org/10.1007/s00410-015-1226-4, 2016.

Gerdes, M. L., Baumgartner, L. P., Person, M. and Rumble, D.: One-and two-dimensional models of fluid flow and stable isotope exchange at an outcrop in the Adamello contact aureole, Southern Alps, Italy, American Mineralogist, 80(9–10), 1004–1019, https://doi.org/10.2138/am-1995-9-1016, 1995a.

Gerdes, M. L., Baumgartner, L. P. and Person, M.: Stochastic permeability models of fluid flow during contact metamorphism, Geology, 23(10), 945–948, https://doi.org/10.1130/0091-7613(1995)023<0945:SPMOFF>2.3.CO;2, 1995b.

Gerya, T. V., Stöckhert, B. and Perchuk, A. L.: Exhumation of high-pressure metamorphic rocks in a subduction channel: A numerical simulation, Tectonics, 21(6), 6–1, https://doi.org/10.1029/2002TC001406, 2002.

Giuntoli, F., Lanari, P. and Engi, M.: Deeply subducted continental fragments-Part 1: Fracturing, dissolution-precipitation, and diffusion processes recorded by garnet textures of the central Sesia Zone (western Italian Alps), Solid Earth, 9(1), 167–167, https://doi.org/10.5194/se-9-167-2018, 2018.

Gorman, P. J., Kerrick, D. M. and Connolly, J. A. D.: Modeling open system metamorphic decarbonation of subducting slabs, Geochemistry, Geophysics, Geosystems, 7(4), https://doi.org/10.1029/2005GC001125, 2006.

Gregory, R. T. and Taylor Jr, H. P.: An oxygen isotope profile in a section of Cretaceous oceanic crust, Samail ophiolite, Oman: Evidence for $\delta^{18}O$ buffering of the oceans by deep (> 5 km) seawater-hydrothermal circulation at mid-ocean ridges, Journal of Geophysical Research: Solid Earth, 86(B4), 2737–2755, https://doi.org/10.1029/JB086iB04p02737, 1981.

Hacker, B. R.: H_2O subduction beyond arcs, Geochemistry, Geophysics, Geosystems, 9(3), 2008.

Hermann, J., Müntener, O. and Scambelluri, M.: The importance of serpentinite mylonites for subduction and exhumation of oceanic crust, Tectonophysics, 327(3–4), 225–238, https://doi.org/10.1016/S0040-1951(00)00171-2, 2000.

Hernández-Uribe, D. and Palin, R. M.: A revised petrological model for subducted oceanic crust: insights from phase equilibrium modelling, Journal of Metamorphic Geology, https://doi.org/10.1111/jmg.12483, 2019.

Heuret, A. and Lallemand, S.: Plate motions, slab dynamics and back-arc deformation, Physics of the Earth and Planetary Interiors, 149(1–2), 31–51, https://doi.org/10.1016/j.pepi.2004.08.022, 2005.

Higashino, F., Rubatto, D., Kawakami, T., Bouvier, A.-S. and Baumgartner, L. P.: Oxygen isotope speedometry in granulite facies garnet recording fluid/melt–rock interaction (Sør Rondane Mountains, East Antarctica), Journal of Metamorphic Geology, 37(7), 1037–1048, https://doi.org/10.1111/jmg.12490, 2018.

Hirauchi, K. and Katayama, I.: Rheological contrast between serpentine species and implications for slab–mantle wedge decoupling, Tectonophysics, 608, 545–551, https://doi.org/10.1016/j.tecto.2013.08.027, 2013.

Hoefs, J.: Stable isotope geochemistry, Springer, Berlin, 1997.

Holland, T. and Powell, R.: Thermodynamics of order-disorder in minerals; II, Symmetric formalism applied to solid solutions, American Mineralogist, 81(11–12), 1425–1437, https://doi.org/10.2138/am-1996-11-1215, 1996.

Holland, T. and Powell, R.: Activity–composition relations for phases in petrological calculations: an asymmetric multicomponent formulation, Contributions to Mineralogy and Petrology, 145(4), 492–501, https://doi.org/10.1007/s00410-003-0464-z, 2003.

Holland, T., Baker, J. and Powell, R.: Mixing properties and activity-composition relationships of chlorites in the system MgO-FeO-Al_2O_3-SiO_2-H_2O, European Journal of Mineralogy, 395–406, 10.1127/ejm/10/3/0395, 1998.

Holland, T. J. B. and Powell, R.: An internally consistent thermodynamic data set for phases of petrological interest, Journal of metamorphic Geology, 16(3), 309–343, https://doi.org/10.1111/j.1525-1314.1998.00140.x, 1998.

Iwamori, H.: Transportation of H_2O and melting in subduction zones, Earth and Planetary Science Letters, 160(1–2), 65–80, https://doi.org/10.1016/S0012-821X(98)00080-6, 1998.

John, T., Scambelluri, M., Frische, M., Barnes, J. D. and Bach, W.: Dehydration of subducting serpentinite: implications for halogen mobility in subduction zones and the deep halogen cycle, Earth and Planetary Science Letters, 308(1–2), 65–76, https://doi.org/10.1016/j.epsl.2011.05.038, 2011.

Kerrick, D. M. and Connolly, J. A. D.: Metamorphic devolatilization of subducted marine sediments and the transport of volatiles into the Earth's mantle, Nature, 411(6835), 293, https://doi.org/10.1038/35077056, 2001.

Kohn, M. J.: Modeling of prograde mineral $\delta^{18}O$ changes in metamorphic systems, Contributions to Mineralogy and Petrology, 113(2), 249–261, https://doi.org/10.1007/BF00283232, 1993.

Konrad-Schmolke, M., O'Brien, P. J., de Capitani, C. and Carswell, D. A.: Garnet growth at high-and ultra-high pressure conditions and the effect of element fractionation on mineral modes and composition, Lithos, 103(3–4), 309–332, https://doi.org/10.1016/j.lithos.2007.10.007, 2008.

Konrad-Schmolke, M., Zack, T., O'Brien, P. and Barth, M.: Fluid migration above a subducted slab — Thermodynamic and trace element modelling of fluid–rock interaction in partially overprinted eclogite-facies rocks (Sesia Zone, Western Alps), Earth and Planetary Science Letters, 311(3–4), 287-298, https://doi.org/10.1016/j.epsl.2011.09.025, 2011.

Kuhn, B. K., Reusser, E., Powell, R. and Günther, D.: Metamorphic evolution of calc-schists in the Central Alps, Switzerland, Schweizerische mineralogische und petrographische Mitteilungen, 85(2–3), 175–190, https://doi.org/10.5169/seals-1659, 2005.

Lanari, P. and Duesterhoeft, E.: Modeling Metamorphic Rocks Using Equilibrium Thermodynamics and Internally Consistent Databases: Past Achievements, Problems and Perspectives, Journal of Petrology, 60(1), 19–56, https://doi.org/10.1093/petrology/egy105, 2019.

Lanari, P. and Engi, M.: Local bulk composition effects on metamorphic mineral assemblages, Reviews in Mineralogy and Geochemistry, 83(1), 55–102, https://doi.org/10.2138/rmg.2017.83.3, 2017.

Lanari, P., Giuntoli, F., Loury, C., Burn, M. and Engi, M.: An inverse modeling approach to obtain P–T conditions of metamorphic stages involving garnet growth and resorption, European Journal of Mineralogy, 29(2), 181–199, https://doi.org/10.1127/ejm/2017/0029-2597, 2017.

Laurent, V., Lanari, P., Naïr, I., Augier, R., Lahfid, A. and Jolivet, L.: Exhumation of eclogite and blueschist (Cyclades, Greece): Pressure–temperature evolution determined by thermobarometry and garnet equilibrium modelling, Journal of Metamorphic Geology, 36(6), 769–798, https://doi.org/10.1111/jmg.12309, 2018.

Liou, J. G., Tsujimori, T., Zhang, R. Y., Katayama, I. and Maruyama, S.: Global UHP metamorphism and continental subduction/collision: the Himalayan model, International Geology Review, 46(1), 1–27, https://doi.org/10.2747/0020-6814.46.1.1, 2004.

Manning, C. E.: The chemistry of subduction-zone fluids, Earth and Planetary Science Letters, 223(1–2), 1–16, https://doi.org/10.1016/j.epsl.2004.04.030, 2004.

Martin, L. A., Rubatto, D., Crépisson, C., Hermann, J., Putlitz, B. and Vitale-Brovarone, A.: Garnet oxygen analysis by SHRIMP-SI: Matrix corrections and application to high-pressure metasomatic rocks from Alpine Corsica, Chemical geology, 374, 25–36, https://doi.org/10.1016/j.chemgeo.2014.02.010, 2014.

Mattey, D., Lowry, D. and Macpherson, C.: Oxygen isotope composition of mantle peridotite, Earth and Planetary Science Letters, 128(3–4), 231–241, https://doi.org/10.1016/0012-821X(94)90147-3, 1994.

Mével, C.: Serpentinization of abyssal peridotites at mid-ocean ridges, Comptes Rendus Geoscience, 335(10–11), 825–852, https://doi.org/10.1016/j.crte.2003.08.006, 2003.

Miller, J. A. and Cartwright, I.: Distinguishing between seafloor alteration and fluid flow during subduction using stable isotope geochemistry: examples from Tethyan ophiolites in the Western Alps, Journal of Metamorphic Geology, 18(5), 467–482, 10.1046/j.1525-1314.2000.00274.x, 2000.

Miller, J. A., Cartwright, I., Buick, I. S. and Barnicoat, A. C.: An O-isotope profile through the HP–LT Corsican ophiolite, France and its implications for fluid flow during subduction, Chemical Geology, 178(1–4), 43–69, https://doi.org/10.1016/S0009-2541(00)00428-9, 2001.

Muehlenbachs, K. and Clayton, R. N.: Oxygen isotope studies of fresh and weathered submarine basalts, Canadian Journal of Earth Sciences, 9(2), 172–184, https://doi.org/10.1139/e72-014, 1972.

Nakakuki, T. and Mura, E.: Dynamics of slab rollback and induced back-arc basin formation, Earth and Planetary Science Letters, 361, 287–297, https://doi.org/10.1016/j.epsl.2012.10.031, 2013.

O'Neil, J. R. and Adami, L. H.: Oxygen isotope partition function ratio of water and the structure of liquid water, The Journal of Physical Chemistry, 73(5), 1553–1558, https://pubs.acs.org/doi/pdf/10.1021/j100725a062, 1969.

O'Neil, J. R. and Taylor, H. P.: The oxygen isotope and cation exchange chemistry of feldspars, American Mineralogist, 52, 1414–1437, 1967.

Padrón-Navarta, J. A., Hermann, J., Garrido, C. J., Sánchez-Vizcaíno, V. L. and Gómez-Pugnaire, M. T.: An experimental investigation of antigorite dehydration in natural silica-enriched serpentinite, Contributions to Mineralogy and Petrology, 159(1), 25–42, https://doi.org/10.1007/s00410-009-0414-5, 2010.

Padrón-Navarta, J. A., Sánchez-Vizcaíno, V. L., Hermann, J., Connolly, J. A., Garrido, C. J., Gómez-Pugnaire, M. T. and Marchesi, C.: Tschermak's substitution in antigorite and consequences for phase relations and water liberation in high-grade serpentinites, Lithos, 178, 186–196, https://doi.org/10.1016/j.lithos.2013.02.001, 2013.

Page, F. Z., Kita, N. T. and Valley, J. W.: Ion microprobe analysis of oxygen isotopes in garnets of complex chemistry, Chemical Geology, 270(1–4), 9–19, https://doi.org/10.1016/j.chemgeo.2009.11.001, 2010.

Page, F. Z., Essene, E. J., Mukasa, S. B. and Valley, J. W.: A garnet–zircon oxygen isotope record of subduction and exhumation fluids from the Franciscan Complex, California, Journal of Petrology, 55(1), 103–131, https://doi.org/10.1093/petrology/egt062, 2013.

Page, F. Z., Cameron, E. M., Flood, C. M., Dobbins, J. W., Spicuzza, M. J., Kitajima, K., Strickland, A., Ushikubo, T., Mattinson, C. G. and Valley, J. W.: Extreme oxygen isotope zoning in garnet and zircon from a metachert block in mélange reveals metasomatism at the peak of subduction metamorphism, Geology, 47(7), 655–658, https://doi.org/10.1130/G46135.1, 2019.

Parra, T., Vidal, O. and Agard, P.: A thermodynamic model for Fe–Mg dioctahedral K white micas using data from phase-equilibrium experiments and natural pelitic assemblages, Contributions to Mineralogy and Petrology, 143(6), 706–732, https://doi.org/10.1007/s00410-002-0373-6, 2002.

Peacock, S. A.: Fluid processes in subduction zones, Science, 248(4953), 329–337, 10.1126/science.248.4953.329, 1990.

Peacock, S. M.: The importance of blueschist→ eclogite dehydration reactions in subducting oceanic crust, Geological Society of America Bulletin, 105(5), 684–694, https://doi.org/10.1130/0016-7606(1993)105<0684:TIOBED>2.3.CO;2, 1993.

Penniston-Dorland, S. C., Kohn, M. J. and Manning, C. E.: The global range of subduction zone thermal structures from exhumed blueschists and eclogites: Rocks are hotter than models, Earth and Planetary Science Letters, 428, 243–254, https://doi.org/10.1016/j.epsl.2015.07.031, 2015.

Piccoli, F., Vitale Brovarone, A., Beyssac, O., Martinez, I., Ague, J. J. and Chaduteau, C.: Carbonation by fluid–rock interactions at high-pressure conditions: implications for carbon cycling in subduction zones, Earth and Planetary Science Letters, 445, 146–159, https://doi.org/10.1016/j.epsl.2016.03.045, 2016.

Plank, T.: The chemical composition of subducting sediments, Treatise on geochemistry, 4, 607–629, https://doi.org/10.1016/B978-0-08-095975-7.00319-3, 2014.

Plank, T. and Langmuir, C. H.: The chemical composition of subducting sediment and its consequences for the crust and mantle, Chemical geology, 145(3), 325–394, https://doi.org/10.1016/S0009-2541(97)00150-2, 1998.

Poli, S. and Schmidt, M. W.: Petrology of subducted slabs, Annual Review of Earth and Planetary Sciences, 30(1), 207–235, https://doi.org/10.1146/annurev.earth.30.091201.140550, 2002.

Powell, R. and Holland, T. J. B.: On thermobarometry, Journal of Metamorphic Geology, 26(2), 155–179, https://doi.org/10.1111/j.1525-1314.2007.00756.x, 2008.

Putlitz, B., Matthews, A. and Valley, J. W.: Oxygen and hydrogen isotope study of high-pressure metagabbros and metabasalts (Cyclades, Greece): implications for the subduction of oceanic crust, Contributions to Mineralogy and Petrology, 138(2), 114–126, https://doi.org/10.1007/s004100050012, 2000.

Rubatto, D. and Angiboust, S.: Oxygen isotope record of oceanic and high-pressure metasomatism: a P–T–time–fluid path for the Monviso eclogites (Italy), Contributions to mineralogy and petrology, 170(5–6), 44, https://doi.org/10.1007/s00410-015-1198-4, 2015.
Rumble, D.: Stable isotope fractionation during metamorphic devolatilization reactions, Reviews in Mineralogy and Geochemistry, 10(1), 327–353, 1982.
Russell, A. K., Kitajima, K., Strickland, A., Medaris, L. G., Schulze, D. J. and Valley, J. W.: Eclogite-facies fluid infiltration: constraints from $\delta^{18}O$ zoning in garnet, Contributions to Mineralogy and Petrology, 165(1), 103–116, https://doi.org/10.1007/s00410-012-0794-9, 2013.
Scambelluri, M. and Philippot, P.: Deep fluids in subduction zones, Lithos, 55(1–4), 213–227, https://doi.org/10.1016/S0024-4937(00)00046-3, 2001.
Scambelluri, M., Fiebig, J., Malaspina, N., Müntener, O. and Pettke, T.: Serpentinite subduction: implications for fluid processes and trace-element recycling, International Geology Review, 46(7), 595–613, https://doi.org/10.2747/0020-6814.46.7.595, 2004.
Schmidt, M. W. and Poli, S.: The stability of lawsonite and zoisite at high pressures: Experiments in CASH to 92 kbar and implications for the presence of hydrous phases in subducted lithosphere, Earth and Planetary Science Letters, 124(1–4), 105–118, https://doi.org/10.1016/0012-821X(94)00080-8, 1994.
Sharp, Z.: Principles of stable isotope geochemistry, https://doi.org/10.25844/h9q1-0p82, 2017.
Sharp, Z. D. and Barnes, J. D.: Water-soluble chlorides in massive seafloor serpentinites: a source of chloride in subduction zones, Earth and Planetary Science Letters, 226(1–2), 243–254, https://doi.org/10.1016/j.epsl.2004.06.016, 2004.
Siron, G., Baumgartner, L., Bouvier, A.-S., Putlitz, B. and Vennemann, T.: Biotite reference materials for secondary ion mass spectrometry $^{18}O/^{16}O$ measurements, Geostandards and Geoanalytical Research, 41(2), 243–253, https://doi.org/10.1111/ggr.12148, 2017.
Spandler, C. and Hermann, J.: High-pressure veins in eclogite from New Caledonia; Implications for fluid migration and seismic activity in subduction zones, Geochimica et Cosmochimica Acta Supplement, 69, A664, 2005.
Spear, F. S.: Metamorphic fractional crystallization and internal metasomatism by diffusional homogenization of zoned garnets, Contributions to Mineralogy and Petrology, 99(4), 507–517, https://doi.org/10.1007/BF00371941, 1988.
Spear, F. S., Pattison, D. R. M. and Cheney, J. T.: The metamorphosis of metamorphic petrology, in The Web of Geological Sciences: Advances, Impacts, and Interactions II, Geological Society of America., 2017.
Staudigel, H.: Chemical fluxes from hydrothermal alteration of the oceanic crust, In: Treatise on Geochemistry (Second edition)., edited by Turekian, H. D. H. K., Elsevier, Oxford, United Kingdom, 583–606, 2014.
Staudigel, H., Plank, T., White, B. and Schmincke, H.-U.: Geochemical fluxes during seafloor alteration of the basaltic upper oceanic crust: DSDP Sites 417 and 418, Subduction: top to bottom, 96, 19–38, https://doi.org/10.1029/GM096p0019, 1996.
Stern, R. J.: Subduction zones, Reviews of geophysics, 40(4), 3–1, https://doi.org/10.1029/2001RG000108, 2002.
Sun, S.-S. and McDonough, W. F.: Chemical and isotopic systematics of oceanic basalts: implications for mantle composition and processes, Geological Society, London, Special Publications, 42(1), 313–345, https://doi.org/10.1144/GSL.SP.1989.042.01.19, 1989.
Syracuse, E. M., van Keken, P. E. and Abers, G. A.: The global range of subduction zone thermal models, Physics of the Earth and Planetary Interiors, 183(1–2), 73–90, https://doi.org/10.1016/j.pepi.2010.02.004, 2010.
Tracy, R. J.: Compositional zoning and inclusions in metamorphic minerals. Characterization of Metamorphism through Mineral Equilibria, Review in Mineralogy, 355–397, 1982.
Valley, J.: Stable isotope geochemistry of metamorphic rocks, Reviews in Mineralogy and Geochemistry, 16, 445–489, 1986.
Vho, A., Lanari, P. and Rubatto, D.: An internally-consistent database for oxygen isotope fractionation between minerals, Journal of Petrology, 10.1093/petrology/egaa001, 2020.
Vidal, O., Lanari, P., Munoz, M., Bourdelle, F., de Andrade, V. and Walker, J.: Deciphering temperature, pressure and oxygen-activity conditions of chlorite formation, Clay Minerals, 51(4), 615–633, https://doi.org/10.1180/claymin.2016.051.4.06, 2016.
Vielzeuf, D., Veschambre, M. and Brunet, F.: Oxygen isotope heterogeneities and diffusion profile in composite metamorphic-magmatic garnets from the Pyrenees, American Mineralogist, 90(2–3), 463–472, https://doi.org/10.2138/am.2005.1576, 2005a.
Vielzeuf, D., Champenois, M., Valley, J. W., Brunet, F. and Devidal, J. L.: SIMS analyses of oxygen isotopes: matrix effects in Fe–Mg–Ca garnets, Chemical Geology, 223(4), 208–226, https://doi.org/10.1016/j.chemgeo.2005.07.008, 2005b.
Wada, I., Wang, K., He, J. and Hyndman, R. D.: Weakening of the subduction interface and its effects on surface heat flow, slab dehydration, and mantle wedge serpentinization, Journal of Geophysical Research: Solid Earth, 113(B4), https://doi.org/10.1029/2007JB005190, 2008.
Walter, M. J.: Melting of garnet peridotite and the origin of komatiite and depleted lithosphere, Journal of Petrology, 39(1), 29–60, https://doi.org/10.1093/petroj/39.1.29, 1998.
White, W. M. and Klein, E. M.: Composition of the Oceanic Crust, Treatise on Geochemistry (Second Edition), http://dx.doi.org/10.1016/B978-0-08-095975-7.00315-6, 2014.
Whitney, D. L. and Evans, B. W.: Abbreviations for names of rock-forming minerals, American mineralogist, 95(1), 185–187, https://doi.org/10.2138/am.2010.3371, 2010.
Williams, M. J.: Tracing Fluids from Seafloor to Deep Subduction Environments: An In-situ Geochemical Investigation of Fluid-Mobile Elements in Oceanic Crust, Ph.D thesis, Australian National University, Canberra, 10.25911/5d650de5b5cfd, 325 pp., 2019.
Zack, T. and John, T.: An evaluation of reactive fluid flow and trace element mobility in subducting slabs, Chemical Geology, 239(3–4), 199–216, https://doi.org/10.1016/j.chemgeo.2006.10.020, 2007.
Zheng, Y. F.: Oxygen isotope fractionation in metal monoxides, Mineralogical Magazine, 58, 1000–1001, 10.1180/minmag.1994.58A.2.255, 1994.~~Abers, G. A., van Keken, P. E., Kneller, E. A., Ferris, A. and Stachnik, J. C.: The thermal~~

structure of subduction zones constrained by seismic imaging: Implications for slab dehydration and wedge flow, Earth and Planetary Science Letters, 241(3–4), 387–397, 2006.
Airaghi, L., Lanari, P., de Sigoyer, J. and Guillot, S.: Microstructural vs compositional preservation and pseudomorphic replacement of muscovite in deformed metapelites from the Longmen Shan (Sichuan, China), Lithos, 282, 262–280, 2017.
Albarède, F.: The survival of mantle geochemical heterogeneities, Washington DC American Geophysical Union Geophysical Monograph Series, 160, 27–46, 2005.
Alt, J. C., Muehlenbachs, K. and Honnorez, J.: An oxygen isotopic profile through the upper kilometer of the oceanic crust, DSDP Hole 504B, Earth and Planetary Science Letters, 80(3), 217–229, doi:10.1016/0012-821X(86)90106-8, 1986.
Auer, S., Bindeman, I., Wallace, P., Ponomareva, V. and Portnyagin, M.: The origin of hydrous, high $\delta^{18}O$ voluminous volcanism: diverse oxygen isotope values and high magmatic water contents within the volcanic record of Klyuchevskoy volcano, Kamchatka, Russia, Contributions to Mineralogy and Petrology, 157(2), 209, 2009.
Barnes, J. D. and Straub, S. M.: Chorine stable isotope variations in Izu Bonin tephra: implications for serpentinite subduction, Chemical Geology, 272(1), 62–74, 2010.
Barnicoat, A. C. and Cartwright, I.: Focused fluid flow during subduction: oxygen isotope data from high pressure ophiolites of the western Alps, Earth and Planetary Science Letters, 132(1–4), 53–61, 1995.
Baumgartner, L. P. and Rumble, D.: Transport of stable isotopes: I: Development of a kinetic continuum theory for stable isotope transport, Contributions to Mineralogy and Petrology, 98(4), 417–430, 1988.
Baumgartner, L. P. and Valley, J. W.: Stable isotope transport and contact metamorphic fluid flow, Reviews in Mineralogy and Geochemistry, 43(1), 415–467, 2001.
Baxter, E. F. and Caddick, M. J.: Garnet growth as a proxy for progressive subduction zone dehydration, Geology, 41(6), 643–646, 2013.
Bebout, G. E. and Penniston Dorland, S. C.: Fluid and mass transfer at subduction interfaces—The field metamorphic record, Lithos, 240, 228–258, 2016.
Bebout, G. E., Agard, P., Kobayashi, K., Moriguti, T. and Nakamura, E.: Devolatilization history and trace element mobility in deeply subducted sedimentary rocks: Evidence from Western Alps HP/UHP suites, Chemical Geology, 342, 1–20, 2013.
Bostock, M. G., Hyndman, R. D., Rondenay, S. and Peacock, S. M.: An inverted continental Moho and serpentinization of the forearc mantle, Nature, 417(6888), 536, 2002.
Bowman, J. R., Willett, S. D. and Cook, S. J.: Oxygen isotopic transport and exchange during fluid flow: One-dimensional models and applications, American Journal of Science;(United States), 294(1), 1994.
Bulle, F., Rubatto, D., Ruggieri, G., Luisier, C., Villa, I. M. and Baumgartner, L.: Episodic hydrothermal alteration recorded by microscale oxygen isotope analysis of white mica in the Larderello-Travale Geothermal Field, Italy, Chemical Geology, 119288, 2019.
Caddick, M. J., Konopásek, J. and Thompson, A. B.: Preservation of garnet growth zoning and the duration of prograde metamorphism, Journal of Petrology, 51(11), 2327–2347, 2010.
de Capitani, C. and Brown, T. H.: The computation of chemical equilibrium in complex systems containing non-ideal solutions, Geochimica et Cosmochimica Acta, 51(10), 2639–2652, 1987.
de Capitani, C. and Petrakakis, K.: The computation of equilibrium assemblage diagrams with Theriak/Domino software, American Mineralogist, 95(7), 1006–1016, 2010.
Cartwright, I. and Barnicoat, A. C.: Stable isotope geochemistry of Alpine ophiolites: a window to ocean-floor hydrothermal alteration and constraints on fluid-rock interaction during high-pressure metamorphism, International Journal of Earth Sciences, 88(2), 219–235, 1999.
Cartwright, I. and Barnicoat, A. C.: Geochemical and stable isotope resetting in shear zones from Täschalp: constraints on fluid flow during exhumation in the Western Alps, Journal of Metamorphic Geology, 21(2), 143–161, 2003.
Cook-Kollars, J., Bebout, G. E., Collins, N. C., Angiboust, S. and Agard, P.: Subduction zone metamorphic pathway for deep carbon cycling: I. Evidence from HP/UHP metasedimentary rocks, Italian Alps., Chemical Geology, 386, 31–48, 2014.
Diener, J. F. A., Powell, R., White, R. W. and Holland, T. J. B.: A new thermodynamic model for clino- and orthoamphiboles in the system Na2O–CaO–FeO–MgO–Al2O3–SiO2–H2O–O, Journal of Metamorphic Geology, 25(6), 631–656, 2007.
Dorendorf, F., Wiechert, U. and Wörner, G.: Hydrated sub-arc mantle: a source for the Kluchevskoy volcano, Kamchatka/Russia, Earth and Planetary Science Letters, 175(1), 69–86, 2000.
Dubacq, B., Vidal, O. and De Andrade, V.: Dehydration of dioctahedral aluminous phyllosilicates: thermodynamic modelling and implications for thermobarometric estimates, Contributions to Mineralogy and Petrology, 159(2), 159, 2010.
Eiler, J. M.: Oxygen isotope variations of basaltic lavas and upper mantle rocks, Reviews in mineralogy and geochemistry, 43(1), 319–364, 2001.
Eiler, J. M., Farley, K. A., Valley, J. W., Hauri, E., Craig, H., Hart, S. R. and Stolper, E. M.: Oxygen isotope variations in ocean island basalt phenocrysts, Geochimica et Cosmochimica Acta, 61(11), 2281–2293, 1997.
Eiler, J. M., McInnes, B., Valley, J. W., Graham, C. M. and Stolper, E. M.: Oxygen isotope evidence for slab-derived fluids in the sub-arc mantle, Nature, 393(6687), 777, 1998.
Engi, M., Giuntoli, F., Lanari, P., Burn, M., Kunz, B. and Bouvier, A. S.: Pervasive Eclogitization Due to Brittle Deformation and Rehydration of Subducted Basement: Effects on Continental Recycling?, Geochemistry, Geophysics, Geosystems, 19(3), 865–881, 2018.
Errico, J. C., Barnes, J. D., Strickland, A. and Valley, J. W.: Oxygen isotope zoning in garnets from Franciscan eclogite blocks: evidence for rock-buffered fluid interaction in the mantle wedge, Contributions to Mineralogy and Petrology, 166(4), 1161–1176, 2013.
Evans, T. P.: A method for calculating effective bulk composition modification due to crystal fractionation in garnet-bearing schist: implications for isopleth thermobarometry, Journal of Metamorphic Geology, 22(6), 547–557, 2004.

Ferry, J. t and Spear, F. S.: Experimental calibration of the partitioning of Fe and Mg between biotite and garnet, Contributions to mineralogy and petrology, 66(2), 113–117, 1978.
Frey, M., Capitani, C. de and Liou, J. G.: A new petrogenetic grid for low-grade metabasites, Journal of Metamorphic Geology, 9(4), 497–509, 1991.
Früh-Green, G. L., Scambelluri, M. and Vallis, F.: O–H isotope ratios of high pressure ultramafic rocks: implications for fluid sources and mobility in the subducted hydrous mantle, Contributions to Mineralogy and Petrology, 141(2), 145–159, 2001.
Gale, A., Dalton, C. A., Langmuir, C. H., Su, Y. and Schilling, J. G.: The mean composition of ocean ridge basalts, Geochemistry, Geophysics, Geosystems, 14(3), 489–518, 2013.
Gerdes, M. L., Baumgartner, L. P., Person, M. and Rumble, D.: One- and two-dimensional models of fluid flow and stable isotope exchange at an outcrop in the Adamello contact aureole, Southern Alps, Italy, American Mineralogist, 80(9–10), 1004–1019, 1995a.
Gerdes, M. L., Baumgartner, L. P. and Person, M.: Stochastic permeability models of fluid flow during contact metamorphism, Geology, 23(10), 945–948, 1995b.
Gerya, T. V., Stöckhert, B. and Perchuk, A. L.: Exhumation of high-pressure metamorphic rocks in a subduction channel: A numerical simulation, Tectonics, 21(6), 6–1, 2002.
Giuntoli, F., Lanari, P. and Engi, M.: Deeply subducted continental fragments-Part 1: Fracturing, dissolution-precipitation, and diffusion processes recorded by garnet textures of the central Sesia Zone (western Italian Alps), Solid Earth, 9(1), 167–167, 2018.
Gregory, R. T. and Taylor Jr, H. P.: An oxygen isotope profile in a section of Cretaceous oceanic crust, Samail ophiolite, Oman: Evidence for $\delta^{18}O$ buffering of the oceans by deep (> 5 km) seawater-hydrothermal circulation at mid-ocean ridges, Journal of Geophysical Research: Solid Earth, 86(B4), 2737–2755, 1981.
Hacker, B. R.: H2O subduction beyond arcs, Geochemistry, Geophysics, Geosystems, 9(3), 2008.
Hermann, J., Müntener, O. and Scambelluri, M.: The importance of serpentinite mylonites for subduction and exhumation of oceanic crust, Tectonophysics, 327(3–4), 225–238, 2000.
Hernández-Uribe, D. and Palin, R. M.: A revised petrological model for subducted oceanic crust: insights from phase equilibrium modelling, Journal of Metamorphic Geology, 2019.
Heuret, A. and Lallemand, S.: Plate motions, slab dynamics and back-arc deformation, Physics of the Earth and Planetary Interiors, 149(1–2), 31–51, 2005.
Higashino, F., Rubatto, D., Kawakami, T., Bouvier, A.-S. and Baumgartner, L. P.: Oxygen isotope speedometry in granulite facies garnet recording fluid/melt–rock interaction (Sør Rondane Mountains, East Antarctica), Journal of Metamorphic Geology, 2018.
Hirauchi, K.-I. and Katayama, I.: Rheological contrast between serpentine species and implications for slab–mantle wedge decoupling, Tectonophysics, 608, 545–551, 2013.
Hoefs, J.: Stable isotope geochemistry, Springer, Berlin., 1997.
Holland, T. and Powell, R.: Thermodynamics of order-disorder in minerals; II, Symmetric formalism applied to solid solutions, American Mineralogist, 81(11–12), 1425–1437, 1996.
Holland, T. and Powell, R.: Activity–composition relations for phases in petrological calculations: an asymmetric multicomponent formulation, Contributions to Mineralogy and Petrology, 145(4), 492–501, 2003.
Holland, T., Baker, J. and Powell, R.: Mixing properties and activity-composition relationships of chlorites in the system MgO-FeO-Al2O3-SiO2-H2O, European Journal of Mineralogy, 395–406, 1998.
Holland, T. J. B. and Powell, R.: An internally consistent thermodynamic data set for phases of petrological interest, Journal of metamorphic Geology, 16(3), 309–343, 1998.
Iwamori, H.: Transportation of H_2O and melting in subduction zones, Earth and Planetary Science Letters, 160(1–2), 65–80, 1998.
John, T., Scambelluri, M., Frische, M., Barnes, J. D. and Bach, W.: Dehydration of subducting serpentinite: implications for halogen mobility in subduction zones and the deep halogen cycle, Earth and Planetary Science Letters, 308(1–2), 65–76, 2011.
Kerrick, D. M. and Connolly, J. A. D.: Metamorphic devolatilization of subducted marine sediments and the transport of volatiles into the Earth's mantle, Nature, 411(6835), 293, 2001.
Kohn, M. J.: Modeling of prograde mineral $\delta^{18}O$ changes in metamorphic systems, Contributions to Mineralogy and Petrology, 113(2), 249–261, 1993.
Konrad-Schmolke, M., O'Brien, P. J., de Capitani, C. and Carswell, D. A.: Garnet growth at high-and ultra-high pressure conditions and the effect of element fractionation on mineral modes and composition, Lithos, 103(3–4), 309–332, 2008.
Kuhn, B. K., Reusser, E., Powell, R. and Günther, D.: Metamorphic evolution of calc-schists in the Central Alps, Switzerland, Schweizerische mineralogische und petrographische Mitteilungen, 85(2–3), 175–190, 2005.
Lanari, P. and Duesterhoeft, E.: Modeling Metamorphic Rocks Using Equilibrium Thermodynamics and Internally Consistent Databases: Past Achievements, Problems and Perspectives, Journal of Petrology, 60(1), 19–56, doi:10.1093/petrology/egy105, 2018.
Lanari, P. and Engi, M.: Local bulk composition effects on metamorphic mineral assemblages, Reviews in Mineralogy and Geochemistry, 83(1), 55–102, 2017.
Lanari, P., Giuntoli, F., Loury, C., Burn, M. and Engi, M.: An inverse modeling approach to obtain P-T conditions of metamorphic stages involving garnet growth and resorption, European Journal of Mineralogy, 29(2), 181–199, 2017.
Laurent, V., Lanari, P., Naïr, I., Augier, R., Lahfid, A. and Jolivet, L.: Exhumation of eclogite and blueschist (Cyclades, Greece): Pressure–temperature evolution determined by thermobarometry and garnet equilibrium modelling, Journal of Metamorphic Geology, 36(6), 769–798, 2018.
Liou, J. G., Tsujimori, T., Zhang, R. Y., Katayama, I. and Maruyama, S.: Global UHP metamorphism and continental subduction/collision: the Himalayan model, International Geology Review, 46(1), 1–27, 2004.
Manning, C. E.: The chemistry of subduction-zone fluids, Earth and Planetary Science Letters, 223(1–2), 1–16, 2004.

Martin, L. A., Rubatto, D., Crépisson, C., Hermann, J., Putlitz, B. and Vitale Brovarone, A.: Garnet oxygen analysis by SHRIMP-SI: Matrix corrections and application to high-pressure metasomatic rocks from Alpine Corsica, Chemical geology, 374, 25–36, 2014.

Mattey, D., Lowry, D. and Macpherson, C.: Oxygen isotope composition of mantle peridotite, Earth and Planetary Science Letters, 128(3–4), 231–241, 1994.

Mével, C.: Serpentinization of abyssal peridotites at mid-ocean ridges, Comptes Rendus Geoscience, 335(10–11), 825–852, 2003.

Miller, J. A. and Cartwright, I.: Distinguishing between seafloor alteration and fluid flow during subduction using stable isotope geochemistry: examples from Tethyan ophiolites in the Western Alps—Miller—2000—Journal of Metamorphic Geology—Wiley Online Library, Journal of Metamorphic Geology, 18(5), 467–482, 2000.

Miller, J. A., Cartwright, I., Buick, I. S. and Barnicoat, A. C.: An O isotope profile through the HP–LT Corsican ophiolite, France and its implications for fluid flow during subduction, Chemical Geology, 178(1–4), 43–69, 2001.

Muehlenbachs, K. and Clayton, R. N.: Oxygen isotope studies of fresh and weathered submarine basalts, Canadian Journal of Earth Sciences, 9(2), 172–184, 1972.

Nakakuki, T. and Mura, E.: Dynamics of slab rollback and induced back-arc basin formation, Earth and Planetary Science Letters, 361, 287–297, 2013.

O'Neil, J. R. and Taylor, H. P.: The oxygen isotope and cation exchange chemistry of feldspars, American Mineralogist, 52, 1414–1437, 1967.

Padrón Navarta, J. A., Hermann, J., Garrido, C. J., Sánchez Vizcaíno, V. L. and Gómez Pugnaire, M. T.: An experimental investigation of antigorite dehydration in natural silica-enriched serpentinite, Contributions to Mineralogy and Petrology, 159(1), 25, 2010.

Padrón Navarta, J. A., Sánchez Vizcaíno, V. L., Hermann, J., Connolly, J. A., Garrido, C. J., Gómez Pugnaire, M. T. and Marchesi, C.: Tschermak's substitution in antigorite and consequences for phase relations and water liberation in high-grade serpentinites, Lithos, 178, 186–196, 2013.

Page, F. Z., Kita, N. T. and Valley, J. W.: Ion microprobe analysis of oxygen isotopes in garnets of complex chemistry, Chemical Geology, 270(1–4), 9–19, 2010.

Page, F. Z., Essene, E. J., Mukasa, S. B. and Valley, J. W.: A garnet–zircon oxygen isotope record of subduction and exhumation fluids from the Franciscan Complex, California, Journal of Petrology, 55(1), 103–131, 2013.

Page, F. Z., Cameron, E. M., Flood, C. M., Dobbins, J. W., Spicuzza, M. J., Kitajima, K., Strickland, A., Ushikubo, T., Mattinson, C. G. and Valley, J. W.: Extreme oxygen isotope zoning in garnet and zircon from a metachert block in mélange reveals metasomatism at the peak of subduction metamorphism, Geology, 47(7), 655–658, 2019.

Parra, T., Vidal, O. and Agard, P.: A thermodynamic model for Fe–Mg dioctahedral K-white micas using data from phase-equilibrium experiments and natural pelitic assemblages, Contributions to Mineralogy and Petrology, 143(6), 706–732, 2002.

Peacock, S. A.: Fluid processes in subduction zones, Science, 248(4953), 329–337, 1990.

Peacock, S. M.: The importance of blueschist → eclogite dehydration reactions in subducting oceanic crust, Geological Society of America Bulletin, 105(5), 684–694, 1993.

Penniston-Dorland, S. C., Kohn, M. J. and Manning, C. E.: The global range of subduction zone thermal structures from exhumed blueschists and eclogites: Rocks are hotter than models, Earth and Planetary Science Letters, 428, 243–254, 2015.

Plank, T.: The chemical composition of subducting sediments, Treatise on geochemistry, 4, 607–629, 2014.

Plank, T. and Langmuir, C. H.: The chemical composition of subducting sediment and its consequences for the crust and mantle, Chemical geology, 145(3), 325–394, 1998.

Poli, S. and Schmidt, M. W.: Petrology of subducted slabs, Annual Review of Earth and Planetary Sciences, 30(1), 207–235, 2002.

Powell, R. and Holland, T. J. B.: On thermobarometry, Journal of Metamorphic Geology, 26(2), 155–179, 2008.

Putlitz, B., Matthews, A. and Valley, J. W.: Oxygen and hydrogen isotope study of high-pressure metagabbros and metabasalts (Cyclades, Greece): implications for the subduction of oceanic crust, Contributions to Mineralogy and Petrology, 138(2), 114–126, 2000.

Rubatto, D. and Angiboust, S.: Oxygen isotope record of oceanic and high-pressure metasomatism: a P–T–time–fluid path for the Monviso eclogites (Italy), Contributions to mineralogy and petrology, 170(5–6), 44, 2015.

Rumble, D.: Stable isotope fractionation during metamorphic devolatilization reactions, Reviews in Mineralogy and Geochemistry, 10(1), 327–353, 1982.

Russell, A. K., Kitajima, K., Strickland, A., Medaris, L. G., Schulze, D. J. and Valley, J. W.: Eclogite facies fluid infiltration: constraints from $\delta^{18}O$ zoning in garnet, Contributions to Mineralogy and Petrology, 165(1), 103–116, 2013.

Scambelluri, M. and Philippot, P.: Deep fluids in subduction zones, Lithos, 55(1–4), 213–227, 2001.

Scambelluri, M., Fiebig, J., Malaspina, N., Müntener, O. and Pettke, T.: Serpentinite subduction: implications for fluid processes and trace-element recycling, International Geology Review, 46(7), 595–613, 2004.

Schmidt, M. W. and Poli, S.: The stability of lawsonite and zoisite at high pressures: Experiments in CASH to 92 kbar and implications for the presence of hydrous phases in subducted lithosphere, Earth and Planetary Science Letters, 124(1–4), 105–118, 1994.

Sharp, Z.: Principles of stable isotope geochemistry, 2017.

Sharp, Z. D. and Barnes, J. D.: Water-soluble chlorides in massive seafloor serpentinites: a source of chloride in subduction zones, Earth and Planetary Science Letters, 226(1–2), 243–254, 2004.

Siron, G., Baumgartner, L., Bouvier, A.-S., Putlitz, B. and Vennemann, T.: Biotite reference materials for secondary ion mass spectrometry $^{18}O/^{16}O$ measurements, Geostandards and Geoanalytical Research, 41(2), 243–253, 2017.

Spandler, C. and Hermann, J.: High-pressure veins in eclogite from New Caledonia; Implications for fluid migration and seismic activity in subduction zones, Geochimica et Cosmochimica Acta Supplement, 69, A664, 2005.

Spear, F. S.: Metamorphic fractional crystallization and internal metasomatism by diffusional homogenization of zoned garnets, Contributions to Mineralogy and Petrology, 99(4), 507–517, 1988.
Spear, F. S., Pattison, D. R. M. and Cheney, J. T.: The metamorphosis of metamorphic petrology, in The Web of Geological Sciences: Advances, Impacts, and Interactions II, Geological Society of America., 2017.
Staudigel, H.: Chemical fluxes from hydrothermal alteration of the oceanic crust, 2014.
Staudigel, H., Plank, T., White, B. and Schmincke, H. U.: Geochemical fluxes during seafloor alteration of the basaltic upper oceanic crust: DSDP Sites 417 and 418, Subduction: top to bottom, 96, 19–38, 1996.
Stern, R. J.: Subduction zones, Reviews of geophysics, 40(4), 3–1, 2002.
Sun, S. S. and McDonough, W. F.: Chemical and isotopic systematics of oceanic basalts: implications for mantle composition and processes, Geological Society, London, Special Publications, 42(1), 313–345, 1989.
Syracuse, E. M., van Keken, P. E. and Abers, G. A.: The global range of subduction zone thermal models, Physics of the Earth and Planetary Interiors, 183(1–2), 73–90, 2010.
Tracy, R. J.: Compositional zoning and inclusions in metamorphic minerals., Characterization of Metamorphism through Mineral Equilibria, Review in Mineralogy, 355–397, 1982.
Valley, J.: Stable isotope geochemistry of metamorphic rocks, Rev. Mineral., 16, 445–489, 1986.
Vho, A., Lanari, P. and Rubatto, D.: An internally-consistent database for oxygen isotope fractionation between minerals, Journal of Petrology, *in review*.
Vielzeuf, D., Veschambre, M. and Brunet, F.: Oxygen isotope heterogeneities and diffusion profile in composite metamorphic-magmatic garnets from the Pyrenees, American Mineralogist, 90(2–3), 463–472, 2005a.
Vielzeuf, D., Champenois, M., Valley, J. W., Brunet, F. and Devidal, J. L.: SIMS analyses of oxygen isotopes: matrix effects in Fe–Mg–Ca garnets, Chemical Geology, 223(4), 208–226, 2005b.
Wada, I., Wang, K., He, J. and Hyndman, R. D.: Weakening of the subduction interface and its effects on surface heat flow, slab dehydration, and mantle wedge serpentinization, Journal of Geophysical Research: Solid Earth, 113(B4), 2008.
Walter, M. J.: Melting of garnet peridotite and the origin of komatiite and depleted lithosphere, Journal of Petrology, 39(1), 29–60, 1998.
White, W. M. and Klein, E. M.: Composition of the Oceanic Crust, Treatise on Geochemistry (Second Edition), 2014.
Whitney, D. L. and Evans, B. W.: Abbreviations for names of rock-forming minerals, American mineralogist, 95(1), 185–187, 2010.
Zack, T. and John, T.: An evaluation of reactive fluid flow and trace element mobility in subducting slabs, Chemical Geology, 239(3–4), 199–216, 2007.

Table 1. Bulk compositions used for the simulations.

	SiO_2	TiO_2	Al_2O_3	FeO_T	MnO	MgO	CaO	Na_2O	K_2O	TOTAL	H_2O	CO_2
Normal MORB[1]	50.47	1.68	14.70	10.43	0.18	7.58	11.39	2.79	0.16	99.38	na	na
~~Normal MORB~~Metabasalt$_{(h)}$*	50.47	1.68	14.70	10.43	0.0	7.58	11.39	2.79	0.16	99.20	5.17[§]	0.00
Altered ~~MORB~~[2]basalt[2]	43.47	1.06	14.74	5.98	0.16	6.32	12.22	1.96	0.53	86.44	7.63	2.80
Metabasalt$_{(a)}$~~Altered MORB~~*	43.47	1.06	14.74	5.98	0.0	6.32	12.22	1.96	0.53	86.28	5.55[§]	2.80
Terrigenous sediment[3]	49.80	0.60	14.70	7.30	2.10	3.10	3.50	3.10	3.60	87.80	10.50	0.00
Metasediment$_{(t)}$~~Terrigenous sediment~~*	49.80	0.60	14.70	7.30	0.00	3.10	3.50	3.10	3.60	85.70	4.43[§]	0.00
Carbonate ~~Sediment~~[4]sediment[4]	32.36	0.40	8.78	2.91	0.12	1.45	23.16	1.96	1.66	72.80	8.78	18.20
Metasediment$_{(c)}$~~Carbonate sediment~~*	32.36	0.40	8.78	2.91	0.00	1.45	23.16	1.96	1.66	72.68	1.95[§]	18.20

[1] Gale et al. (2013)
[2] Baxter and Caddick (2013) after Staudigel et al. (1996)
[3] Mariana clay from Plank and Langmuir (1998)
[4] Nanno Ooze from Plank (2014)
* used for the thermodynamic modelling
[§] water content at saturation at 350 °C and 1.3 GPa. The calculated initial water content is consistent with values from the literature at these conditions (e.g. Poli and Schmidt, 1998; Hacker et al., 2003).

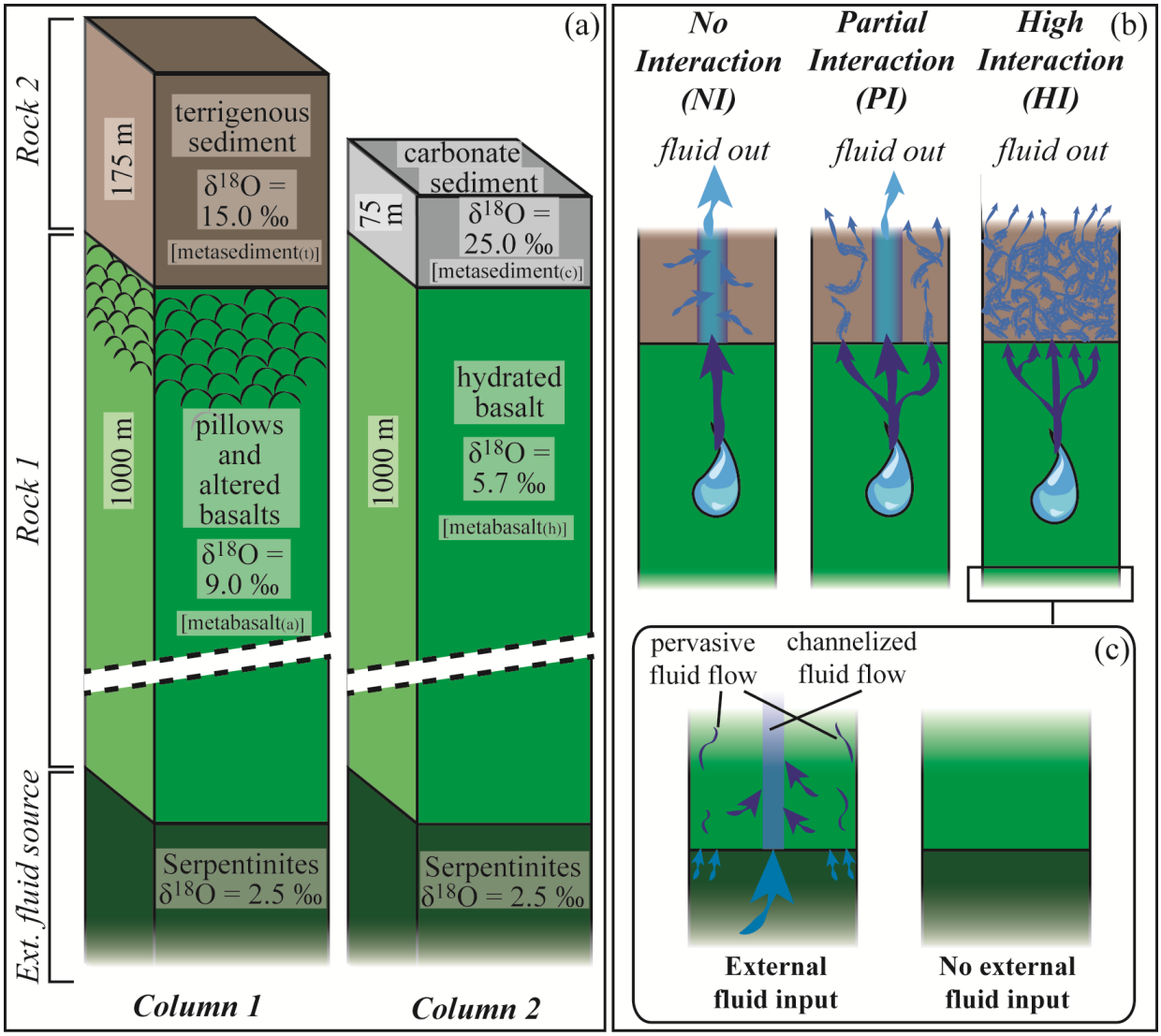

Figure 1. Schematic geometry of the subduction models discussed in the text. The rock column is composed ~~by~~ of two rock types (*Rock1* and *Rock2*) that can be infiltrated by an external fluid deriving from a third layer located beneath them. (a) Example columns used in the calculation along the *P-T* path shown in Fig. 2 to produce the results presented in figures #3 – 6. See text for details. (b) Schematic representation of the three interaction cases discussed in the text. *No Interaction* case (*NI*): the fluid released by the ~~MORB~~ metabasalt does not interact with the ~~sedimentary cover~~metasediment. The fluid leaving the system is a ~~mixing~~ mixture of metabasalt~~MORB~~-derived and metasediment-derived fluids. *Partial Interaction* case (*PI*): 50 % of the metabasalt~~MORB~~-derived fluid does not ~~exchange~~ interact with the ~~sedimentary cover~~metasediment, and 50 % of it equilibrates with the metasediments. The final fluid released by the system is the ~~mixing~~ mixture between the unmodified metabasalt-derived~~mafic~~ fluid and the fluid deriving from the metasediment after it equilibrates with 50 % of the metabasalt-derived~~mafic~~ fluid. *High Interaction* case (*HI*): all the fluid released by the metabasalt~~MORB~~ equilibrates with the metasediment. The fluid leaving the system exits the metasediment. (c) Possible scenario at the base of the column. As a consequence of serpentine breakdown, serpentinite-derived~~ultramafic~~ fluids may infiltrate the metabasalt~~MORB~~, exchange with it and affect the fluid infiltrating the metasediment~~sedimentary cover~~.

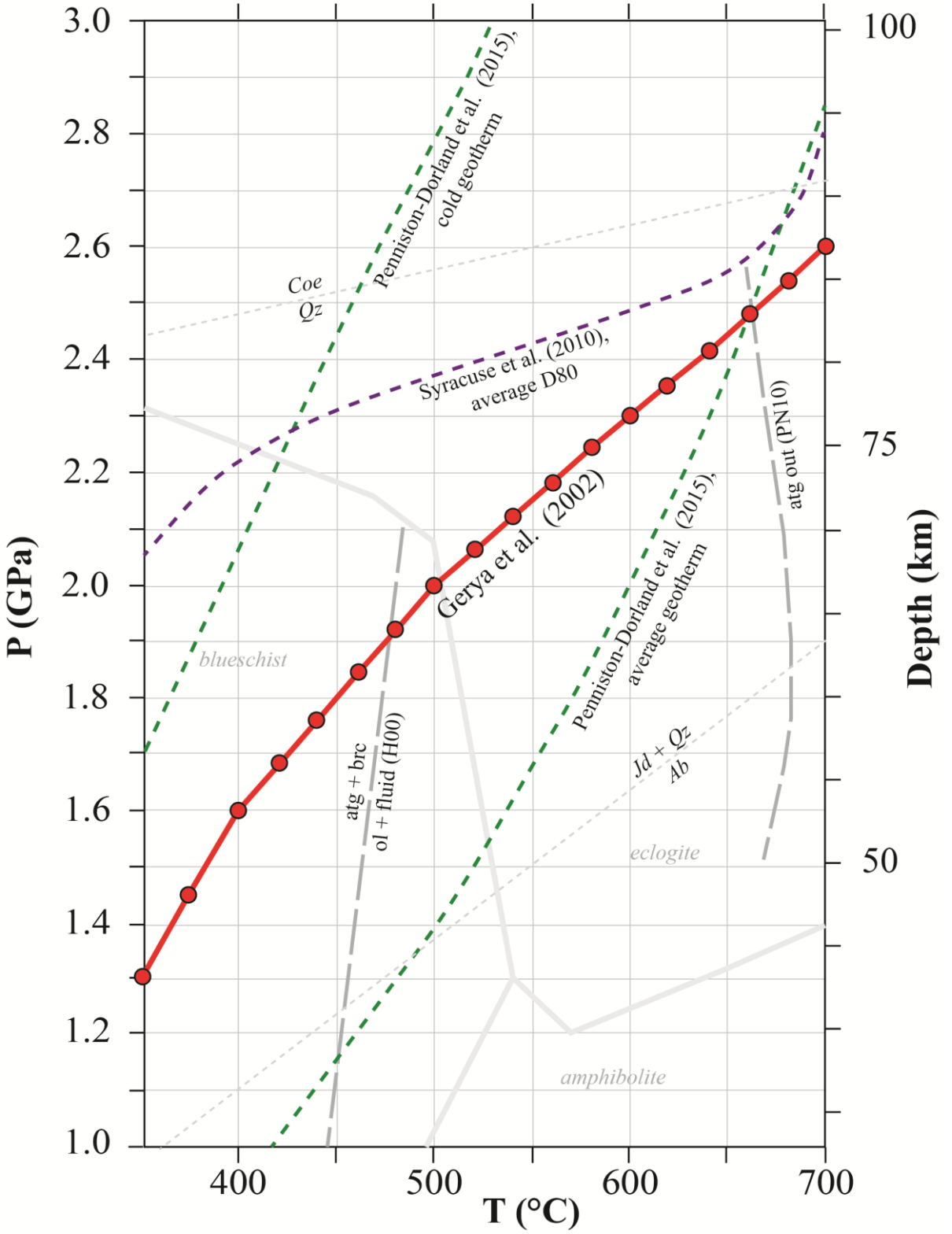

Figure 2. ~~Pressure-Temperature (~~*P*-*T*~~)~~ diagram showing typical oceanic subduction geotherms and the intermediate geotherm used in the calculation (red line, Gerya et al., 2002). The red spots represent the modelling steps. The average D80 geotherm from Syracuse et al. (2010), i.e. the geotherm dominated by a steep *T* gradient at 80 km depth, which occurs at the transition from partial to full coupling, as reported by Penniston-Dorland et al. (2015) (purple dashed~~dotted~~ line) and the average slab-top geotherm from Penniston-Dorland et al. (2015) (green dashed~~dotted~~ line) are shown for comparison. Metamorphic facies modified from Peacock (1993) and Liou et al. (2004). Serpentine breakdown reactions from Padrón-Navarta et al. (2010) (PN10) and Hermann et al. (2000) (H00). Mineral abbreviations ~~are~~ from Whitney and Evans (2010).

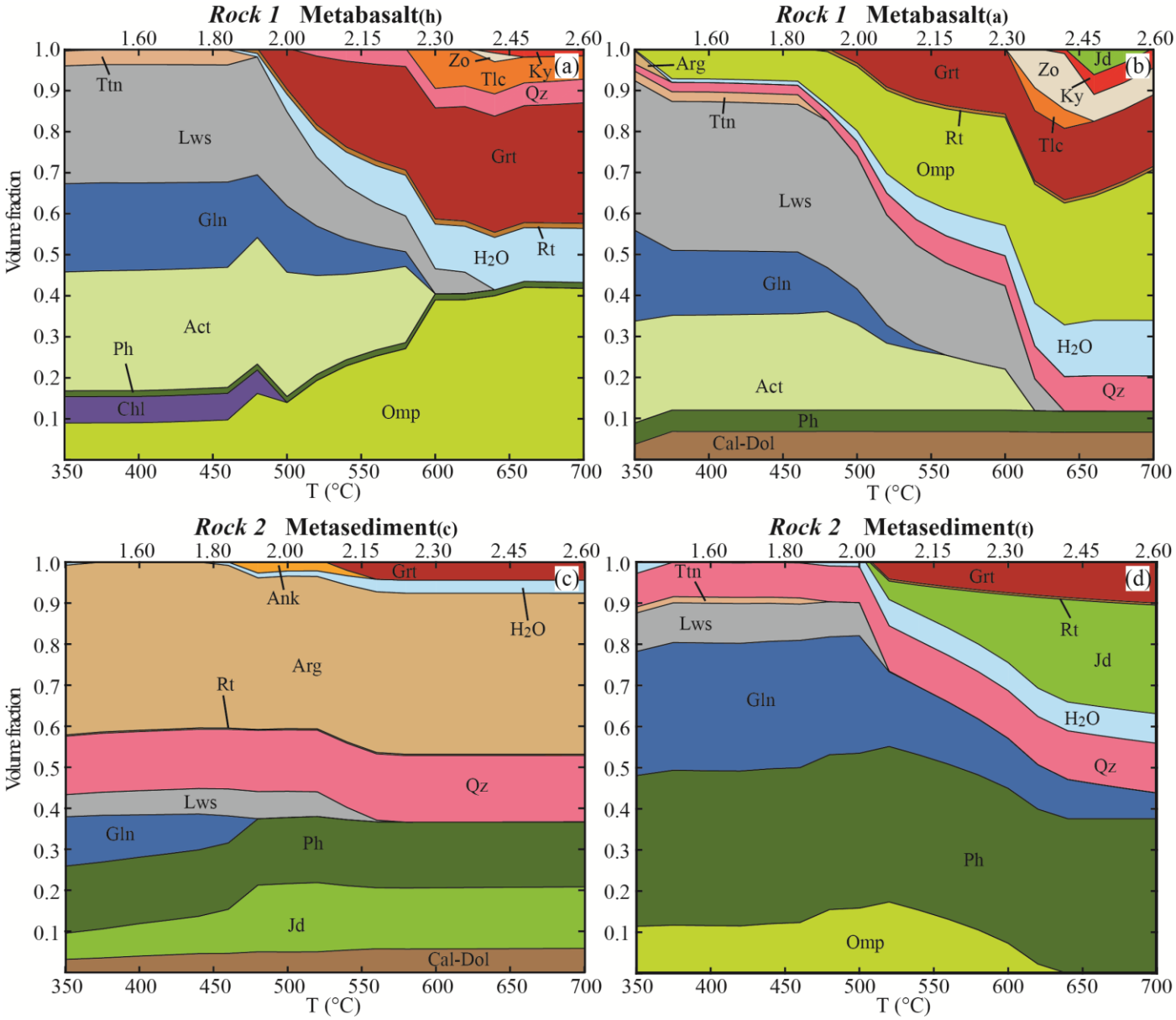

Figure 3. Mode-box diagrams showing the evolution of the mineral assemblages and fluid during subduction of the different rock types along the geotherm shown in Fig. 2. The initial H_2O content is < 1 vol% in the metabasalts and in the metasediment$_{(c)}$, ~ 3 vol% in the metasediment$_{(t)}$ (see Table 1 for details). Garnet fractionation is applied to all the lithologies. The volume fraction of garnet shown at each step represents the sum of the fractionated and newly grown garnet. The phase proportions refer to the *NI* case, where the H_2O content is the excess (free) H_2O produced by each rock type evolving independently. The excess water is fractionated at each step and the volume fraction displayed represents the sum of the fractionated and the newly produced water. Mineral abbreviations from Whitney and Evans (2010).

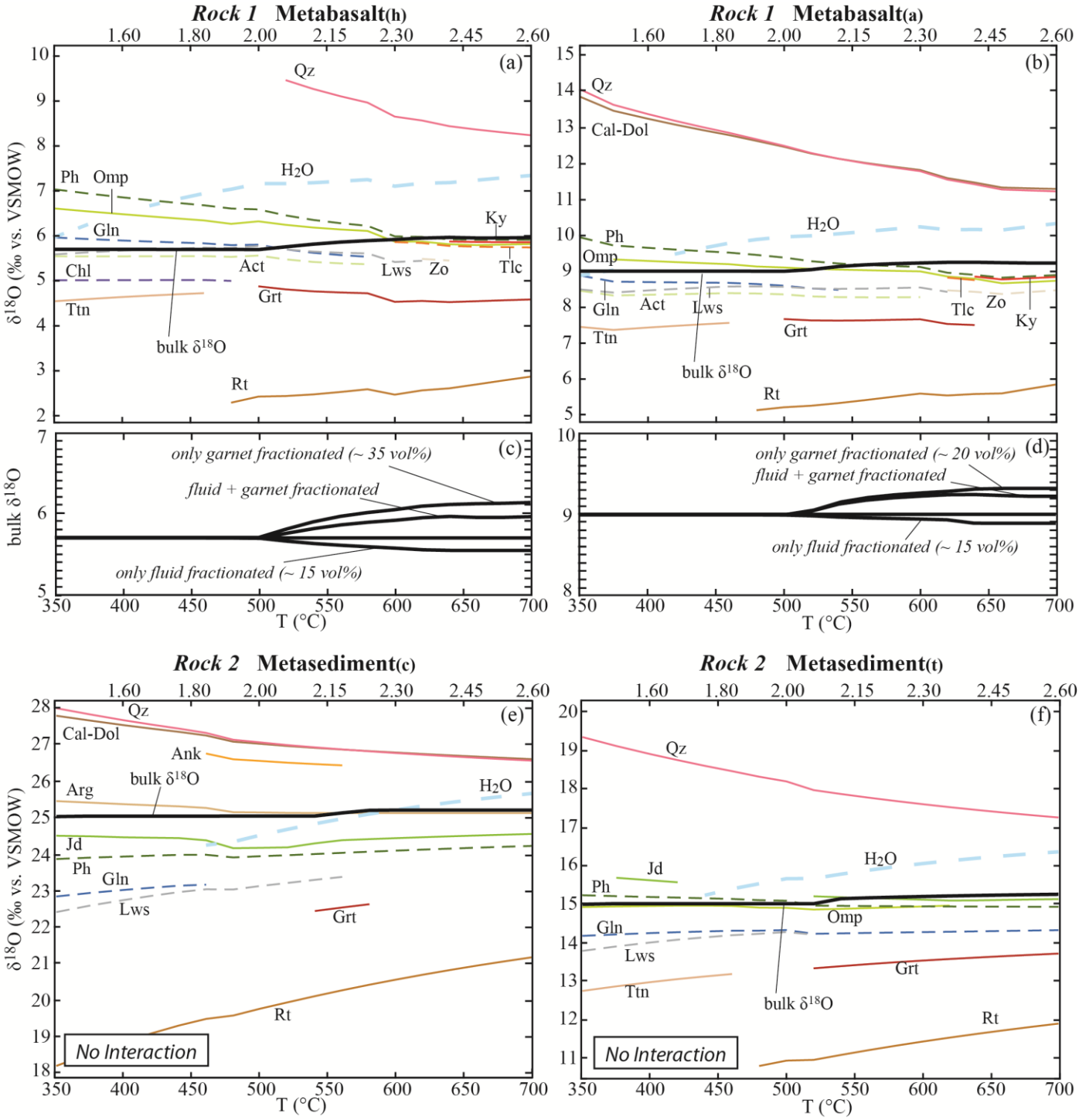

Figure 4. Calculated bulk and mineral $\delta^{18}O$ values along the geotherm shown in Fig. 2. Bulk $\delta^{18}O$: black solid line. Hydrous mineral $\delta^{18}O$: coloured dashed~~dotted~~ lines. Anhydrous mineral $\delta^{18}O$: coloured solid lines. Released H_2O: thick blue dashed~~dotted~~ lines. (a, b) Modelled mineral, bulk and released fluid $\delta^{18}O$ values ~~from fresh and altered MORBs~~ for the metabasalt$_{(h)}$ and the metabasalt$_{(a)}$ considering garnet fractionation and excess fluid loss and in absence of external fluid input. (c, d) Quantification of the effects of garnet fractionation and fluid loss on the bulk $\delta^{18}O$ of the metabasalts~~of the MORB compositions~~. (e, f) Modelled mineral, bulk and released fluid $\delta^{18}O$ values for the metasediment$_{(c)}$ and the metasediment$_{(t)}$ ~~from carbonate and terrigenous sediments~~ considering garnet fractionation and excess fluid loss and in the absence of external fluid input. Mineral abbreviations from Whitney and Evans (2010). ~~(g, h) Modelled $\delta^{18}O$ values from carbonate and terrigenous sediments considering garnet fractionation and excess fluid loss in case of *PI* (*) and *HI* (**). Only bulk, released H_2O and representative mineral $\delta^{18}O$ values are shown for clarity.~~

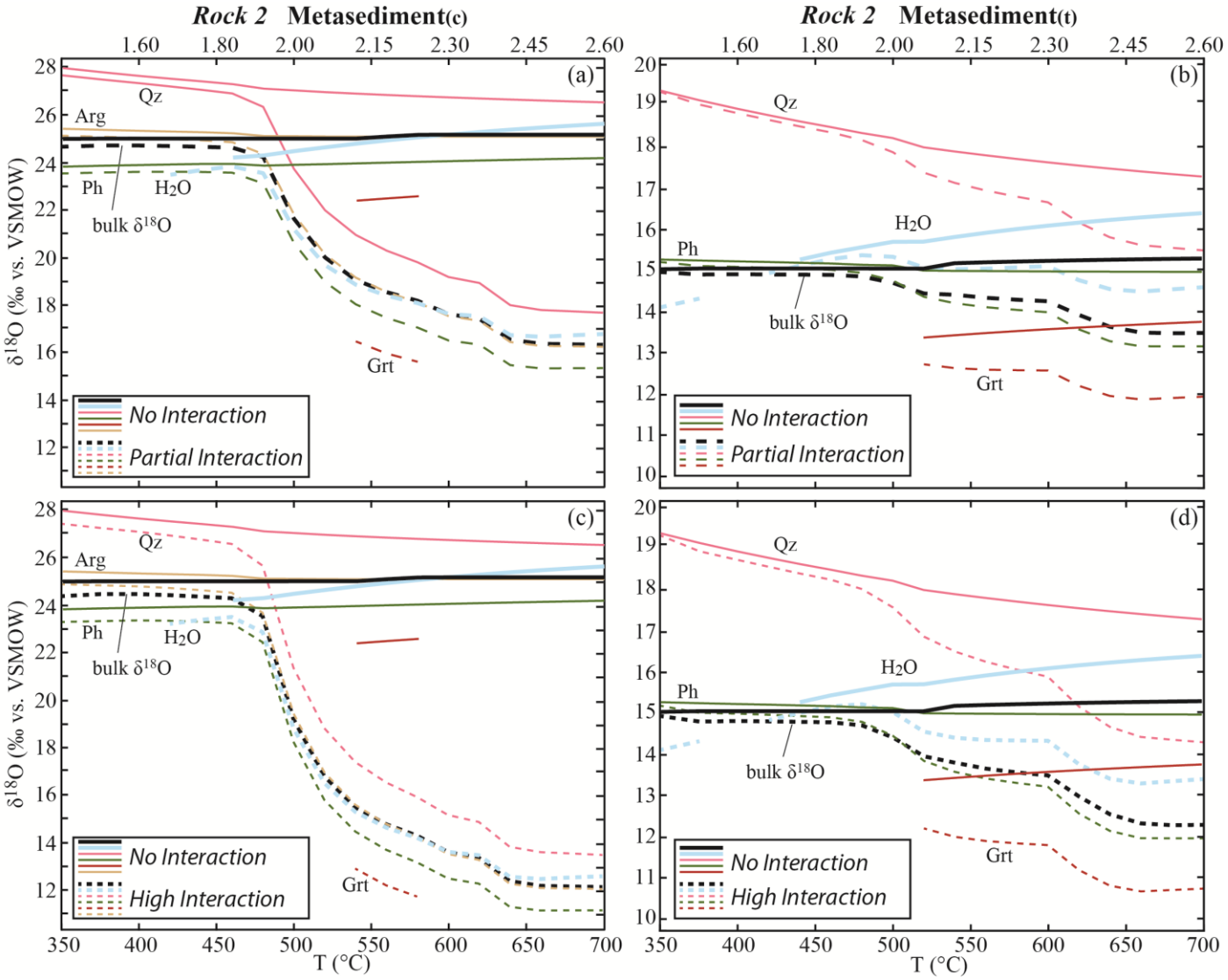

Figure 5. Calculated bulk and mineral $\delta^{18}O$ values in the metasediments along the geotherm shown in Fig. 2 in case of interaction with the metabasalt-derived fluid. Only bulk, released H_2O and representative mineral $\delta^{18}O$ values are shown for clarity. Garnet fractionation and excess fluid loss are considered. (a) $Metasediment_{(c)}$: evolution of the $\delta^{18}O$ values in case of *NI* (continuous lines) and *PI* (dashed lines). (b) $Metasediment_{(t)}$: evolution of the $\delta^{18}O$ values in case of *NI* (continuous lines) and *PI* (dashed lines). (c) $Metasediment_{(c)}$: evolution of the $\delta^{18}O$ values in case of *NI* (continuous lines) and *HI* (dashed lines). (d) $Metasediment_{(t)}$: evolution of the $\delta^{18}O$ values in case of *NI* (continuous lines) and *HI* (dashed lines). Mineral abbreviations are from Whitney and Evans (2010).

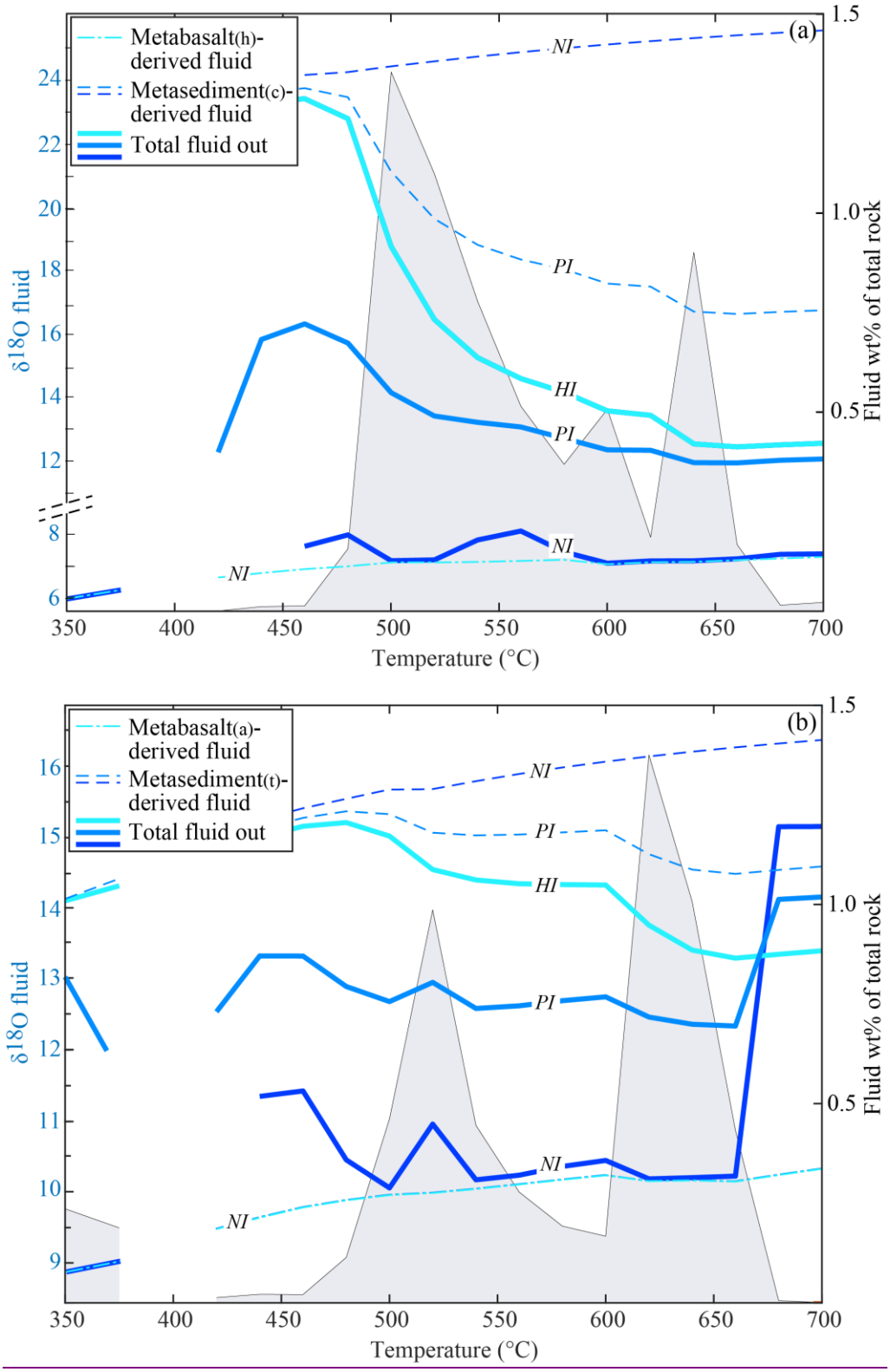

Figure ~~5~~6. Double plot diagrams showing the oxygen isotope composition of the released fluids (left axis, coloured lines) and the amount (in wt% of the total rock) of the total fluid released by the systems (right axis, grey field) for each interaction case in absence of serpentinite-derived~~ultramafic~~ fluid input. (a) Modelled fluid $\delta^{18}O$ values and amount for the system metabasalt$_{(h)}$ + metasediment$_{(c)}$~~fresh MORB + carbonate sediment~~. (b) Modelled fluid $\delta^{18}O$ values and amount for the system metabasalt$_{(a)}$ + metasediment$_{(t)}$~~altered MORB + terrigenous sediment~~. Dashed~~Dotted~~ lines show the $\delta^{18}O$ values of the fluids released by each rock type, solid lines the $\delta^{18}O$ values of the final fluids released by each system. In case of *HI*, all the metabasalt-derived~~MORB-derived~~ fluid infiltrates the metasediment. Hence the final fluid released overlaps with the fluid expelled by the metasediment and only one line is represented (light blue, marked as *HI*). Because the $\delta^{18}O$ values of the fluids released by the ~~MORB-~~metabasalts are not affected by the degree of interaction, all three cases are represented by one line (marked as *NI*).

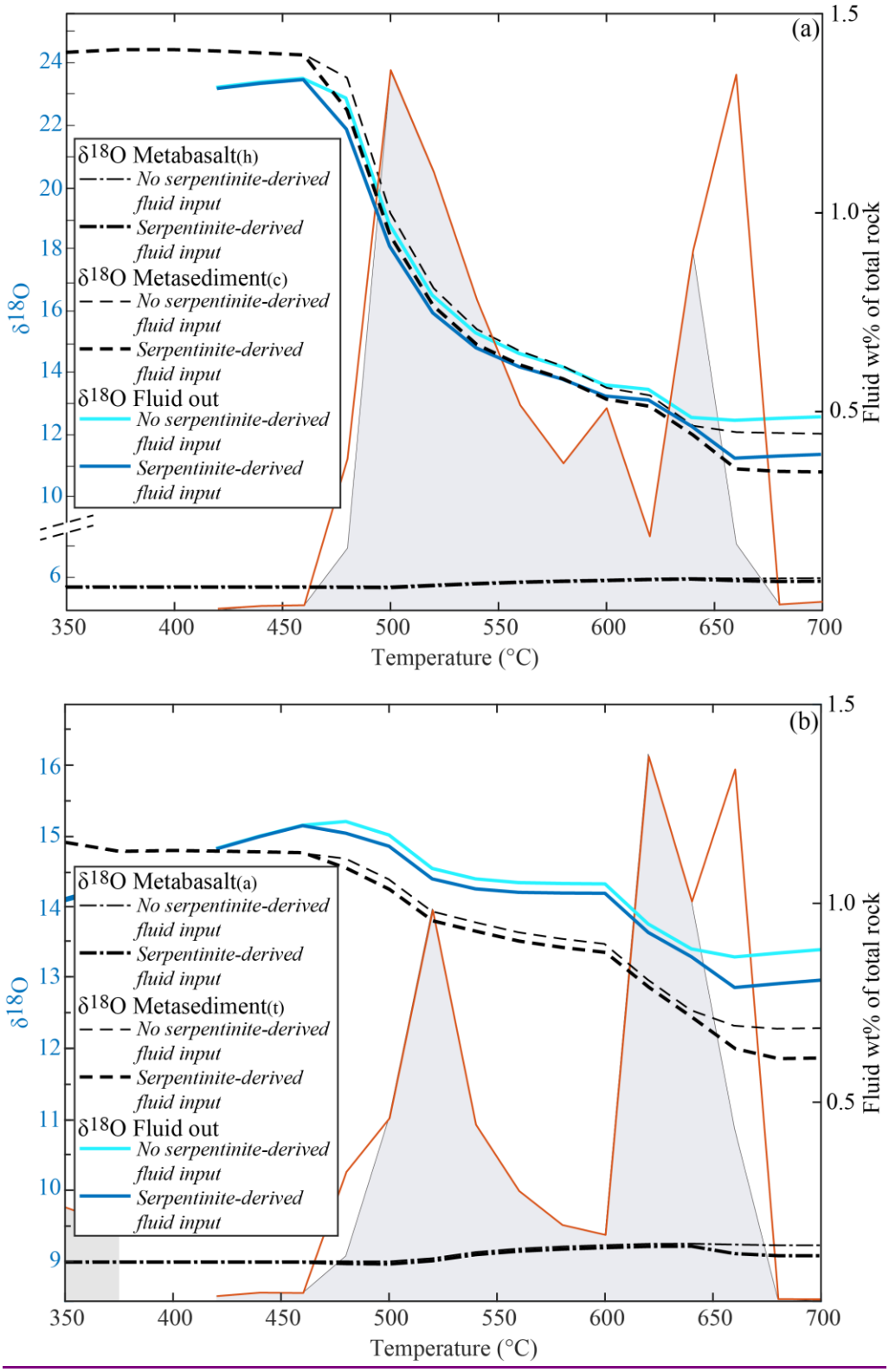

Figure ~~6~~7. Double plot diagrams showing the effect of the input of the serpentinite-derived~~ultramafic~~ fluid deriving from a layer of 150 m of pure serpentine (see text for details) on the $\delta^{18}O$ of the rock types and of the of the total released H_2O (left axis) and on the amount and distribution of the H_2O released by the systems (right axis). All the values are calculated assuming *HI* between the metabasalts and the metasediments~~MORBs and the sediments~~. Black dashed~~dotted~~ lines represent the bulk $\delta^{18}O$ ~~for~~ of the different lithologies and the blue lines the $\delta^{18}O$ of the final fluid released by the systems. The final H_2O released by each system is represented with a red line. The amount and distribution of the final fluids in case of no serpentinite-derived~~ultramafic~~ fluid input (grey fields) are shown for comparison. (a) Modelled $\delta^{18}O$ values released fluid amount for the system metabasalt$_{(h)}$ + metasediment$_{(c)}$~~fresh MORB + carbonate sediment~~. (b) Modelled $\delta^{18}O$ values released fluid amount for the system metabasalt$_{(a)}$ + metasediment$_{(t)}$~~altered MORB + terrigenous sediment~~.

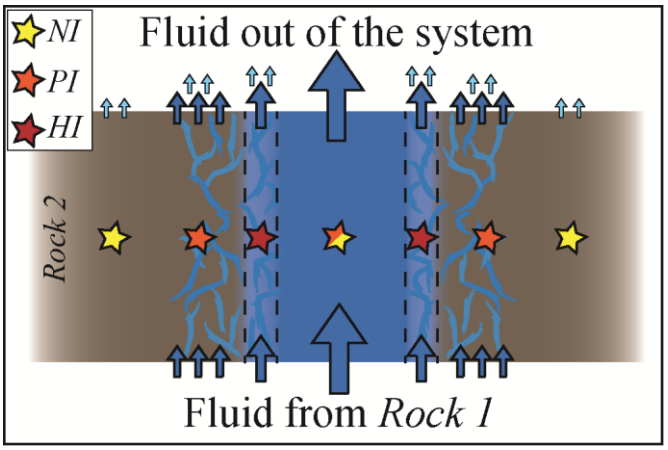

Figure ~~7~~8. Schematic section of a channelled fluid flow where different degrees of exchange between the fluid and the rock may occur in spatial proximity. From the host rock perspective, the *NI* case describes the distal portion of the rock walls where no fluid infiltrates; the *PI* case the intermediate portion where a limited amount of external fluid is available and the *HI* case the pervasively infiltrated rock proximal to the vein. From the fluid perspective, the *NI* case describes the fluid flow in the centre of the channel, for which the exchange with the rock walls is negligible; the *PI* case the case for which part of the fluid does not react with the wall rock and part equilibrates with it and the *HI* case the situation in which no fluid flows without equilibrating with the host rock.

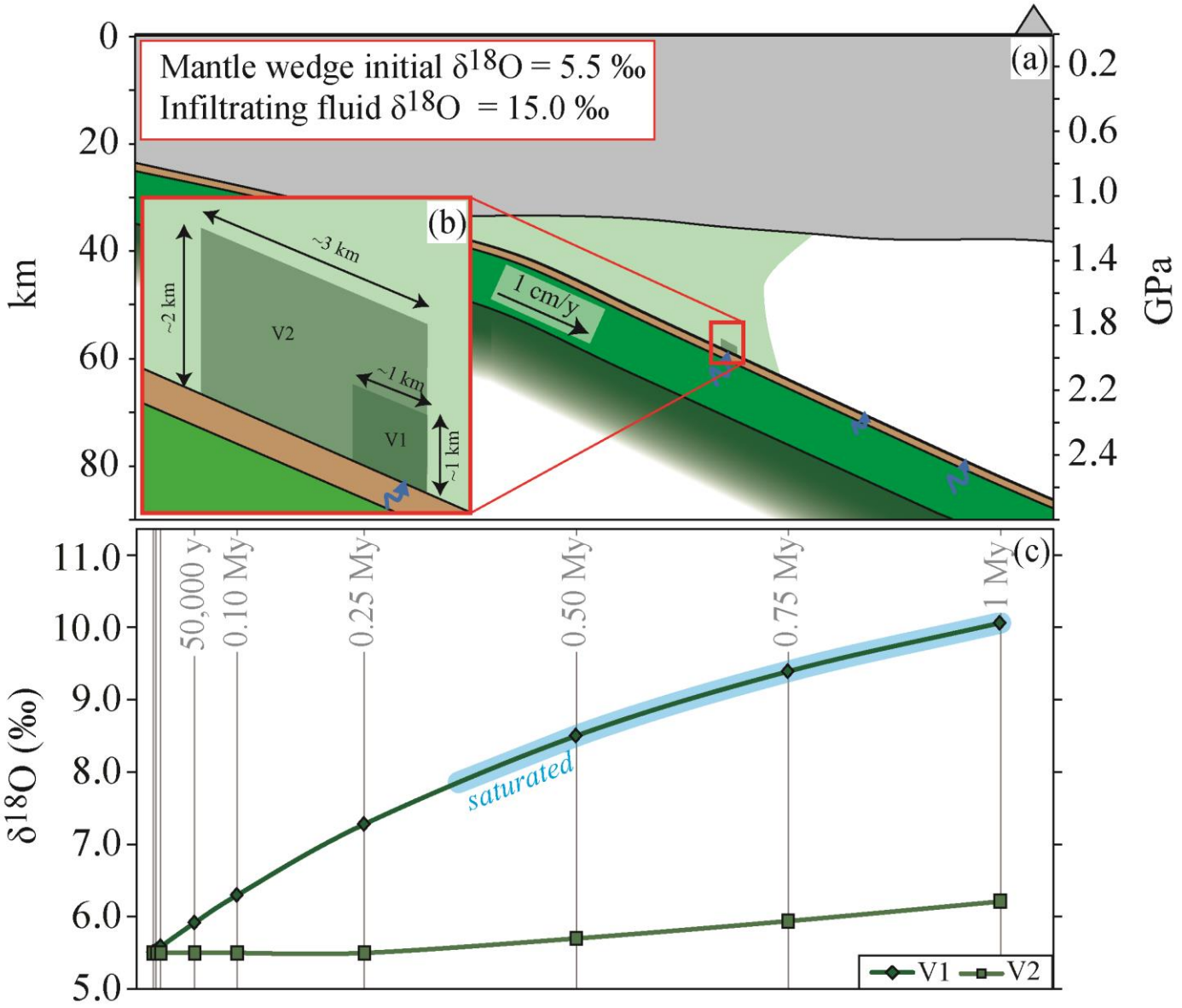

Figure ~~8~~9. Case model for mantle wedge hydration. (a) Sketch of a subduction zone (modified after Bostock et al., 2002). The subducting slab is composed of metabasalt$_{(a)}$ and metasediment$_{(t)}$~~altered MORB and terrigenous sediments~~ as shown in Fig. 1a, left column. (b) Geometry of the model. The blue arrow represents slab dehydration at 500 – 520 °C. Abbreviations: V1 represents the volume of mantle rocks at the interface and V2 the surrounding volume (see text for details). (c) Plot of the bulk $\delta^{18}O$ variations of V1 and V2 as consequence of continuous slab dehydration over 1 Myr.